NCHRP Report 438

Recommended LRFD Specifications for Plastic Pipe and Culverts

Transportation Research Board
National Research Council

Report 438

Recommended
LRFD Specifications for
Plastic Pipe and Culverts

T. J. McGRATH
V. E. SAGAN
Simpson Gumpertz & Heger Inc.
Arlington, MA

Subject Areas

Bridges, Other Structures, and Hydraulics and Hydrology

TRANSPORTATION RESEARCH BOARD
NATIONAL RESEARCH COUNCIL

NATIONAL ACADEMY PRESS
Washington, D.C. 2000

NATIONAL COOPERATIVE HIGHWAY RESEARCH PROGRAM

Systematic, well-designed research provides the most effective approach to the solution of many problems facing highway administrators and engineers. Often, highway problems are of local interest and can best be studied by highway departments individually or in cooperation with their state universities and others. However, the accelerating growth of highway transportation develops increasingly complex problems of wide interest to highway authorities. These problems are best studied through a coordinated program of cooperative research.

In recognition of these needs, the highway administrators of the American Association of State Highway and Transportation Officials initiated in 1962 an objective national highway research program employing modern scientific techniques. This program is supported on a continuing basis by funds from participating member states of the Association and it receives the full cooperation and support of the Federal Highway Administration, United States Department of Transportation.

The Transportation Research Board of the National Research Council was requested by the Association to administer the research program because of the Board's recognized objectivity and understanding of modern research practices. The Board is uniquely suited for this purpose as it maintains an extensive committee structure from which authorities on any highway transportation subject may be drawn; it possesses avenues of communications and cooperation with federal, state and local governmental agencies, universities, and industry; its relationship to the National Research Council is an insurance of objectivity; it maintains a full-time research correlation staff of specialists in highway transportation matters to bring the findings of research directly to those who are in a position to use them.

The program is developed on the basis of research needs identified by chief administrators of the highway and transportation departments and by committees of AASHTO. Each year, specific areas of research needs to be included in the program are proposed to the National Research Council and the Board by the American Association of State Highway and Transportation Officials. Research projects to fulfill these needs are defined by the Board, and qualified research agencies are selected from those that have submitted proposals. Administration and surveillance of research contracts are the responsibilities of the National Research Council and the Transportation Research Board.

The needs for highway research are many, and the National Cooperative Highway Research Program can make significant contributions to the solution of highway transportation problems of mutual concern to many responsible groups. The program, however, is intended to complement rather than to substitute for or duplicate other highway research programs.

FOREWORD

By Staff
Transportation Research
Board

This report presents the results of an investigation of the capacity of thermoplastic culvert pipe in hoop compression and the resistance of profile wall pipe sections to failure by local buckling. The work was carried out to support development of design provisions (for plastic pipes and culverts) to be included in the AASHTO load and resistance factor design (LRFD) specifications. At present, design methodology and properties for plastic pipes and culverts are governed through procedures developed for metal products. The use of plastic pipe is increasing and, therefore, so is the need for provisions to assist structural engineers to make safe, cost-effective use of these materials. The contents of the report are, therefore, of immediate interest to both highway and rail transit professionals responsible for designing, installing, inspecting, maintaining, and upgrading nonpressure drainage pipes as well as to those charged with specifying materials for such pipe.

Simpson Gumpertz & Heger Inc., of Arlington, Massachusetts, conducted this research as Task 89 of NCHRP Project 20-07, *LRFD Specifications for Plastic Pipe and Culverts*. The principal investigator directed the research and authored the report; an advisory panel established for Task 89 of NCHRP Project 20-07 wrote the scope of work and reviewed the report, and the necessary majority accepted the report.

The objective of the research was to develop LRFD design provisions for plastic pipe and culvert. The objective was accomplished through (1) a review of past work related to local buckling of thin sections, (2) laboratory testing to investigate the local buckling behavior of currently available profile wall thermoplastic pipe, and (3) investigation of a design model to predict the capacity of profile wall thermoplastic pipe in compression as governed by local buckling.

The key product of the research is a proposed revision to the AASHTO LRFD specifications for thermoplastic pipe (presented in Appendix E of this report). This revision is based on the results of the "stub compression" tests conducted in the project on HDPE and PVC pipe sections. Calculated values derived from the empirical design equations of Winter correlated well with these test results. Thus, the proposed revision incorporates these equations into current standards.

The design method proposes strain limits for compressive strength on the basis of the 50-year strength and stiffness values for thermoplastic pipe currently in the AASHTO standards. The report cautions that these limits are for sections made up of elements with low width to thickness ratios and that sections with higher ratios will be limited to lower average strain levels. The method also provides limits on allowable deflection and depth of fill; the latter limits assume that parallel research results for improving the load computation method for thermoplastic culverts will also be implemented by AASHTO.

CONTENTS

RECOMMENDED LRFD SPECIFICATIONS FOR PLASTIC PIPE AND CULVERTS

SUMMARY   This project was developed to investigate the capacity of thermoplastic culvert pipe in hoop compression—specifically, the resistance of profile wall pipe sections to failure by local buckling. The project was necessitated by the advent of large-diameter pipe with high bending stiffness and low cross-sectional area, a structural combination that has not been dealt with in prior research on buried pipe. The project consisted of a review of the literature for past work related to local buckling of thin sections, tests to investigate the local buckling behavior of currently available profile wall thermoplastic pipe, and investigation of a design model to predict the capacity of profile wall thermoplastic pipe in compression, as governed by local buckling.

The literature showed that the classical buckling equation proposed by Bryan (1891) is still used to predict the onset of buckling in thin plates. The empirical equations of Winter (1946) are used to predict the ultimate capacity of thin steel sections, which includes some post buckling strength. No detailed work has been undertaken to apply this work to thermoplastic pipe. Introductory tests have been conducted at the University of Massachusetts and at the University of Western Ontario.

Testing consisted of a series of "stub compression" tests on high-density polyethylene (HDPE) and polyvinyl chloride (PVC) pipe sections. Several sample sizes and end conditions were investigated. The best results were obtained with relatively short specimens, and a recommended length for future tests is that the specimen length be approximately 1.5 times the height of the wall profile. The recommended end conditions are one end fixed and one end pinned. Additional work should be conducted before implementing the test as a standard or a quality control test.

The results of the compression tests correlated well with the empirical equations of Winter. A design method based on these equations is proposed for incorporation into AASHTO standards. The design equations rely on the 50-year strength and stiffness values currently in AASHTO to establish proposed strain limits for compressive strength. This is the limiting strain for thick sections. Thinner sections (i.e., sections with high ratios of width to thickness) are limited to lower strains.

The proposed design method provides limits on depth of fill and on allowable deflection levels. The allowable depths of fill were calculated assuming that parallel research for improving the load computation method for thermoplastic culverts will

be implemented. This work shows that the load depends on the type and density of the backfill—thus these parameters also affect the allowable depth of fill. For HDPE pipe, the allowable depths of fill vary widely based on the specific profile being evaluated— from 6 to 16 m (20 to 36 ft) in dense granular material compacted to 100 percent of maximum standard Proctor density and from 3.6 to 6.4 m (12 to 21 ft) in silty soil compacted to 90 percent of maximum standard Proctor density. For the one PVC pipe evaluated, the allowable depth of fill is 17 m (50 ft) in the dense granular material and 14 m (45 ft) in the silty soil.

Additional research is recommended to further develop the stub compression test for use as a standard. Investigation should focus on time effects and on strain limits. Although the current AASHTO parameters appear to correlate well with the pipe tested, this may not always be the case. Additional research should also investigate the relationship between bending strain and hoop compression strain. Understanding this relationship could lead to improved design methods that may be less conservative than proposed here. Additional research should also be conducted to investigate the effect of soil support. If soil support has a significant effect, then the current recommendations could be quite conservative.

The recommendations in this report for evaluating hoop compression strength and local buckling should be implemented simultaneously with parallel research on methods for computing loads and for improving HDPE resins. The current criteria in AASHTO for loads are known to be overly conservative for some types of pipe, and implementation of the proposed local buckling criteria would be an additional and unnecessary conservatism. The need for improved HDPE resins is also important. The application of a design model that uses post-buckling capacity demands resins that are not sensitive to cracking.

CHAPTER 1

INTRODUCTION AND RESEARCH APPROACH

The use of thermoplastic profile wall pipe for culverts, under drains, and other highway applications has continued to increase in recent years. The advent of technology to manufacture thermoplastic pipe with profile walls in larger diameters is further increasing interest in these products as the geometry provides pipe with high bending stiffness and low cross-sectional area. This trend has resulted in pipe with structural characteristics that have not been dealt with in prior research on buried pipe. The low cross-sectional area and the lower modulus of elasticity results in increased compression strain that must be considered in the structural design of the pipe.

The structural efficiency of profile wall pipe is achieved through designing wall sections that are deep, but with as little area as possible, which means that individual elements of the pipe wall are kept as thin as possible. However, because a properly installed flexible pipe carries stresses largely in compression, the thin elements in the pipe wall are susceptible to instability in compression, or local buckling. This report presents the results of an investigation into the local buckling capacity of profile wall thermoplastic pipe.

The approach taken to this project was as follows:

- Investigate the literature for past work related to local buckling of thin sections,
- Conduct tests to investigate the local buckling behavior of currently available profile wall thermoplastic pipe, and
- Develop a design model to predict the capacity of profile wall thermoplastic pipe in compression, as governed by local buckling.

TERMINOLOGY

Several wall profiles are used to manufacture pipe for drainage applications. Figure 1a shows just a few of these. Most of the work reported here pertains to thermoplastic pipe with a corrugated profile. The terminology used to describe the portions of this profile are presented in Figure 1b.

Corrugated wall

Honeycomb wall (D-profile)

Standing Rib Wall

a. Types of Profile Wall (not inclusive)

b. Idealized Corrugation and Terminology
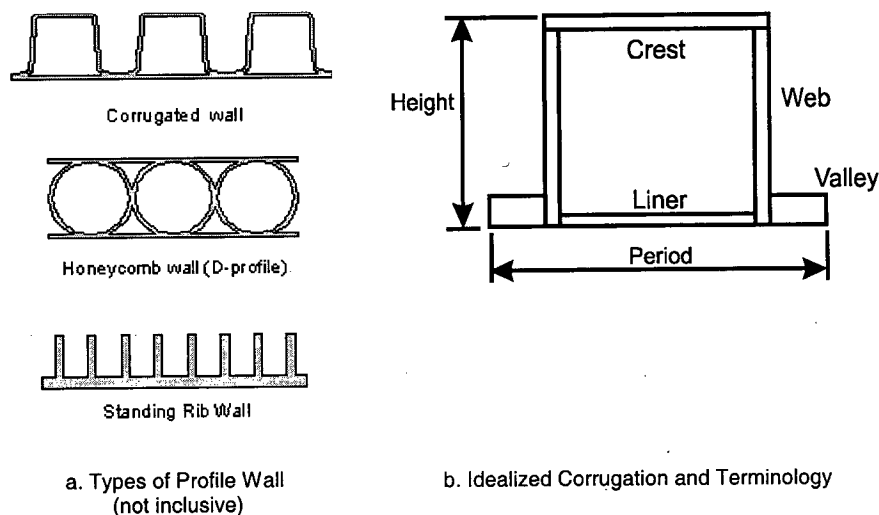
Figure 1. Pipe profiles and terminology.

CHAPTER 2

FINDINGS

STATE OF THE ART

Current knowledge related to local buckling of thin sections was reviewed and is presented in Appendix A. Details pertinent to the design method proposed later in this section are presented here.

Strain Capacity

The focus of this report is the compression capacity of profile wall thermoplastic culvert pipe and the resistance of such pipe to local buckling. The presence of tension in the pipe wall affects the buckling performance in some instances, but tension capacity is not evaluated.

Current AASHTO Design Parameters

Currently, AASHTO[1] provides "initial" and "50-year" values for modulus and strength and lists allowable tension strain limits. All are summarized in Table 1. In design according to AASHTO, the strength values are used to evaluate the hoop compression strength, and thus the ratio of the strength to modulus becomes a compression strain limit. These values are summarized in Table 1. However, the strain limits for compression represent strength limit states, while the strain limits for tension are specified as allowable strains. The basis for most of the limits specified in AASHTO are not clear.

HDPE and PVC Behavior in Compression

Very little research has been conducted on the behavior of thermoplastic pipe materials in compression. Compression stress-strain curves for polyethylene, from Zhang and Moore (1997), are presented in Figure 2. The strain rate for the test shown in Figure 2a was relatively slow, 0.05 percent per second, while the strain rates for the several tests reported in Figure 2b vary from 0.001 percent per second to 10 percent per

second. The figures are plotted as true stress versus true strain, but the deviation from engineering stress and strain in the region of interest (4 to 8 percent strain level) is small. The figure shows that, for all strain rates, the strain at yield in compression is in the range of 15 percent; however, the material is highly nonlinear and the stiffness above strains of 6 percent is quite low. For all strain rates, the stress-strain curves are relatively linear up to about 2 percent strain and relatively flat for strains greater than about 6 percent strain. The similarities of these curves based on strain levels suggest that design based on a strain limit rather than a stress limit is reasonable. The curves suggest that compression limits for high-density polyethylene (HDPE) pipe should likely be set in the range of 4 to 6 percent. No similar data are currently available for polyvinyl chloride (PVC) pipe materials.

Profile Wall Pipe Behavior in Parallel Plate Tests

AASHTO specifications for both PE and PVC pipe require a flattening test to at least 20 percent deflection (standards for PVC pipe require that the pipe be loaded to deflection of 60 percent), which the pipe must survive without buckling, cracking, or other loss of load-carrying capacity. Table 2 presents results of calculations of strain levels in the parallel plate test for pipe produced by several manufacturers. The calculations are discussed in more detail in Appendix C. The table shows that, at 20 percent deflection, typical corrugated PE pipe reaches strain levels on the order of 2.5 to 5.5 percent on the inside and 4.5 to 10 percent on the outside. These levels at first suggest that the strain limits in AASHTO (Table 1) are conservative; however, the highest strain levels are reached on the outside surface where the pipe bears on the loading plate. Thus, the plate may be either providing support to the pipe or restraining it from reaching the theoretical strain level. Thus, the fact that pipes are subjected to and pass this test is encouraging, but it is not definitive in providing assurance that the theoretical strain limits are achievable.

Selig et al. (1994) reported on long-term parallel plate tests at the University of Massachusetts in which corrugated PE pipe was held at deflection levels of 5 percent, 10 percent, and 15 percent for a period of more than 1 year. No pipe tested at 15 percent developed any type of failure condition, including

---

[1] Unless otherwise noted, references to "AASHTO" refer to Section 18 of the *Standard Specifications for Highway Bridges, 16th Edition*. The provisions for design of thermoplastic pipe in Section 12 of the *LRFD Bridge Design Specifications* are identical, and thus the two codes need not be distinguished for purposes of this report.

TABLE 1 Apparent strain limits based on AASHTO properties for HDPE and PVC

Material	HDPE				PVC			
Resin	335420C		334433C		12454C		12364C	
Design period (1)	Short	Long	Short	Long	Short	Long	Short	Long
Strength, MPa	21	6.2	21	7.7	48	25	41	18
Modulus, MPa	760	152	551	138	2,760	965	3,030	1,090
Compression Strain Limit (2)	2.8%	4.1%	3.8%	5.6%	1.7%	2.6%	1.4%	1.7%
AASHTO Allowable Tensile Strain (3)	5.0%		5.0%		5.0%		3.5%	

Notes:
1. Short = AASHTO initial values, Long = AASHTO 50-year values.
2. Taken as strength divided by modulus.
3. AASHTO Standard Specifications, Section 18.
4. 1 MPa = 145 psi

local buckling. These results are also encouraging, but again are not definitive for the same reasons cited above.

Profile Wall Pipe Behavior in Hoop Compression

Selig et al. (1994) developed a test to evaluate the capacity of profile wall thermoplastic pipe in hoop compression by placing a test pipe in a steel cylinder lined with an inflatable bladder. The annulus between the pipe and the bladder is filled with soil and then the bladder is inflated. Changes in diameter, which for pure circumferential stresses relate directly to strain, are recorded. Moore and Laidlaw (1997) have also applied

this test. These researchers report buckling in corrugated PE pipe at strain levels between 2.2 and 4 percent with the capacity closely related to the width thickness ratios of the corrugated elements. One test by Selig et al. (1994) reported a buckle at the intersection of the crest and web at a strain level of 3 percent. This test has not been used for PVC pipe at the current time.

Observed Behavior in Ground

The research team has inspected many pipes in the ground under high deflection. These pipes sometimes show
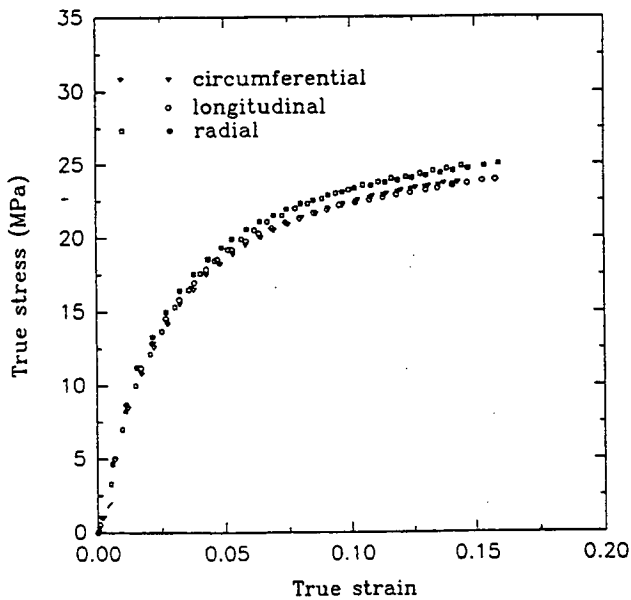
a. General stress-strain curve   b. Effect of variable strain rate
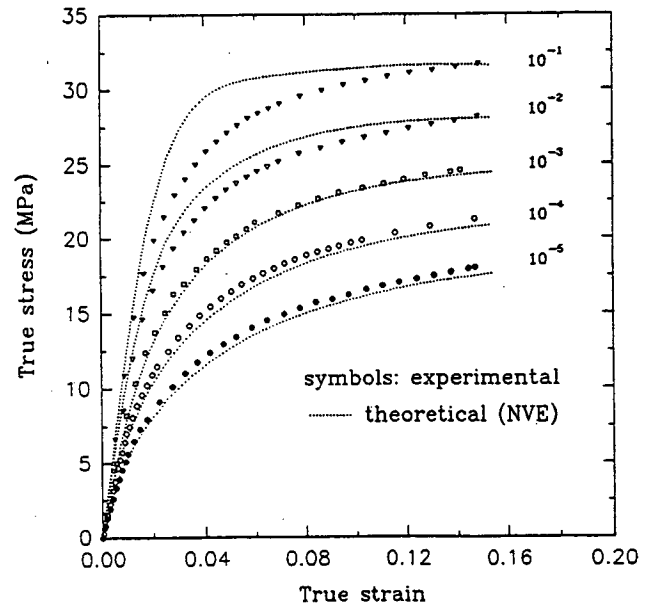
*Figure 2.   Stress-strain curves for PE in compression (*Zhang and Moore, 1997*).*

TABLE 2   Compression strain levels at 20% deflection in parallel plate test

Material	Diameter (mm)	Profile Type	Inside Springline (%)	Outside Crown (2) (%)
PE	460	Corrugated	2.9	8.4
	610	Corrugated	4.0	8.9
	910	Corrugated	2.4	7.1
	910	Corrugated	3.0	8.2
	1220	Corrugated	2.1	5.7
	1220	Honeycomb	2.4	4.2
PVC	610	Corrugated	1.9	4.2

Notes: 1. 1 in. = 25.4 mm
2. Crown and invert are at the same strain level in the parallel plate test
3. Calculations based on linear parallel plate theory

liner buckling but, under modest depths of fill, generally do not show buckling or compressive failure of the corrugation valley, unless deflections are greater than 15 percent. Under deeper fills, compression failures are evident at lower deflections because of the increased hoop compression strain.

Plate Buckling Design Equations

Most research on buckling of thin wall sections has been conducted for metals. This section presents elements of the state of the art related to local buckling.

The onset of buckling in a plate subjected to in-plane compression forces was first addressed by Bryan (1891), who proposed

$$\sigma_{cr} = \frac{k\pi^2 E}{12(1-v^2)(w/t)^2} \tag{1}$$

where

σ_{cr} = critical buckling stress, MPa, psi
k = edge support coefficient
E = modulus of elasticity of plate material, MPa, psi
v = Poisson's ratio of plate material
w = plate width, mm, in.
t = plate thickness, mm, in.

The key elements of Equation 1 are the material modulus of elasticity, the width to thickness ratio (w/t) of the plate, and the edge support conditions. The edge support coefficient varied from 0.43 for a free edge (no support at all on one edge), to 4 for a plate with edges simply supported, to 7 for a plate with both edges fixed against rotation. Equation 1 is presented in *ASCE Manual of Practice No. 63*, "Structural Plastics Design Manual" (ASCE, 1984), although the application discussed in the manual is primarily composites. Table 3, taken from the ASCE Manual, shows that the edge support coefficient for a plate subjected to pure bending can be as high as 24.

In the 1940s, as light-gauge steel members were being developed, Winter (1946) noted that thin plates had substantial post-buckling capacity and suggested that design methods could be developed to take advantage of this capacity. Winter proposed an equation that was eventually adopted into *Specification for the Design of Cold-Formed Steel Structural Members with Commentary* (AISI, 1997) and is called the "effective width approach." The basis of this approach is that the center portion of a plate will be ineffective when it buckles, but the edges of the plate remain effective in resisting increased total load on the member. This is demonstrated in Figure 3.

The Winter effective width approach is carried out in three steps:

1. Compute slenderness factor, λ based on the strain, width thickness ratio, and edge support coefficient:

$$\lambda = \sqrt{\frac{12(1-v^2)}{\pi^2 k}}\left(\frac{w}{t}\right)\sqrt{\frac{\sigma_c}{E}} > 0.673 \tag{2}$$

where

σ_c = compression stress on the element, MPa, psi

2. Compute effective width reduction factor, ρ:

$$\rho = \frac{(1 - 0.22/\lambda)}{\lambda} \tag{3}$$

3. Compute effective width:

$$b = \rho w \tag{4}$$

where

b = effective width of element, mm, in.
w = unsupported width of element, mm, in.

TABLE 3 Edge support coefficients for edge-supported plates (ASCE, 1984)

Case	Loading	Ratio of Bending Stress to Uniform Compression Stress	Minimum Buckling Coefficient,* k					
					Top Edge Free		Bottom Edge Free	
			Unloaded Edges Simply Supported	Unloaded Edges Fixed	Bottom Edge Simply Supported	Bottom Edge Fixed	Top Edge Simply Supported	Top Edge Fixed
1		0.0 (pure compression)	4.0	6.97	0.45**	1.33	0.45**	1.33
	(min. a/b for long plate)		(1.0)	(0.6)	(5.+)**	(1.5)	(5.+)	(1.5)
2		0.50	5.8					
3		1.00	7.8	13.6	0.57	1.61	1.70	5.93
4		2.00	11.0					
5		5.00	15.7					
6		∞ (pure bending)	23.9	39.6	0.85	2.15		
	(min. a/b for long plate)		(0.6)					

* Values given are based on plates having loaded edges simply supported and are conservative for plates having loaded edges fixed.

** A more accurate value of k for plates with one longitudinal support free and the other simply supported with a/b 0.7 is (6.11):

$k = 0.45 + (b/a)^2.$
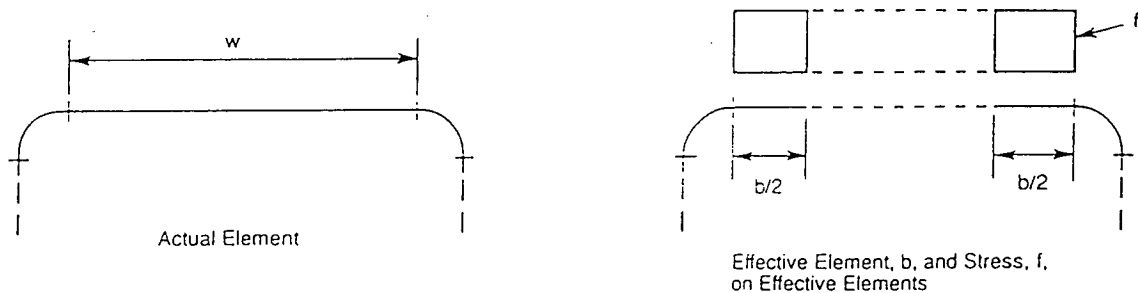
Figure 3. Effective width concept from AISI standard for cold-formed sections.

The area of the cross section used in design is the reduced width, b, rather than the actual width, w.

Given that the Winter equation uses the ratio of stress to modulus, the calculation can be completed in terms of strain or stress. This is a common simplifying assumption for thermoplastics.

The Bryan and Winter equations are compared in Figure 4 for the two PE resins and the two PVC resin types listed in Table 1 and using the limiting compressive strain listed in the table for long-term properties. The figure indicates the difference between the onset of buckling (the Bryan curve) and the ultimate post-buckling capacity (the Winter curves). Materials with higher strain capacity have more post-buckling capacity than lower strain limit materials.

The AISI specifications, which have rules for considering different design conditions, have recently been modified to include the work of Pekoz (1987). Schafer (1997) has studied the design of longitudinal stiffeners.
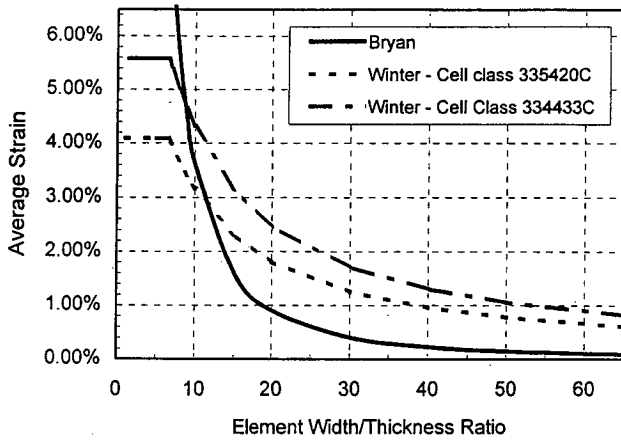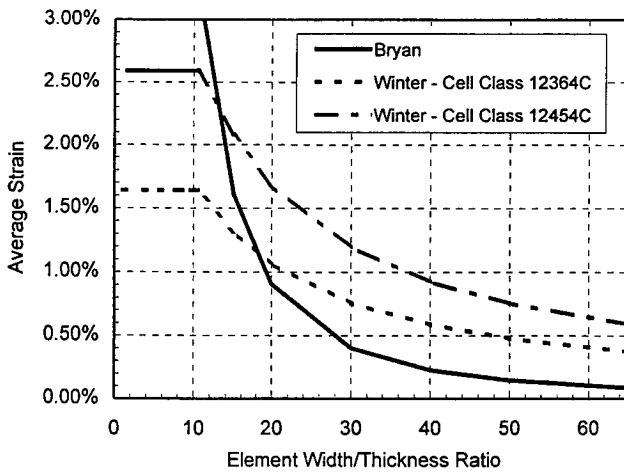
Figure 4. Comparison of Bryan and Winter equations for thermoplastic pipe.

Allowable Deflection

Given that the compressive strain that can be developed in a pipe is a function of both the hoop compression load and bending, a design method for local buckling must also consider the effects of deflection, which can be correlated with bending strain. The most established method for doing this is presented in AWWA Manual of Practice M45 *Fiberglass Pipe Design*. This method is based on a parameter called the shape factor which is expressed as

$$\epsilon_b = D_f \left(\frac{c}{R}\right)\left(\frac{\Delta}{D}\right) \tag{5}$$

where

ϵ_b = bending strain
D_f = shape factor
c = distance from centroid to location of strain calculation, mm, in.
R = radius to centroid of pipe wall, mm, in.
Δ = change in vertical diameter (deflection), mm, in.
D = diameter to centroid of pipe wall, mm, in.

Equation 5 can be derived for known loading conditions and it can be shown that D_f is 4.28 for bending strain at the invert in the parallel plate test. For a pipe deflected into a perfect ellipse, D_f is 3.0, the lowest value it can take. Research (Turkopp et al., 1985) shows that at design deflection levels, D_f can vary from 3.5 for relatively stiff pipe in backfill that does not require substantial compactive effort to 8 for low stiffness ($F/\Delta y = 62$ kPa, 9 psi) in soil that requires substantial compaction. The table of D_f values from Manual M45 is presented as Table 4.

Typically the parallel plate test is considered a severe load condition, and it is surprising that design values of D_f are higher for this test; however, flexible pipes are subjected to local deformations during compaction of backfill resulting in the high shape factors.

Manual M45 uses the shape factor equation to back calculate allowable deflection based on the strain limits, and the same could be done for thermoplastic pipe.

COMPRESSION TESTS

Evaluation of local buckling capacity requires testing sections in compression. Testing was conducted both to evaluate the compression capacity of pipe currently on the market and to investigate testing procedures that might be used in a quality control program. This section presents procedures used to test profile wall thermoplastic pipe sections in compression. Goals of the effort were to develop a simple test that may be conducted relatively quickly to verify that a given section meets requirements being developed to control local buckling. The work is summarized here and presented in detail in Appendix B.

TABLE 4   Shape factors, D_f (AWWA Manual M45)

Pipe Stiffness		Pipe-Zone Embedment Material and Compaction			
		Gravel[*]		Sand[†]	
		Dumped to Slight[‡]	Moderate to High[§]	Dumped to Slight[‡]	Moderate to High[§]
psi	kPa	Shape Factor D_f (dimensionless)			
9	62	5.5	7.0	6.0	8.0
18	124	4.5	5.5	5.0	6.5
36	248	3.8	4.5	4.0	5.5
72	496	3.3	3.8	3.5	4.5

[*] GW, GP, GW–GC, GW–GM, GP–GC, and GP–GM per ASTM D2487 (includes crushed rock).
[†] SW, SP, SM, SC, GM, and GC or mixtures per ASTM D2487.
[‡] < 85% Proctor density (ASTM D698), <40% relative density (ASTM D4253 and D4254).
[§] ≥ 85% Proctor density (ASTM D698), ≥40% relative density (ASTM D4253 and D4254).

Test Specimens

All test specimens included three corrugation or periods (Figure 5) of the test pipe. The arc length of the specimen was varied. Specimens were cut from pipe samples and the ends were cut plane and then further smoothed with a belt sander. Sample ends were not milled to achieve truly parallel ends. This is an option for future testing.

Corrugation cross sections were measured with calipers at specimen ends. Average corrugation dimensions were used to compute section properties using an idealized corrugation cross section as shown in Figure 1. The idealization for the honeycomb, or "D" profile, is shown in Figure 6. Pipe sections from different manufacturers were identified by letter. Width thickness ratios of the various pipe sections tested are summarized in Table 5. The table shows wide variations in the profile geometries for corrugate PE pipe and that the PVC section considered in the test program has elements with substantially lower width thickness ratios (i.e., thicker elements).

Test Apparatus and Procedures

Tests were conducted on a universal tension/compression machine with a maximum capacity of 100 kN (22,500 lbs). End load plates could be free to rotate or fixed. A dial gauge was placed at midheight on the exterior surface of the center corrugation to measure the lateral deflection of the specimen.

Specimens were typically compressed between the end plates at a rate of 1.3 mm (0.05 in.) per minute until an ultimate load condition was reached. Load and vertical end dis-
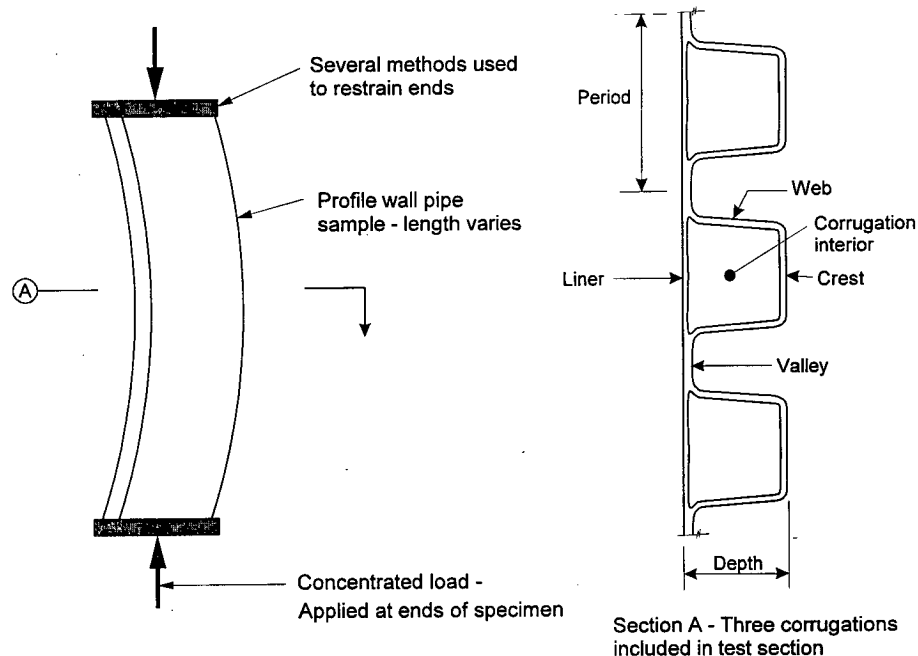
Figure 5.   Typical configuration for compression tests.
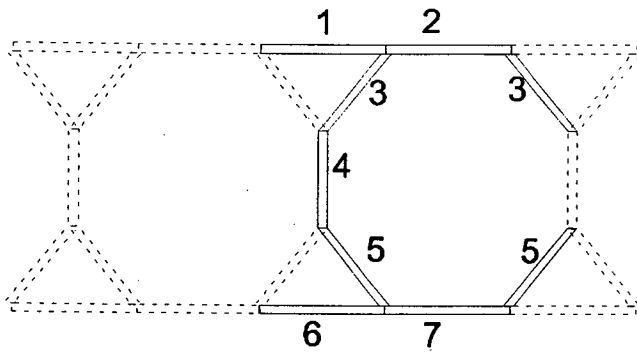
Figure 6. Idealization of honeycomb profile.

placement were continuously recorded on a paper chart. Lateral displacement was recorded regularly from the dial gauge reading. A few tests were conducted at load rates of 13 mm (0.5 in.) per minute and 0.13 mm (0.005 in.) per minute.

Experiments were conducted on a series of end conditions to investigate the condition that could minimize end effects where the section bears against the load plate. These included

- Neoprene bearing pads;
- Plaster encasement;
- Plywood bracing of crest; and
- No special provisions (i.e., direct bearing on end plate).

Most of the means of end support were time consuming or ineffective. The condition of no special provisions proved most reliable.

Most tests were conducted with the samples and instrumentation as noted above; details of all tests are provided in Appendix B. Forty-three tests were conducted.

The arc length of the test specimens varied from 7 to 90 deg. The longer arc length specimens deflected substantially, and the ends also rotated substantially. It was difficult to develop test fixtures with sufficient rotation capacity. In addition, the longer specimens were stressed primarily in bending, with compression on the inside surface. The specimens with the shortest arc lengths were in compression across the entire section.

The test was continued until the load carried by the specimen began to drop. Test times varied from roughly 1 min for the fast tests to roughly 30 min for the slow tests. The test time was affected by the length of the specimen and the modulus of elasticity of the material, as well as the load rate. Buckling was observed in many sections before reaching an ultimate (peak) load condition.

Table 6 summarizes the test parameters and load and strain levels achieved in the tests that were conducted with several lengths of specimens and end conditions. These tests are representative of the overall test results. The strains were computed using statics, considering the moment as a result of the offset at the midheight of the specimen. Because buckling

TABLE 5 Width/thickness ratios for all tested specimens

Diameter mm (in.) / Material	Testing Designation	Width / Thickness ratio, w/t			
		Crest	Web	Liner	Valley
Corrugated PE Profiles (Fig. 1)					
300 (12) / PE	A12	40.1	8.3	30.1	1.0
450 (18) / PE	B18	23.1	13.4	28.4	5.2
450 (18) / PE	B18	21.3	10.7	24.5	5.4
600 (24) / PE	A24	27.1	18.9	24.2	2.2
900 (36) / PE	B36	20.0	11.1	21.3	6.3
900 (36) / PE	B36	30.1	13.5	27.0	3.6
900 (36) / PE	E36	16.9	10.9	22.0	5.8
1200 (48) / PE	B48	25.5	13.0	29.7	6.5
	Maximum	40.1	18.9	30.1	6.5
	Minimum	16.9	8.3	21.3	1.0
	Average	25.5	12.5	25.9	4.5
Honeycomb PE Profile (Fig. 6)					
1200 (48) / PE	D48	9.6*	8.0*	7.5*	NA
Corrugated PVC Profile (Fig. 1)					
600 (24) / PVC	C24	8.1	5.3	9.4	1.7

* w/t ratios are for Elements 6, 4, and 7, respectively

TABLE 6 Summary of test results for selected sections

Material	Test No.	Diameter mm	Profile Type	Wall Area mm²/mm	Wall Moment of Inertia mm⁴/mm	Arc Length deg.	End Condition	Peak Load kN	Max. Strain % In.	Max. Strain % Out.
PE	A24F-1	600	Corrug.	7.8	5,020	15	P-F	19.0	3.9	3.9
	A24I-1	600	Corrug.	7.8	5,020	15	P-F	15.9	4.0	4.0
	B36E-1	900	Corrug.	9.94	6,075	35	P-F	39.2	5.3	NA
	B48A-1	1,200	Corrug.	10.5	8,470	45	F-F	29.2	2.4	3.2
	B48C-1	1,200	Corrug.	10.5	8,470	25	F-F	44.8	2.6	2.9
	E36D-1	900	Corrug.	14.2	12,310	15	P-F	62.0	2.4	2.7
	D48D-2	1,200	Honeycomb	10.7	7,830	15	P-F	31.6	2.4	2.7
PVC	C24C-1	600	Corrug.	9.3	975	7	P-F	59.1	1.7	1.8
	C24D-1	600	Corrug.	9.3	975	7	P-F	49.6	1.5	1.6
	C24E-1	600	Corrug.	9.3	975	7	P-F	58.4	1.7	1.8

Notes 1. 1 in. = 25.4 mm, 1 lb = 0.00445 kN
2. Inside compressive strain is maximum at the mid-height of the specimen, outside compressive strain is maximum at the specimen end.
3. F-P = fixed pinned end condition, F-F= fixed-fixed end condition.

was evident during the tests, the section could not be considered fully effective at the peak load, therefore, the Winter equations were used to estimate the peak strain in the following manner:

1. Based on statics, and the gross section properties, compute the strain in each of the profile elements:

$$\epsilon_t = \frac{1}{E}\left(\frac{P}{A} + \frac{Mc}{I}\right) \quad (6)$$

where

ϵ_t = strain
E = modulus of elasticity of pipe material, kPa, psi
P = maximum applied axial load in test, kN, lb
A = area of pipe wall of test specimen, mm², in.²
M = moment computed from statics, kN-m, in.-lb
c = distance from centroid of wall section to location at which strain is being computed, mm, in.
I = moment of inertia of pipe wall of test specimen, mm⁴, in.⁴

2. For each of the elements, use Equations 2, 3, and 4 to compute the effective area.
3. Compute new section properties based on the reduced section.
4. Repeat Steps 1, 2, and 3 with the new properties until the predicted strain does not change.

In the above calculations, the variation in the modulus of elasticity was considered time dependent and was computed from the following simplified equations:

$$E_{PE} = 664t^{-0.0859} \quad (7)$$

$$E_{PVC} = 2800t^{-0.067} \quad (8)$$

where

E_{PE} = modulus of elasticity of PE, MPa
E_{PVC} = modulus of elasticity of PVC, MPa
t = time, minutes

Equation 7 is taken from Hashash and Selig (1990) and is based on parallel plate testing of corrugated pipe. Equation 8 was developed for this project based on AASHTO properties for PVC.

COMPRESSION TESTS WITH STRAIN-GAUGED SPECIMENS

A second set of tests was conducted to further investigate the pipe behavior in the stub compression tests under different end conditions and to verify that linear elastic theory for curved beams could be used to evaluate test results. A corrugated PVC and corrugated HDPE specimen were instrumented with strain gauges and tested with three end conditions: fixed-fixed, fixed-free, and free-free. As in the basic test, each specimen included three full corrugations. Both specimens had a 35-deg arc length. Eight strain gauges were bonded to each specimen: four gauges at the specimen mid-height and four at the quarter point, as illustrated in Figure 7. At each location, one gauge each was bonded to the crest and liner of the middle corrugation, and one gauge was bonded to each of the valleys on either side of the middle corrugation.

The specimens were tested to a maximum strain level of about 1 percent. The strain conditioner contained only four inputs, thus each test was repeated two or three times to col-
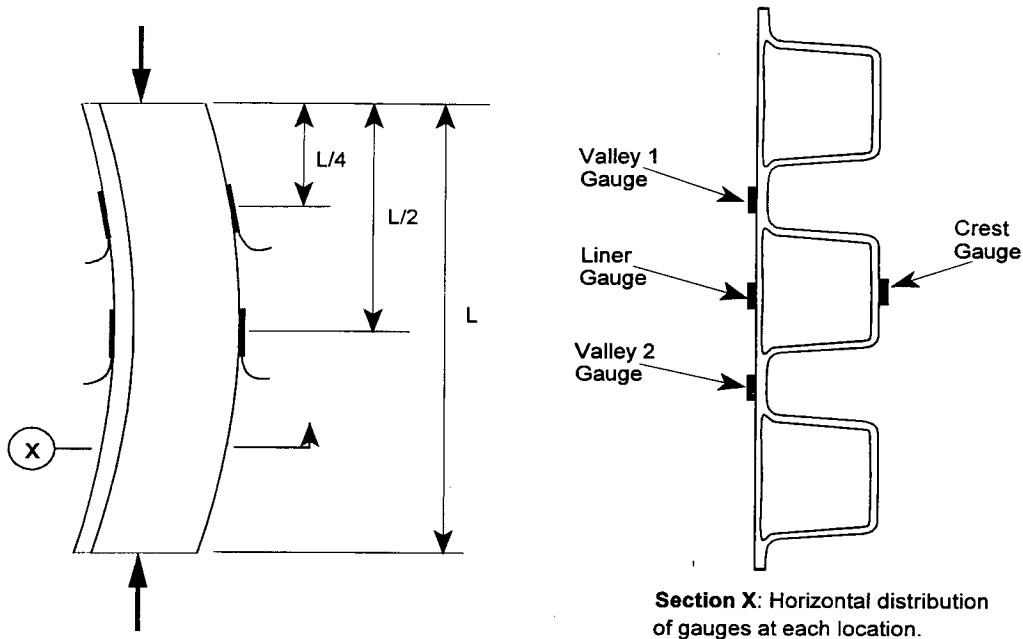
Figure 7. Strain gauge locations on corrugation profile.

lect the midheight and quarter-point data (three times for the fixed-free condition and two times for the fixed-fixed and free-free conditions). Specimens were allowed to recover for 15 to 30 min after each test before the next test began.

Results

Measured strain levels from the tests with the fixed-pinned end condition are compared with calculated strain levels in Table 7. Results from all the tests are presented in Appendix B. Test results were evaluated using linear elas-

tic curved beam theory. Axial loads and moments were calculated and superimposed to determine the total stresses along the length of the specimen. Strains were estimated by dividing the total stresses by the AASHTO short-term modulus of elasticity values of 440,000 psi for PVC and 110,000 psi for PE.

The following trends were noted:

- PVC strains were much closer to prediction than PE. Strains measured in the valley of the PVC pipe were generally within 10 percent of predicted values.

TABLE 7   Comparison of test and theoretical strains, fixed-pinned end conditions

a. PVC

Calculated Strain (%)		Measured Strain (%)		
Valley/Liner	Crest	Valley	Liner	Crest
0.38	0.39	0.45	0.35	0.18
0.70	-0.01	0.78	0.66	-0.13
0.70	-0.01	0.61	0.50	-0.06

b. PE

Calculated Strain (%)		Measured Strain (%)		
Valley/Liner	Crest	Valley	Liner	Crest
0.75	0.76	0.58	--	0.28
0.99	0.40	0.60	0.24	0.19
0.99	0.40	0.57	--	0.30

Note: Positive strain values indicate compression

- In the PE specimen, the measured strains achieved in the liner/valleys were generally less than predicted.
- Slight crippling of the crest and web were observed at the fixed ends of the PE at approximately 75 percent of total test load.
- In the PVC specimen, the liner strains were about 80 percent of those measured in the valley; for the PE specimen, the measured liner strains were 40 percent of the valley strain.

The test program indicates a general agreement between the calculated and measured strain values for the PE and PVC specimens. The agreement is much better for the PVC. The differences likely result from several conditions, including uncertainty in the value of the modulus of elasticity and effects because of the higher width-to-thickness ratios of the elements. Strain gauging of PE is known to be difficult. The modulus of elasticity of PE is so low that the gauge can have a reinforcing effect and modify the strain field.

CHAPTER 3

INTERPRETATION, APPRAISAL, AND APPLICATION

EVALUATION OF TEST RESULTS

The compression test results can be compared with the Winter (Equations 2 and 3) and Bryan (Equation 1) buckling equations by plotting the average strain in an element at the peak load versus the w/t ratio for the element. The average strain is computed by multiplying the peak strain (Table 5) by the effective width reduction factor, ρ, and plotting versus the w/t ratio (Table 6). The results of these calculations are presented in Table 8 and shown graphically in Figure 8 for the PVC and PE data. The PE data are compared with the curve for Cell Class 335420C and the PVC data are compared with the curve for Cell Class 12364C.

Considering the uncertainties of the test, such as end effects and end restraint, and the uncertainty of the material properties, the match between the data and the Winter curves is quite good. In the case of PVC, the w/t ratios were low and all of the ultimate strain values were governed by the limiting strain. For the PE, the w/t ratios varied widely and many of the elements failed at strains well below the limiting values. The figures suggest that elements with width-thickness ratios greater than about 10 for PE and 15 for PVC have substantial capacity after the onset of buckling.

STRAIN LIMITS

A key design parameter is the establishment of the limiting strain value for profile elements that do not buckle (i.e., elements with high w/t ratios). This parameter establishes the maximum strain that the reduced width of any profile element can carry. For an elastic material, such as steel, the limiting value would be the yield strength (i.e., the point on the stress-strain curve where the slope is zero). The yield strains for PE and PVC are quite high (See for example, Figure 2 for PE), and the test data presented in Chapter 2 clearly demonstrate that the sections buckle before reaching this strain. This section discusses appropriate strain limits for elements subject to pure bending and to bending plus compression.

Strain Limit for Pure Compression

Although the basis for design values for strength and stiffness provided in AASHTO are not clear, and the applicabil-

ity of these values to compressive strength even less so, Figure 8 suggests that for the two types of resin tested, one PE and one PVC, the AASHTO values are appropriate. The ratio of the AASHTO long-term strength to modulus is recommended as the strain limit for pipe under pure hoop compression. It would be appropriate to study the behavior of PE and PVC in compression and establish a standard by which compression strength should be established. The work of Zhang and Moore (1997) may provide a basis for such work.

Strain Limit for Combined Compression and Bending

Information presented in Chapter 2 indicates that the performance of corrugated, profile wall pipe in compression is different if the section is under uniform compression or bending. This appears to be the case even for the crest, valley, and liner, even though these elements are under a relatively uniform stress field whether the force is bending or thrust. The difference in behavior is likely the response of the web to bending. Table 3 shows that the edge support coefficient, k, for a plate under uniform thrust varies between 4 and 7, while the coefficient for a plate under bending is 24. This is because the center of the plate is subjected to low stresses in bending. In a corrugated pipe subject to bending alone, such as in a parallel plate test, the web does not buckle, and this likely increases the overall compression capacity of the profile. In the hoop compression tests conducted by Selig et al. (1994) and Moore and Laidlaw (1997), the entire corrugation is under uniform compression and the capacity appears to drop to 3 to 4 percent strain, while in the parallel plate test, the pipe carried up to 9 percent strain for HDPE and 4 percent for the one PVC pipe profile studied (see Table 2). This has not been studied in detail at this time, yet it appears conservative to select a strain level for combined bending and thrust that is 50 percent larger than the hoop compression limit.

Proposed Design Limits for Thermoplastic Pipe In Compression

Based on the discussion in the previous two sections, Table 9 provides proposed compression strain limits for use in design of thermoplastic drain pipe. These values represent

TABLE 8 Summary of test results for selected sections

Material	Test No.	Diam. (mm)	Profile Type	Peak Strain (%)					-
				Liner		Valley		Crest	
				w/t	Strain	w/t	Strain	w/t	Strain
PE	A24F-1	600	Corrug.	24.2	1.5	2.2	3.9	34.8	0.9
	A24I-1	600	Corrug.	24.2	1.6	2.2	4.0	34.8	0.8
	B36E-1	900	Corrug.	27.0	1.5	3.6	5.3	30.2	T
	B48A-1	1,200	Corrug.	29.7	0.9	6.5	2.4	22.3	T
	B48C-1	1,200	Corrug.	29.7	1.2	6.5	3.6	22.3	T
	E36D-1	900	Corrug.	22.0	1.2	5.9	2.4	16.9	2.1
	D48D-2	1,200	Honeycomb	9.57	3.5				
PVC	C24C-1	600	Corrug.	9.4	1.7	1.7	1.7	8.1	1.6
	C24D-1	600	Corrug.	9.4	1.5	1.7	1.5	8.1	1.4
	C24E-1	600	Corrug.	9.4	1.8	1.7	1.8	8.1	1.6

Note: T = element in tension

ultimate strain values and should be reduced by a factor of safety to determine service strain levels.

HOOP COMPRESSION CAPACITY DETERMINED BY TEST

The testing suggests that the overall hoop compression capacity of profile wall thermoplastic pipe sections can be determined by a relatively simple stub compression test. Key parameters for consideration in testing are the length of the specimen and the end conditions.

Long specimens (large included arc length, L in Figure 7) undergo large rotations when subject to compression loads, and test fixtures can become somewhat complicated to accommodate this rotation. In addition, bending effects will dominate the section response in specimens with long lengths, and only the inside wall of the pipe (liner and valley for the corrugated profile) will be tested. Both of these facts suggest that sections should be relatively short. The minimum length of a specimen is governed by the w/t ratios of the elements. The specimen should allow a full buckling wavelength to develop. The testing in Section 2 and analysis above suggests that 7 deg was an acceptable length for the PVC pipe and 15 deg was acceptable for the PE pipe. The ratio of the length to the depth of the PVC pipe was 1.3 and of the PE pipes varied from 1.4 to 2.2. This leads to the conclusion that the specimen should be at least 1.5 times the depth of the cross section.

In tests with the end plates fixed against rotation (fixed ends), the pipe specimens develop positive bending (compression on the outside) at the crest, which led to localized crimping of the specimen near the end support. This would argue for pinned-end conditions in the test, but the test can be difficult to set up and run with rotating ends. A test condition with one end fixed and one pinned is suggested.

Although the testing was successful in demonstrating the capacity of the thermoplastic pipe sections, it is believed to be premature at the current time to propose it as a formal test for adoption by AASHTO. Additional testing should be conducted on other types of profile walls, with the participation of several other laboratories to establish the consistency of the test.

One possible shortcoming of establishing a test method to verify capacity of pipe in hoop compression is that tests often are set up on a pass-fail basis. That is, all pipe must pass a test to be used for a certain application. This may not be the best approach for thermoplastic pipe, given that many profiles are on the market, and all may have certain applications for which they would be suitable, yet would have very different capacities in the stub compression test. There are two alternatives available to address this. One is a test that establishes the strength of the pipe based on the test result (i.e., pipes that have greater capacity in the test can be buried deeper). The second alternative is to evaluate pipe capacity by design equations, as is proposed in the next section. In this method, a section can be evaluated and the end use parameters, such as allowable depth of fill, will be established based on the properties of the individual section being evaluated.

The benefit of a test method over a design method is that users do not need to get involved in measuring and calculating section capacity for each pipe section as a method of quality control. This may be desirable in the long term.
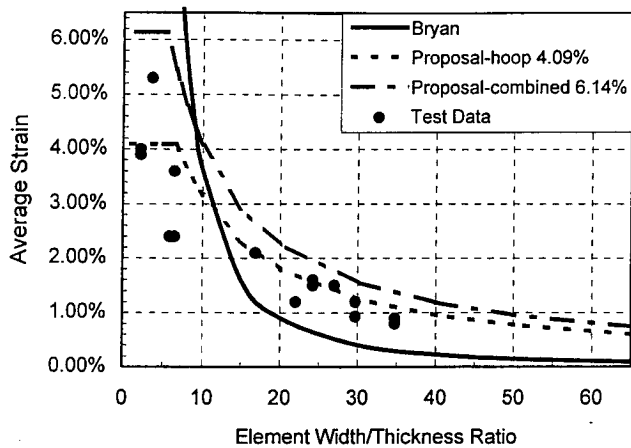
a. PE Pipe
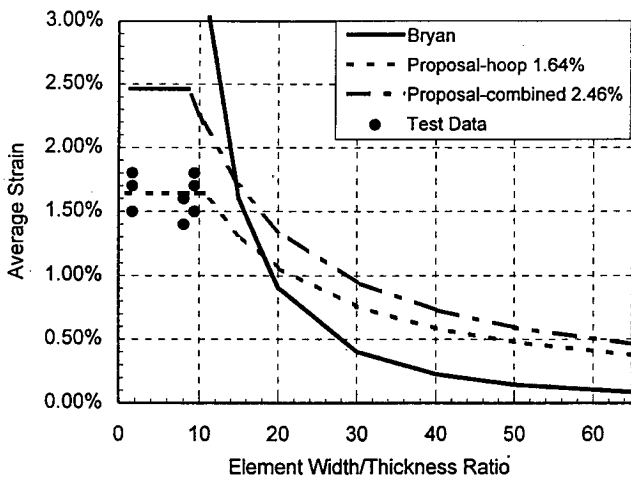
b. PVC Pipe

Figure 8.   Comparison of Bryan and Winter plate-buckling equations with data.

HOOP COMPRESSION CAPACITY DETERMINED BY DESIGN

The test results suggest that the Winter equations are appropriate for use in design of thermoplastic pipe sections for hoop compression capacity. A design method using this approach would proceed as follows:

1. Establish material properties and profile wall section properties; idealize section as a series of flat plate elements (See Figures 1 and 6).
2. Establish project design parameters, such as depth of cover over pipe, type and density of backfill, and ground water level.
3. Evaluate section capacity based on gross area. If inadequate, then select a pipe with a higher cross-sectional area or improve the type or density of the backfill to

TABLE 9   Proposed strain limits for thermoplastic pipe

Material	Hoop strain limit	Combined strain limit
PE Cell Class 335420C	4.1%	6.2%
PE Cell Class 334433C	5.6%	8.4%
PVC Cell Class 12454	2.6%	3.9%
PVC Cell Class 12364	1.6%	2.4%

reduce the load on the pipe (See below for discussion of possible changes to current AASHTO load calculation method).

4. If the gross area of the section is adequate, then check each of the elements of the profile for the effective width and compute a reduced effective area. Evaluate the section capacity based on the reduced section area. If inadequate, take the same actions as recommended in Step 3.
5. If the section is adequate based on the reduced area, compute the allowable deflection based on the remaining capacity of the section and the combined strain limit. If the allowable deflection is considered too small to be practical, then select an alternate pipe section or redesign the installation to reduce the load and/or deflections.

The calculations for Step 4 include an evaluation of each element of the profile using the following steps:

4.1 Compute slenderness factor, λ based on the strain, w/t ratio, and edge support coefficient:

$$\lambda = \frac{w}{t} \sqrt{\frac{\varepsilon}{k}} > 0.673 \qquad (9)$$

4.2 Compute effective width reduction factor, ρ:

$$\rho = \frac{(1 - 0.22/\lambda)}{\lambda} \qquad (10)$$

4.3 Compute effective width:

$$b = \rho w \qquad (11)$$

Equation 9 is a simplification of Equation 2, making the assumption that Poisson's ratio is equal to 0.42. This is a reasonable value for the thermoplastics in the long term and has an effect of less than 10 percent on the computed value of λ. Other items to consider in applying the equations include

- A value of the edge support coefficient, k, should be taken as 4.0 for all elements that intersect other elements at an angle of 90 deg. The intersection of the web and crest is

considered such an intersection. For free-standing elements, k should be taken as 0.43.

- For elements with stiffeners, such as shown in Figure 9, the thickness of the element may be taken as the thickness which provides the correct total area of the element. No other effect of the stiffener should be considered.
- In establishing the idealized cross section (Figures 1 and 6), radii should be ignored and the idealized section should be carried to a sharp corner, just as in Figure 1.

The proposed procedure is demonstrated in the design examples in Appendix D. A summary of results of these calculations for pipes subjected to several levels of hoop compression strain is presented in Table 10 for some of the pipes that were considered in the testing program. The calculations were completed using the load theory discussed in the next section.

Table 10 shows very different results for the various sections that were included in the testing. The PVC, C24, has the largest allowable depth of fill. It has the greatest compressive strength (17.9 MPa [2,600 psi] versus 6.2 MPa [900 psi] for HDPE). The PVC also has the largest ratio of area to diameter. PVC does have the lowest strain limit of the materials investigated and this causes a reduced allowable deflection. Of the HDPE sections, the honeycomb pipe, D48, has the highest allowable fill, mostly because it is made up of a series of elements with low w/t ratios. The E36 pipe has the next highest allowable depth of fill because it has the largest area to diameter ratio of the HDPE pipe. The HDPE pipe with the lowest allowable depth of fill actually has a relatively large ratio of area to diameter; however, this pipe has elements with very high w/t ratios.
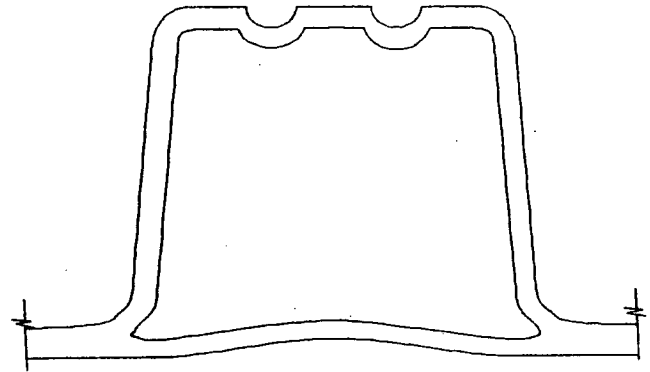
Figure 9. Corrugation with stiffeners.

The relative safety of the design method is demonstrated in Figure 10 which compares factored stress and deflection with stress and deflections calculated with all load and resistance factors set to 1.0. The calculations were conducted for a 900-mm (36-in.)-diameter, corrugated PE pipe buried in soil with a density of 18.8 kN/m³ (120 pcf) with the groundwater table below the pipe. The figure indicates that the intended factors of safety of 1.95 on hoop thrust and 1.5 on bending are preserved.

Load Theory

Under the proposed design method, the depth of burial under which a pipe can be buried and still meet the specified design criteria is a function of the effective area of the section. The effective area is calculated based on the width-to-thickness ratios of the elements of the profile wall. Obviously,

TABLE 10 Results of calculations with proposed design method

Pipe Designation/Type	Diameter (mm)	Area (mm²/mm)	Area/Diam. Ratio	Soil Type - Sn-100 M_s = 33 MPa		Soil Type - Si-90 M_s = 14 MPa	
				Allowable Depth of Fill (m)	Allowable Deflection (Bending only) (%)	Allowable Depth of Fill (m)	Allowable Deflection (Bending only) (%)
A24 - HDPE Corrugated	24	7.8	0.33	6.0	3.8	3.6	3.8
C24 - PVC Corrugated	24	9.3	0.39	16.6	2.8	14.3	2.8
E36 - HDPE Corrugated	36	14.2	0.39	10.2	3.9	6.4	3.9
B48 - HDPE Corrugated	48	10.6	0.22	6.5	5.3	3.8	5.3
D48 - HDPE Honeycomb	48	10.9	0.23	11.1	4.9	6.3	4.9

Notes:
1. Sn-100 is an SW material compacted to 100% of maximum standard Proctor density, or crushed stone. Si-90 is an ML material compacted to 90% of maximum standard Proctor density.
2. Allowable deflection is computed on the basis of a D_f = 6.0; higher and lower values are possible.
3. All computations completed assuming maximum hoop compression thrust allowed by AASHTO, 6.2 MPa (900 psi) for HDPE and 17.9 MPa (2,600 psi) for PVC.
4. 1 ft = 0.305 m, 1 in. = 25.4 mm
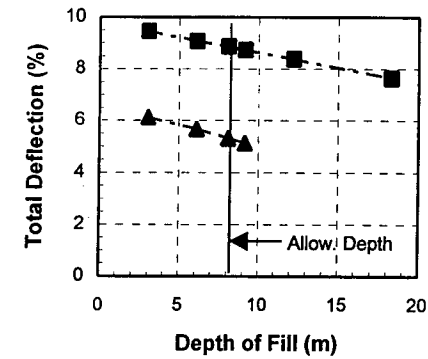
a. Sn95 Backfill **b. Cl95 Backfill**
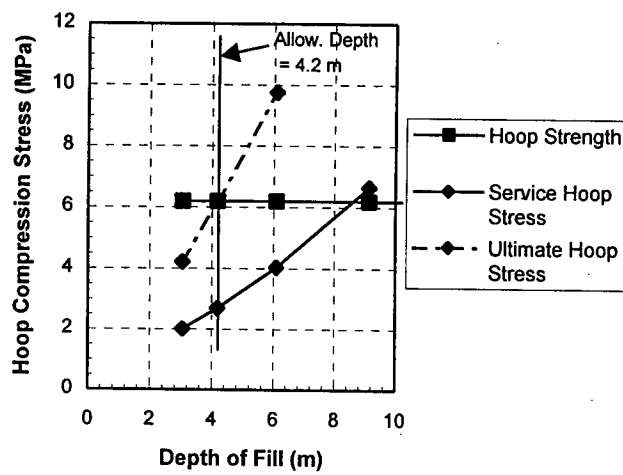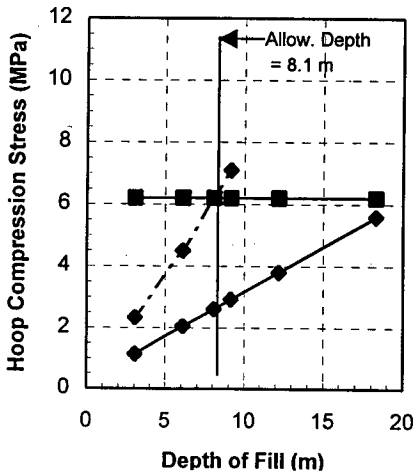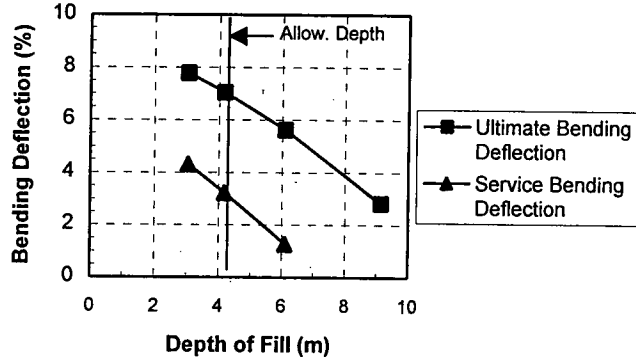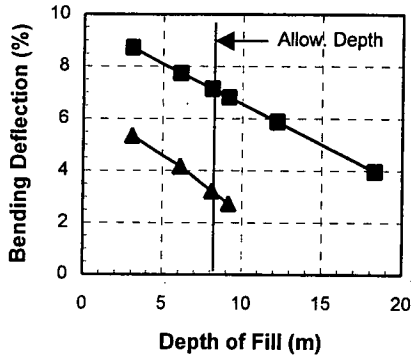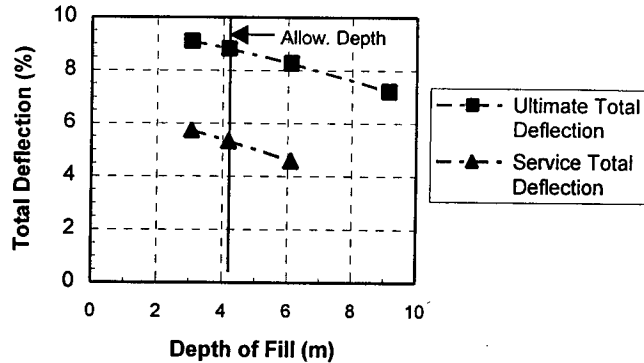
Figure 10. Design parameters vs. depth of fill, 900-mm (36-in.)-diameter corrugated PE pipe.

the load that is transmitted from the soil to the pipe is also a factor. Research by Hashash and Selig (1990), and McGrath (1998, 1999) has shown that some thermoplastic pipe carry loads far less than the weight of the soil directly over the pipe (the soil prism load) that is assumed in the current AASHTO code. The AASHTO Flexible Culvert Liaison Committee has been developing this theory for proposal to the AASHTO Bridge Committee for incorporation into design standards. Current AASHTO standards for loads on some thermoplastic pipe are so conservative that the revised load theory should be considered at the same time as the proposals developed from this project.

CHAPTER 4

CONCLUSIONS AND RECOMMENDATIONS

A review of past work on the design of thermoplastic culvert pipe revealed little work in the way of design methods. Although some testing work has been completed, no design method had been documented in the literature. The bulk of the research on buckling of thin sections has been completed by the light-gauge steel industry. The most commonly cited works are those of Bryan and Winter. The principal parameters in these equations are the width-to-thickness ratio and the stress level in the plate.

A preliminary stub compression test has been developed to evaluate local buckling and general capacity in compression. The test is relatively simple to execute; however, questions remain about end effects that should be investigated further before establishing the test as standard. The results of the test correlate well with the buckling equations proposed by Winter for thin metal sections. This method takes advantage of the post-buckling capacity of the sections.

Design equations have been developed for implementation within AASHTO. These equations are relatively simple to apply. The design criteria set for the time being is based on current AASHTO strength and stiffness properties for 50 years. The design equations evaluate the capacity of thin sections in compression and in combined bending and compression. The check on combined bending and compression produces a limiting deflection for the field. The deflection limit decreases with increasing depth of fill as the combined bending and hoop stresses increase. For pipe under 20 or more feet of fill, this deflection limit is well under 7.5 percent for some pipe. The effect of the design method varies, with the individual profiles produced by different manufacturers. Some profiles are quite thin and have relatively low allowable fill heights. Allowable fill heights depend on the method of load computation. This report assumes that parallel work on this subject will also be adopted by AASHTO. If this is the case, then fill heights for HDPE sections evaluated in this report will vary from roughly 6 to 9 m (20 to 30 ft) in dense granular material compacted to 100 percent of maximum

standard Proctor density and from 3.6 to 6.4 m (12 to 21 ft) in silty soil compacted to 90 percent of maximum standard Proctor density. For the PVC pipe, the allowable depth of fill is 17 m (55 ft) in the dense granular material and 14 m (45 ft) in the silty soil.

The subject of local buckling deserves more research. The proposed test should be investigated further and developed into a standard. This should improve the ability of users to conduct quick evaluations of new products. The combined tools of a design method and a test will provide powerful tools for manufacturers and designers. Users can quickly evaluate profile sections for product approval, and new profile shapes can be evaluated without developing expensive prototype sections. The test should be developed as a means of evaluating capacity, rather than as a pass-fail test. This will ensure that all products are treated on the basis of their individual qualities. Additional testing should also investigate loading over longer terms than those used in the current testing program.

Strain limits in compression should be investigated. Strains computed from the current 50-year strength and stiffness values in AASHTO appear to be suitable; however, insufficient data were collected to provide assurance on this subject. Criteria for evaluating this parameter should be established, because the resins used for thermoplastic culvert pipe are subject to change.

The recommendations in this report for evaluating hoop compression strength and local buckling should be implemented simultaneously with parallel research on methods for computing loads and for improving HDPE resins. The current criteria in AASHTO for loads are known to be overly conservative for some types of pipe, and implementation of the proposed local buckling criteria would be an additional and unnecessary conservatism. The need for improved HDPE resins is also important. The application of a design model that uses post-buckling capacity demands resins that are not sensitive to cracking.

REFERENCES

AASHTO (1994) "AASHTO LRFD Bridge Design Specifications, First Edition," American Association of State Highway and Transportation Officials, Washington, DC.

AASHTO (1996) "Standard Specifications for Highway Bridges, Sixteenth Edition—1996," American Association of State Highway and Transportation Officials, Washington, DC.

AISI (1997) *Specification for the Design of Cold-Formed Steel Structural Members with Commentary*, American Iron and Steel Institute, Washington, DC.

Aluminum Design Manual, Sixth Edition (1994) The Aluminum Association, Inc., Washington, DC.

ASCE (1984) "Structural Plastics Design Manual—ASCE Manual of Practice No. 63," American Society of Civil Engineers, New York, NY.

AWWA (1996) "Fiberglass Pipe Design," AWWA Manual of Practice M45, First Edition, American Water Works Association, Denver, CO.

Bryan, G. H. (1891) "On the Stability of a Plane Plate Under Thrusts in Its Own Plane, with Applications to the 'Buckling' of the Sides of a Ship," Proceedings of the London Mathematical Society., Vol. 22, London.

Clark, J. W., and Rolf, R. L. (1964) "Design of Aluminum Tubular Members," Journal of the Structural Division, Proceedings ASCE, Vol. 90, No. ST6, December.

Cohen, J. M. (1987) "Local Buckling Behavior of Plate Elements," Department of Structural Engineering Report, Cornell University, Ithaca, NY.

Dhalla, A. K., Errera, S. J., and Winter, G. (1971) "Connections in Thin Low-Ductility Steels," *Journal of the Structural Division*, ASCE, Vol. 97, No. ST10, Proc. Paper 8442, Oct.

Dhalla, A. K., and Winter, G. (1974) "Steel Ductility Measurements," *Journal of the Structural Division*, ASCE, Vol. 100, No. ST2 Proc. Paper 10365, Feb.

Dhalla, A. K., and Winter, G. (1974) "Suggested Steel Ductility Requirements," *Journal of the Structural Division*, ASCE, Vol. 100, No. ST2 Proc. Paper 10366, Feb.

DiFrancesco, L. C., Selig, E. T., and McGrath, T. J. (1994) "Laboratory Testing of High Density Polyethylene Drainage Pipes," Geotechnical Report No. CPP93-412F, Department of Civil Engineering, University of Massachusetts, Amherst, MA.

Gabriel, L. H., and Goddard, J. B. (1999) "Curved Beam Stiffness for Thermoplastic Gravity Flow Drainage Pipes," *Transportation Research Record 1656*, Transportation Research Board, National Research Council, Washington, DC.

Hashash, N., and Selig, E. T. (1990) "Analysis of the Performance of a Buried High Density Polyethylene Pipe," First National Conference on Flexible Pipes, Balkema, Rotterdam, The Netherlands.

Janson, L. E. (1995) "Plastics Pipe for Water Supply and Sewage Disposal," Borealis, Stenungsund, Sweden.

Johnston, B. G., Ed., (1976) "Guide to Stability Design Criteria for Metal Structures," 3rd Edition, Structural Stability Research Council, Wiley, NY.

Li, H., and Donovan, J. A. (1994) "Ring Bending and Hoop Compression Tests on Big "O" HDPE Pipe," Department of Civil Engineering, University of Massachusetts, Amherst, MA.

McGrath, T. J. (1998) "Replacing 'E' with the Constrained Modulus in Flexible Pipe Design," Pipelines in the Constructed Environment, American Society of Civil Engineers, Reston, VA.

McGrath, T. J. (1999) "Calculating Loads on Buried Culverts Based on Pipe Hoop Stiffness," *Transportation Research Record 1656*, Transportation Research Board, National Research Council, Washington, DC, pp 73–79.

Moore, I. D. (1996) Annual Conference of the Canadian Society for Civil Engineering, 29 May to June 1, Edmonton, Alberta, Canada.

Moore, I. D., and Hu, F. (1995) "Response of Profiled High-Density Polyethylene Pipe in Hoop Compression," *Transportation Research Record 1514*, Transportation Research Board, National Research Council, Washington, DC, pp. 29–36.

Moore, I. D., and Laidlaw, T. C. (1997) "Corrugation Buckling in HDPE Pipes—Measurements and Analysis," Paper No. 970565, 1997 Annual Meeting of the Transportation Research Board, Transportation Research Board, Washington, DC.

Moser, A. P. (1998) "The Structural Performance of Buried Profile-Wall HDPE Pipe and the Influence of Pipe Wall Geometry," 1998 Annual Meeting of the Transportation Research Board, Transportation Research Board, Washington, DC.

Pekoz, T. (1987) "Development of a Unified Approach to the Design of Cold-Formed Steel Members," *Report CF 87-1*, American Iron and Steel Institute, Washington, DC.

Plexco/Spirolite Engineering Manual (1992, Revised 1993) PLEXCO Performance Pipe Division—Chevron Chemical Company, Bensenville, IL.

PPI (1993) "Engineering Properties of Polyethylene," The Plastics Pipe Institute of the Society of the Plastics Industry, Inc., Washington, DC.

Schafer, B. (1997) "Cold-Formed Steel Behavior and Design: Analytical and Numerical Modeling of Elements and Members with Longitudinal Stiffeners," A Dissertation Presented to the Faculty of the Graduate School of Cornell University in Partial Fulfillment of the Requirements for the Degree of Doctor of Philosophy.

Selig, E. T., DiFrancesco, L. C., and McGrath, T. J. (1994) "Laboratory Test of Buried Pipe in Hoop Compression," *Buried Plastic Pipe Technology, ASTM STP 1222*, American Society for Testing and Materials, Philadelphia, pp. 119–132.

Turkopp, R. C., Torp, S., and Carlstrom, B. (1985) "Buried Fiberglass Pipe Performance and Installation Requirements and Design Calculations in International Standardization," *Advances in*

Underground Pipeline Engineering, American Society of Civil Engineers, Reston, VA.

UniBell (1991) "UniBell Handbook of PVC Pipe—Design and Construction," UniBell PVC Pipe Association, Dallas, TX.

Weingarten, V. I., Morgan, E. J., and Seide, P. (1965) "Elastic Stability of Thin Walled Cylindrical and Conical Shells Under Axial Compression," *AIAA Journal*, Vol. 3, No. 3, March.

Winter, G. (1946) "Strength of Thin Steel Compression Flanges," *Transactions*, American Society of Civil Engineers, Vol. 112.

Zhang, C., and Moore, I. D. (1997) "Nonlinear Mechanical Response of High Density Polyethylene. Part I: Experimental Investigation and Model Evaluation," *Polymer Science and Engineering*, Vol. 37, No. 2.

APPENDIX A

LITERATURE REVIEW OF LOCAL WALL STABILITY FOR PROFILE WALL PLASTIC PIPE

INTRODUCTION

The efficient use of materials to manufacture pipe for non-pressure applications requires the use of nonsolid or "profiled" wall sections. These sections attempt to maximize the moment of inertia of the section (I, mm⁴/mm, in.⁴/in.) while minimizing the cross-sectional area (A, mm²/mm, in.²/in.). This approach results in thin elements, whose strength can be controlled by local buckling rather than by general failure modes. Local buckling resistance of thin metal sections is addressed by the American Iron and Steel Institute's *Specification for the Design of Cold-Formed Steel Structural Members with Commentary* (AISI, 1997), but has not been studied extensively for plastics. This report presents a review of literature on the behavior and design of steel and plastic sections for resistance to local buckling. The plastic materials considered in this review are polyvinyl chloride (PVC) and polyethylene (PE).

MATERIAL PROPERTIES

PE and PVC are plastics, which have no true elastic constants, nor do they have sharply defined yield points (PPI, 1993). PE and PVC are viscoelastic materials, meaning they have time-dependent mechanical and strength properties, and they are thermoplastic, which means that properties are also affected by temperature. The time dependence of stiffness properties are often characterized by an apparent modulus based on testing under sustained stress or strain. The apparent modulus is the ratio of the applied constant stress to the total accumulated strain after a specified time. Often, the apparent modulus is also computed using the ratio of the stress after being held for a specified time at a constant strain. Although the apparent moduli computed in these two ways is not identical, they are often used interchangeably in practice.

Data on strength and stiffness properties of PVC are presented in Janson (1995) and UniBell (1991). The apparent modulus for PVC under a 50-year sustained load is approximately 33 percent of the short-term modulus. Poisson's ratio for PVC is about 0.35 (Janson, 1995).

Data on strength and stiffness of PE are presented in Janson (1995), PPI (1993), and Plexco (1992, Revised 1993). The apparent modulus for PE under a 50-year sustained load is approximately 20 percent of the short-term modulus. Janson

conducts all calculations on PE with a Poisson's ratio for PE of 0.40. Plexco (1992, Revised 1993) reports values for Poisson's ratio of PE of 0.35 short term and 0.45 long term. Although often neglected in simplified design methods, the modulus of PE is also dependent on the stress level (PPI, 1993).

Strength and stiffness properties of PVC and PE from the AASHTO Standard Specifications for Highway Bridges (the Standard Specifications, AASHTO, 1996) are presented in Table A-1. The service strain limits apply only to tension strain. The same properties are presented in the AASHTO LRFD Bridge Design Specifications (the LRFD Specifications, AASHTO, 1994).

EXISTING DESIGN PROVISIONS

AASHTO

The LRFD Specifications and the Standard Specifications recognize that local buckling of thermoplastic pipe may occur; however, no design guidance is provided. The LRFD requirement is stated as "The buckling resistance of corrugated and profile wall pipes shall be verified by testing" (Section 12.12.3.8), while the Standard Specification requirement is "The manufacturers of corrugated and ribbed pipe should demonstrate the adequacy of their pipes against local buckling when designed and constructed in accordance with this specification" (Section 18.4.1.7).

ASCE

The Structural Plastics Design Manual (ASCE, 1984) "was written to provide practical assistance and guidelines to structural engineers engaged in the design of plastics and reinforced plastics structural components." The manual incorporates both local and overall buckling of thin-walled sections. Many of the design recommendations presented in Chapter 7, Beams and Axially Stressed Members, are based on the Bryan (1891) equation that predicts the onset of local buckling of an edge-supported plate. For use with plastics, these equations have been used mostly with composites with relatively high stiffness and low ductility. Very little literature exists on the application of these equations to design with thermoplastics.

TABLE A-1 AASHTO (1996) properties for PE and PVC

Properties		PE			PVC	
		Smooth	Corrugated	Ribbed	Cell Class 12454C (Note 1)	Cell Class 12364C (Note 1)
Strength MPa (psi)	Short term	21 (3,000)	21 (3,000)	21 (3,000)	48 (7,000)	41 (6,000)
	Long term	9.9 (1,440)	6.2 (900)	7.8 (1,125)	25 (3,700)	18 (2,600)
Stiffness MPa (psi)	Short term	760 (110,000)	760 (110,000)	550 (80,000)	2,750 (400,000)	3,000 (440,000)
	Long term	150 (22,000)	150 (22,000)	138 (20,000)	960 (140,000)	1,100 (158,400)
Service strain limit (%)	Long term	5	5	5	5	3.5

Note:
1. The resin cell classes are based on ASTM D 1784. Both types of resin are allowed for smooth or ribbed pipe.

Moser Recommendations

Recently A. P. Moser (1998) has proposed dimensionless variables to limit corrugation geometries of polyethylene pipe. Moser proposes limits on five dimensionless variables presented in Table A-2. All but one of the proposed variables incorporate the mean pipe radius. One variable is clearly a local buckling limit (t_{min}/ℓ_{uns}). Moser notes that the proposed limits are approximate and the actual values need to be calibrated for implementation. The criteria are also presented as absolute limits and are not dependent on stress levels. The proposed values are based on results from soil box testing and no theoretical basis is supplied.

The provision for the parameter I/r^3 is essentially a limit on the minimum pipe stiffness. The basic equation for pipe stiffness is

$$PS = \frac{F}{\Delta y} = \frac{E\,I}{0.1488\,r^3} \qquad (A.1)$$

TABLE A-2 Moser (1998) recommendations for geometric design limits for profile wall HDPE

Dimensionless Parameter	Proposed Value for HDPE
t_{min}/r	≥ 0.005
t_{min}/ℓ_{uns}	≥ 0.02
I/r^3	≥ 4 x 10⁻⁵
A/r	≥ 0.02
L_p/r	≤ 0.3

Note: t_{min} = minimum thickness of profile element
r = radius to centroid of pipe wall
ℓ_{uns} = unsupported width of profile element
A = area of pipe wall per unit length
I = moment of inertia of pipe wall per unit length
L_p = length of profile section

where

PS = pipe stiffness, kN/m/m (lb/in./in.)
F = load on pipe in parallel plate test, kN/m (lb/in.)
Δy = change in vertical diameter in parallel plate test, m (in.)
E = modulus of elasticity, kPa (psi)
I = pipe wall moment of inertia per unit length, mm⁴/mm (in.⁴/in.)
r = radius to centroid of pipe wall, mm (in.)

Equation A.1 can be rearranged to

$$\frac{I}{r^3} = \frac{0.1488\,PS}{E} \qquad (A.2)$$

Thus, assuming values of E based on Table A-2, the Moser criteria require that the pipe stiffness be greater than about 200 kN/m/m (30 lb/in./in.) or 150 kN/m/m (22 lb/in./in.) for $E = 760$ MPa (110,000 psi) or 550 MPa (80,000 psi), respectively. AASHTO standards currently allow pipe with lower stiffnesses than permitted by Equation A.2.

The overall approach proposed by Moser could be appropriate for AASHTO specifications. Dimensional limits are used in cold-formed steel design. As stated in the commentary on the Cold-Formed Steel Specification (AISI, 1997), such limitations are intended to set practical ranges and "the upper limits will generally keep noticeable deformation to reasonable limits." Dimensionless parameters are desirable, especially when converting between SI and imperial units.

AISI

The American Iron and Steel Institute (AISI, 1997) has historically designed light-gauge steel members based on the

work of Winter (1946). Winter's approach empirically took advantage of the post-buckling capacity of thin elements. Current AISI procedures are discussed below, but are still based on the same design philosophy.

TESTING FOR LOCAL BUCKLING CAPACITY OF THERMOPLASTIC PIPE

Tests on local bucking in PE pipe have been reported by several researchers, including Li and Donovan (1994), DiFrancesco et al. (1994), Moore and Laidlaw (1997), and Moser (1998). This work (excluding Moser's) used a test procedure developed by Selig et al. (1994) called the hoop compression test.

The hoop compression test apparatus consists of a stiff outer cylinder lined with an inflatable bladder. The test pipe is set into the cylinder and the annulus between the pipe outside diameter and the bladder is filled with soil. When the bladder is inflated, the soil and pipe are compressed. This test results in a pure hoop compression stress on the pipe. The magnitude of deformation (hoop compression strain) is monitored by measuring the change in diameter. Because of load sharing between the pipe and the ring of soil, the stress state in the pipe is uncertain, but has been estimated for some tests based on pipe relaxation data (Selig et al., 1994).

Li and Donovan (1994) performed hoop compression tests on 600-mm (24-in.)-diameter corrugated PE pipes. They observed local buckling of a liner with a width-to-thickness ratio (w/t) of approximately 21 at approximately 1.7 percent change in diameter at a bladder pressure of 205 kPa (30 psi). The liner buckling increased with time and pressure, and most of the inner liner was buckled at about 2.8 percent change in diameter.

DiFrancesco et al. (1994) tested 600-mm (24-in.)-diameter corrugated pipe composed of three different resins and observed local buckling in the inner liner during the tests. At the conclusion of one test, local buckling of the corrugation web was observed, as well as buckling at the intersection of the crest and web (see Selig et al., 1994). Also, the liner portion of the corrugation began to ripple at a radial pressure between 139 and 172 kPa (20 and 25 psi) when the diametral shortening was between 11 and 12 mm (0.43 and 0.47 in.). They observed 50 to 60 inward and outward bulging surfaces (inward and outward being away and toward the pipe center, respectively) around the pipe circumference. The average measured pipe wall strain in the hoop compression test for the three tests was 2.2 percent at a bladder pressure of 172 kPa (25 psi).

Moore and Laidlaw (1997) tested unlined corrugated HDPE pipe in a hoop compression testing cell. In six tests, local buckling in the web and valley was observed. They also estimated the local buckling strength of the profiled pipe using local buckling solutions from the ASCE *Structural Plastics Design Manual* (ASCE, 1984). Instead of evaluating stresses

and determining a value of the modulus of elasticity, they evaluated strains. Their procedure is based on the following assumptions:

1. The profile is composed of flat plate segments. The curved components are ignored.
2. The segments can be modeled as having uniform thickness and width.
3. The support conditions at the edges of the segments can be modeled as free, simple, or clamped.
4. Intermediate soil support normal to the segments is negligible.

The predicted strains at which local buckling occurred are lower than what was observed. During testing, local buckling in the crest ($w/t = 16$ to 18) occurred at strains ranging from 2.2 to 3 percent. The valleys ($w/t = 5$) buckled at strains ranging from 2.5 to 4 percent (this was observed in tests where the liner was removed from the pipe). One test indicates that the soil in the corrugations increases the local buckling capacity of the section.

Moore and Hu (1995) investigated whether the regularly spaced ripples observed in the liner of corrugated pipe tested by DiFrancesco et al. (1994) were the result of local shell buckling. Moore and Hu used a linear three-dimensional buckling solution of thin cylindrical shells to determine the radial contraction necessary to cause buckling. The analysis indicated that elastic buckling occurs in the liner ($w/t = 28$) at a radial contraction of 1.8 percent, and with 40 buckles developing around the pipe circumference. Moore and Hu concluded that the ripples observed in the pipe appeared to be the result of local buckling in the pipe liner.

In addition, Moore (1996) analyzed the test data from Li and Donovan (1994), DiFrancesco et al. (1994), and Moser (1996). Local buckling of the inner liner was reported in pipe under large earth loads. Four tests used corrugated HDPE pipe and three (Moser) used helically wound tubular profile PE pipe. The corrugated pipes were tested under hoop compression, while the tubular pipe was tested with a combination hoop compression and ovalling. Moore used linear buckling theory to examine the buckling of the liner. Comparison with the tests indicate that local buckling deformations were observed at anywhere from 0.5 to 1.5 times the critical hoop contractions predicted by linear buckling theory.

Gabriel and Goddard (1999), at California State University, Sacramento, are conducting compression tests on 90-deg pipe segments. The segments are supported on steel angles to prevent lateral displacement and allow end rotation. Compression is applied through hydraulic cylinders. Currently, the test is being conducted primarily to investigate characteristics of pipe stiffness, but it is also applicable to investigating local buckling behavior. The test uses 90-deg segments and, thus, does not evaluate the pipe performance of the corrugation crest in compression because of the high tensile bending strains at this location.

RECENT DEVELOPMENTS IN LOCAL BUCKLING DESIGN PROCEDURES FOR STEEL

The cold-formed steel design approach changed in 1986 to the unified approach. Pekoz (1987) explains the development of the unified approach for the design of cold-formed steel structural members. All compression elements subject to local buckling are designed using a generalized effective width approach. For member design, the approach "treats members that are made up of elements that may or may not be in the post-buckling range." Failure modes for members include flexural, lateral, and torsional buckling. The nominal load-carrying capacities of the member are determined instead of ultimate stresses. These nominal capacities can be used in interaction equations to determine the effects of combined load actions like bending moments and compressive loads.

Schafer (1997) found that the current specification for dealing with multiple longitudinal intermediate stiffeners in the compression flange are inadequate. He developed a simple design method that determines a buckling coefficient for overall buckling of the entire stiffened element as a unit and for local buckling of the subelement plates between stiffeners. The minimum buckling coefficient from the two modes (local and overall) is used to calculate the critical buckling stress for the element. The overall buckling mode dominates the behavior. Using the equation from the current AISI cold-formed steel specification, the effective width of the element is determined. The effective width is distributed as two strips at the corners, in a manner similar to elements without intermediate stiffeners.

In addition, Schafer reports that the existing AISI specification is flawed for webs where the entire web is in compression. The existing procedure is adequate for most cases, but problems may develop for members with deep webs, or members with web stiffeners. Schaefer reports that another approach proposed by Cohen (1987), which was adopted by the Canadian cold-formed steel code, is also adequate. The Cohen approach is simpler to use and would be a good basis for web provisions for thermoplastic pipe.

Cylinders

Cold-formed steel section design is based on modeling the behavior of flat plate segments. However, compared with cold-formed steel members, plastic pipe and culverts have cross sections that have corners with a large radius and resemble cylinders. Curved elements and cylinders are treated differently in the AISI *Specification for the Design of Cold-Formed Steel Structural Members* (1997) and the *Aluminum Design Manual* (1994). The commentary for the AISI specification, Clark and Rolf (1964), and Weingarten et al. (1965), all state that the capacity of thin-walled cylindrical members must be determined by experimental methods. Testing is required to determine the effect of the large-radius curved segments of the plastic pipe. The basis for this conclusion is that buckling of circular elements appears to be controlled by geometric flaws, which tend to be unpredictable. This is a significant issue for plastic pipes that have mold-parting lines and other geometric features that will affect the capacity.

Ductility

In cold-formed steel, Dhalla et al. (1971) distinguish between uniform ductility and local ductility. "Uniform ductility is characterized by the ability of a member made of the subject material to undergo sizeable plastic deformations over significant portions of its length, prior to failure" while "local ductility is the ability to undergo plastic deformation in a localized area."

Dhalla and Winter (1974) suggest the following ductility requirements for cold-formed steel:

- Uniform elongation outside the fracture greater than or equal to 3 percent,
- Local elongation in ½-in. gauge length across the fracture greater than or equal to 20 percent, and
- Tensile strength to yield strength ratio greater than or equal to 1.05.

Similar requirements may be necessary for thermoplastic pipe and culverts to prevent crack propagation; however, the above recommendations were developed in part to ensure that the sections, which are cold-formed, could be fabricated. Thermoplastics are extruded and fabrication deformations should not be an issue.

APPENDIX B

TESTS TO EVALUATE LOCAL WALL STABILITY OF PROFILE WALL PLASTIC PIPE

INTRODUCTION

This appendix presents procedures used to test profile wall thermoplastic pipe sections in compression. Goals of the effort were to develop a simple test that may be conducted relatively quickly to verify that a given section meets requirements being developed to control local buckling. The test program investigated the effect of the arc length of the specimen, but all tests included three corrugation cycles or periods (Figure B-1) of whatever pipe was under test. Several test configurations were evaluated.

TEST SPECIMENS

Test specimens were cut from pipe samples using a reciprocating saw. Each specimen consists of three corrugation cycles (periods) of pipe (Figure B-1). The ends of each specimen were cut plane with a band saw and then further smoothed with a belt sander. Sample ends were not milled to achieve truly parallel ends. This is an option for future testing.

Corrugation cross sections were measured with calipers at specimen ends (Figure B-2). Average corrugation dimensions are used to compute section properties using an idealized corrugation cross section as shown in Figure B-3. The idealization for the honeycomb or "D" profile is shown in Figure B-4.

Pipe from different manufacturers were identified by letter. Width-to-thickness ratios of the various pipe sections tested are summarized in Table B-1.

TEST APPARATUS AND PROCEDURES

The testing was conducted in a controlled environment of 23°C (73°F) and 50 percent relative humidity.

Tests were conducted with a Zwick, Model 1474, tension/compression machine with a maximum capacity of 100 kN (22,500 lb). End load plates could be free to rotate or be fixed. A dial gauge was placed at midheight on the exterior surface of the center corrugation to measure the lateral deflection of the specimen.

Specimens were typically compressed between the two end plates at a rate of 1.3 mm/minute (0.05 in./minute) until an ultimate load condition was reached. Load and vertical end displacement were continuously recorded on a paper chart. Lateral displacement was recorded regularly from the dial gauge reading.

Various end conditions were experimented with to reduce failure resulting from discontinuous support. These included

- Neoprene bearing pads;
- Plaster encasement;
- Plywood bracing of crest; and
- No special provisions (i.e., direct bearing on end plate).

Most of the means of end support were time consuming or ineffective. The condition of no special provisions proved most reliable.

GENERAL TEST SERIES

Most tests were conducted with the samples and instrumentation as noted above. Table B-2 chronologically summarizes these tests, including test parameters, peak forces developed during the test, and observations of buckling behavior and other test features. Notes pertaining to Table B-2 include

- All tests used neoprene loading pads between specimen and loading device unless otherwise noted;
- Arc lengths varied and are noted in degrees;
- (PE) indicates polyethylene; (PVC) indicates polyvinyl chloride;
- End restraints:
  A   = gypsum caps,
  B   = no end restraint,
  C(X) = plywood reinforcement flush with loading surface(s) (number of ends), and
  D(X) = plywood reinforcement near loading surface(s) (number of ends);
- When used, plywood reinforcement extended over negative moment region was attached using four screws per crest and spanned the width of the specimen; and
- Support conditions:
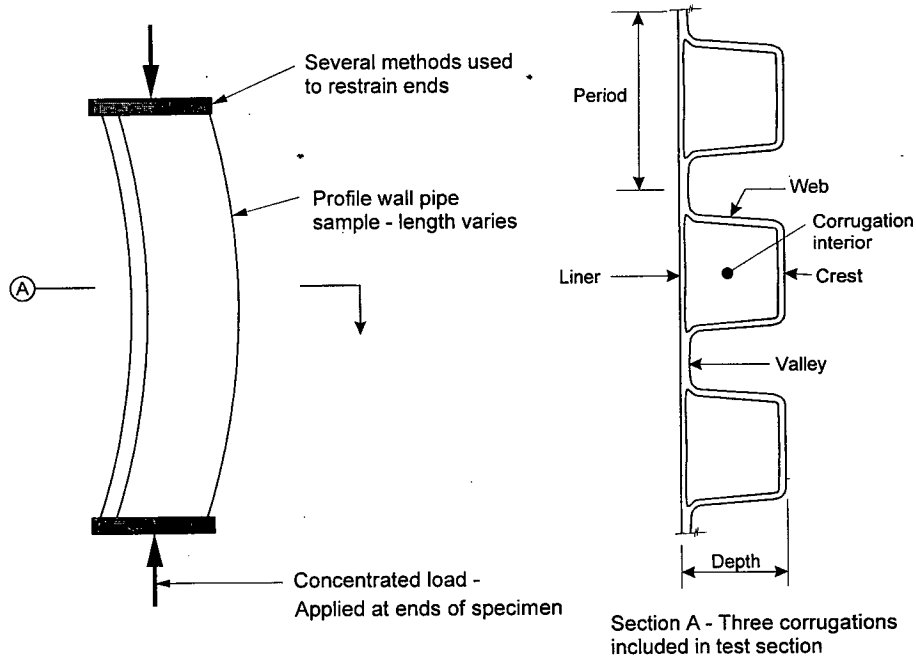
Figure B-1.   General test arrangement and corrugation terminology.

free = specimen unrestrained against rotation at both ends,

one end free = specimen restrained against rotation at one end only, and

fixed = specimen restrained against rotation at both ends.

Table B-3 presents estimated strain levels for all tests. These strains are calculated assuming that all elements of the cross section are fully effective.

COMPRESSION TESTS WITH STRAIN-GAUGED SPECIMENS

A second set of tests was conducted to further investigate the pipe behavior in the stub compression tests under differ-

ent end conditions and to verify that linear elastic theory for curved beams could be used to evaluate test results. A corrugated PVC and corrugated HDPE specimen were instrumented with strain gauges and tested with three end conditions: fixed-fixed, fixed-free, or free-free.

Specimens

One HDPE and one PVC specimen were instrumented. Each specimen included three full corrugations (See Figure B-1) and had a 35-deg arc length. Eight strain gauges were bonded to each specimen: four gauges at the specimen mid-height and four at the quarter point, as illustrated in Figure B-5. At each location, one gauge each was bonded to the crest and liner of the middle corrugation, and one gauge was bonded to each of the valleys on either side of the middle corrugation.
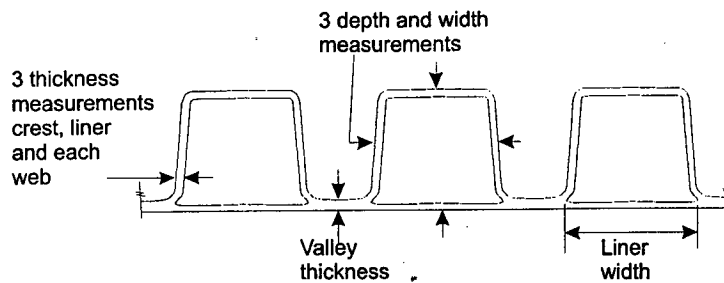
Figure B-2.   Measurement locations to document corrugation geometry.

28
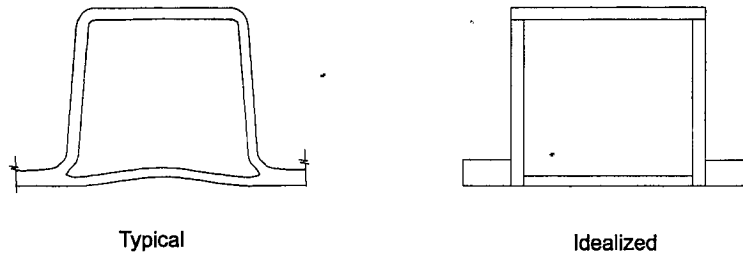
Figure B-3. Idealization of corrugation profile.
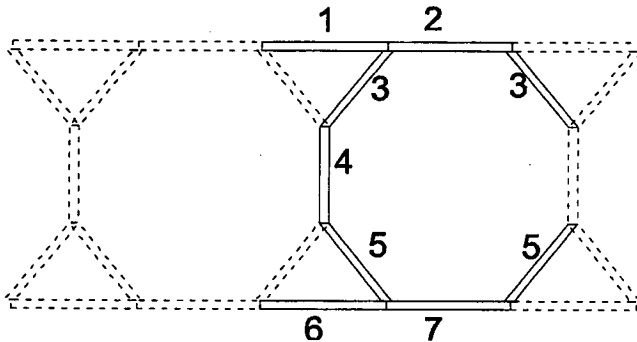
Figure B-4. Idealized profile for honeycomb (D) profile.

Initial specimen preparation was the same as reported above. To prepare the specimen surface for strain gauge application, the surface was first cleaned with Ajax cleanser and paper towels and thoroughly rinsed with distilled water. After rinsing, 220 grit silicon-carbide paper was used to lightly abrade the surface, which was then washed and rinsed

as before. The surface was then scrubbed with isopropyl alcohol to remove any grease or oils and swabbed with Micro-Measurements M-Prep Neutralizer 5A to remove any acidic surface material. The surface was warmed with a heat gun and the gauges were bonded using Micro-Measurements M-Bond 200 Adhesive.

Test Apparatus and Procedures

Tests were conducted on the same Zwick universal compression test machine and with the same general procedures reported for the general test series. Data from the strain gauges, load cell, and crosshead were recorded using a computer-based data acquisition system. The system includes a Vishay strain conditioner and amplifier, an analog-to-digital conversion board, and LABTECH Notebook data acquisition software. Readings from each input were recorded every 20 sec. After testing, the raw data files were imported into Microsoft Excel for analysis and comparison.

TABLE B-1   Width/thickness ratios for all tested specimens

Diameter mm (in.) / Material	Testing Designation	Width / Thickness ratio, w/t			
		Crest	Web	Liner	Valley
300 (12) / PE	A12	40.1	8.3	30.1	1.0
450 (18) / PE	B18	23.1	13.4	28.4	5.2
450 (18) / PE	B18	21.3	10.7	24.5	5.4
600 (24) / PE	A24	27.1	18.9	24.2	2.2
900 (36) / PE	B36	20.0	11.1	21.3	6.3
900 (36) / PE	B36	30.1	13.5	27.0	3.6
900 (36) / PE	E36	16.9	10.9	22.0	5.8
1200 (48) / PE	B48	25.5	13.0	29.7	6.5
	Maximum	40.1	18.9	30.1	6.5
	Minimum	16.9	8.3	21.3	1.0
	Average	25.5	12.5	25.9	4.5
1200 (48) / PE	D48	9.6*	8.0*	7.5*	NA
600 (24) / PVC	C24	10.4	5.5	9.4	1.7

* w/t ratios are for Elements 6, 4, and 7, respectively

TABLE B-2   Summary of test parameters/observations

Test No. (Material Type)	Diam. mm (in.)	Arc Length/ Support Condition	End Restraint (see Text)	Loading Rate mm/min (in./min)	Compr. Load kN (lb)	Moment @ End N-m (in.-lb)	Moment @ Mid-Height N-m (in.-lb)	Observations
A12A-1 (PE)	300 (12)	90/free	A	1.3 (0.05)	1.35 (304)	0 (0)	71 (627)	Insufficient end restraint and confinement. Large lateral deflection. Moment does not account for lateral deflections
A12A-2 (PE)	300 (12)	90/free	B	1.3 (0.05)	0.854 (192)	0 (0)	49 (435)	Load applied at centroid of cross section at mid-height of specimen. Large lateral deflection.
A12A-3 (PE)	300 (12)	90/free	B	1.3 (0.05)	1.04 (234)	0 (0)	52 (464)	Load applied 3/4 in. away from centroid of cross section at mid-height of specimen.
A12A-4 (PE)	300 (12)	90/free	B	1.3 (0.05)	1.29 (290)	0 (0)	63 (556)	Load applied 9/16 in. away from centroid of cross section at mid-height of specimen.
A12A-5 (PE)	300 (12)	45/free	B	1.3 (0.05)	1.88 (423)	0 (0)	44 (393)	Local crushing of corrugation developed at load bearing ends of specimen.
A24A-1 (PE)	600 (24)	45/free	B	1.3 (0.05)	8.19 (1,840)	0 (0)	186 (1,430)	Load applied approximately at centroid of cross section at specimen ends. Local crushing of corrugation developed at load bearing ends of specimen.
A24A-2 (PE)	600 (24)	45/free	B	1.3 (0.05)	7.60 (1,709)	0 (0)	136 (1,200)	Load applied approximately at centroid of cross section at specimen ends. Local crushing of corrugation developed at load bearing ends of specimen.
A12A-6 (PE)	300 (12)	45/one end fixed	A	1.3 (0.05)	4.80 (1,080)	-69 (-607)	70 (621)	Local buckling developed in corrugations at mold line.
A24A-3 (PE)	600 (24)	45/one end fixed	A	1.3 (0.05)	7.20 (1,619)	78 (686)	-94 (-834)	Load applied approximately at centroid of cross section at specimen spring line. Local buckling developed in crest and webs of corrugations.
A24B-1 (PE)	600 (24)	45/one end fixed	A	1.3 (0.05)	12.0 (2,707)	-263 (-2,329)	190 (1,678)	Local buckling developed at base of corrugation webs.
A24C-1 (PE)	600 (24)	45/fixed	A	1.3 (0.05)	15.8 (3,543)	267 (-2,389)	231 (2,046)	Local buckling developed in webs of corrugations.
A24D-1 A24E-1 (PE)	600 (24)	45/fixed	A	1.3 (0.05)	32.8 (7,374)	NA	NA	Back-to-back specimens. Difficult to observe behavior of corrugations. Local buckling developed in corrugation webs.
B48A-1 (PE)	1200 (48)	45/fixed	A	1.3 (0.05)	29.2 (6,564)	-953 (-8,433)	549 (4,859)	Well-defined local buckling developed in liner. Local buckling developed in corrugations at ends.
B48B-1 (PE)	1200 (48)	35/fixed	A , C(2)	1.3 (0.05)	49.5 (11,060)	NA	1,137 (10,059)	Liner buckling at 49.2 kN
B48C-1 (PE)	1200 (48)	25/fixed	A	1.3 (0.05)	44.8 (10,071)	456 (-4,032)	523 (4629)	Local buckling in liner developed at 41 kN
B18A-1 (PE)	450 (18)	35/free	B	1.3 (0.05)	6.96 (1,565)	NA	120 (1,060)	Large end rotations. No buckling observed
B18B-1 (PE)	450 (18)	35/free	A	1.3 (0.05)	8.30 (1,865)	NA	149 (1,319)	Gypsum inside corrugations only. Liner buckles developed after peak load. Large end rotations
C24A-1 (PVC)	600 (24)	25/free	B	1.3 (0.05)	36.4 (8,183)	NA	637 (5,638)	No buckling; liner separated from corrugations at top; stress cracks developed at all liner/web connections

TABLE B-2 *(Continued)*

Test No. (Material Type)	Diam. mm (in.)	Arc Length/ Support Condition	End Restraint (see Text)	Loading Rate mm/min (in./min)	Compr. Load kN (lb)	Moment @ End N-m (in.-lb)	Moment @ Mid-Height N-m (in.-lb)	Observations
B36C-1 (PE)	900 (36)	35/one end fixed	C(1)	1.3 (0.05)	24.8 (5,575)	NA	371 (3,285)	Buckles in web developed at base (free end) of specimen. Test stopped when load curve became nonlinear.
B36D-1 (PE)	900 (36)	35/one end fixed	D(1)	1.3 (0.05)	32.0 (7,194)	NA	528 (4,671)	No buckling observed
D48A-1 (PE)	1200 (48)	35/one end fixed	D(1)	1.3 (0.05)	17.1 (3,844)	NA	289 (2,556)	High frequency ripples from manufacturing observed in liner at beginning of test.
B36E-1 (PE)	900 (36)	35/one end fixed	A , C(1)	1.3 (0.05)	39.2 (8,813)	NA	694 (6,141)	Well-developed buckling at 37 kN. Severe end crushing at peak load. Reinforcement pushed downward.
D48D-1 (PE)	1200 (48)	35/one end fixed	C(1)	1.3 (0.05)	17.0 (3,822)	NA	276 (2,444)	Buckling developed at edges of specimen at 16 kN. Well-defined crimp in end tube at peak. End tube split from scratch made during prep.
E36A-1 (PE)	900 (36)	35/one end fixed	B	1.3 (0.05)	49.9 (11,222)	-1,020 (-9,026)	1,375 (12,169)	Well-developed local buckling in webs.
E36C-1	900 (36)	35/one end fixed	C(1)	1.3 (0.05)	53.2 (11,960)	NA	1,276 (11,294)	Well-developed web buckling at 52 kN. Buckling at ends in web and crest.
C24B-1 (PVC)	600 (24)	25/one end fixed	B	1.3 (0.05)	31.8 (7,149)	-240 (-2,122)	441 (3,899)	No buckling observed.
C24B-2 (PVC)	600 (24)	7/one end fixed	B	1.3 (0.05)	44.1 (9,914)	-25 (-218)	12 (107)	Moment does not account for lateral deflections. Local buckling in liner at 42 kN.
E36D-1 (PE)	900 (36)	15/one end fixed	B	1.3 (0.05)	62.0 (13,938)	-245 (-2,165)	231 (2,040)	No neoprene pads. Well-defined liner buckling at 61 kN.
C24C-1 (PVC)	600 (24)	7/one end fixed	B	1.3 (0.05)	59.1 (13,286)	-33 (-292)	16 (144)	No neoprene pads. Moment does not account for lateral deflections. Local buckling in liner at 48 kN. Crushing at ends.
C24D-1 (PVC)	600 (24)	7/one end fixed	B	1.3 (0.05)	49.6 (11,150)	-28 (-245)	14 (120)	No neoprene pads. Moment does not account for lateral deflections. Liner buckling at 48 kN.
C24E-1 (PVC)	600 (24)	7/one end fixed	B	1.3 (0.05)	58.4 (13,129)	-33 (-289)	16 (142)	No neoprene pads. Moment does not account for lateral deflections. Liner buckling at 52 kN. Buckling in fixed end crest at 58 kN.
E36E-1 (PE)	900 (36)	35/one end fixed	C(1)	1.3 (0.05)	54.6 (12,275)	NA	1046 (9,260)	No neoprene pads. Additional plywood reinf. on inside crest. Slight web buckling observed at 41 kN.
E36F-1 (PE)	900 (36)	15/one end fixed	B	0.13 (0.005)	56.7 (12,747)	-224 (-1,980)	557 (4,925)	No neoprene pads. Slight bulging in end of web at 40 kN. Well-defined web buckling at 50 kN. Slight ripples in liner at 48 kN.
E36G-1 (PE)	900 (36)	15/one end fixed	B	13 (0.5)	104.0 (23,380)	-410 (-3,632)	651 (5,759)	No neoprene pads. Specimen loaded too fast to make detailed observations. Web and crest were bulging at end of test.
C24F-1 (PVC)	600 (24)	7/one end fixed	B	0.13 (0.005)	64.0 (14,388)	-36 (-316)	18 (155)	No neoprene pads. Moment does not account for lateral deflections. Slight bulging in crest at 60 kN. Small dimples in liner at 62 kN.

TABLE B-2 *(Continued)*

Test No. (Material Type)	Diam. mm (in.)	Arc Length/ Support Condition	End Restraint (see Text)	Loading Rate mm/min (in./min)	Compr. Load kN (lb)	Moment @ End N-m (in.-lb)	Moment @ Mid-Height N-m (in.-lb)	Observations
C24G-1 (PVC)	600 (24)	7/one end fixed	B	13 (0.5)	76.0 (17,085)	-42 (-376)	21 (185)	No neoprene pads. Moment does not account for lateral deflections. Crushing of crest at 65 kN. Bottom of specimen shifted 1/4 in. towards liner.
A24F-1 (PE)	600 (24)	15/one end fixed	B	1.3 (0.05)	19.0 (4,271)	-26 (-227)	44 (387)	No neoprene pads. Buckles in crest at 17 kN. Web and liner bulging at 18 kN.
A24G-1 (PE)	600 (24)	15/one end fixed	B	1.3 (0.05)	22.6 (5,080)	-31 (-270)	52 (460)	No neoprene pads. Bulging in crest at 17 kN. Web buckling at 18.5 kN. Waves observed in crest at peak.
A24H-1 (PE)	600 (24)	15/one end fixed	B	13 (0.5)	31.8 (7,138)	-43 (-379)	65 (575)	No neoprene pads. Specimen loaded too quickly to make detailed observations. Severe bulging in web and crest at peak.
A24I-1 (PE)	600 (24)	15/one end fixed	B	0.13 (0.005)	15.9 (3,572)	-21 (-190)	33 (288)	No neoprene pads. Buckling developed in crest at 11.3 kN. Local buckling of crest and web at 11.8 kN and 14.3 kN respectively.
D48C - 1	1200 (28)	15/one end fixed	B	1.3 (0.05)	37.8 (8,498)	-91 (-868)	257 (2,276)	No neoprene pads. High frequency ripples in liner at 30 kN. Liner buckling and crushing of crest at 37 kN.
D48D - 2	1200 (48)	15/one end fixed	B	1.3 (0.05)	31.6 (7,104)	-82 (-726)	191 (1,689)	No neoprene pads. Minor crushing/buckling at ends at 24 kN. End cell liner developed waves at end of test.
D48E - 1	1200 (48)	15/one end fixed	B	1.3 (0.05)	28.4 (6,362)	-73 (-650)	139 (1,227)	No neoprene pads. Slight crushing at ends at 26 kN.

The specimens were tested to a maximum strain level of about 1 percent. The strain conditioner contained only four inputs, thus each test was repeated two or three times to collect the midheight and quarter-point data (three times for the fixed-free condition and two times for the fixed-fixed and free-free conditions). Specimens were allowed to recover for 15 to 30 min after each test before the next test began.

Results

Strain levels from the tests are summarized in Tables B-4 and B-5. Test results were evaluated using linear elastic curved beam theory. Axial loads and moments were calculated and superimposed to determine the total stresses along the length of the specimen. Strains were estimated by dividing the total stresses by the AASHTO short-term modulus of elasticity values.

The researchers noted the following trends:

- For PE, all end conditions induce compression in all elements of the cross section. For the PVC, tension is induced at the crest for the pinned-pinned setup and the fixed-pinned setup.
- In the PE specimen, the strains achieved in the liner/valleys were generally less than predicted.
- For PE, the strains in the crest were generally less than predicted, except for the pinned-pinned condition; however the crest exhibited more linear behavior than the other elements.
- Slight crippling of the crest and web were observed at the fixed ends of the PE fixed-fixed and fixed-pinned tests at approximately 75 percent of total test load.
- PVC strains were much closer to prediction than PE. Strains measured in valley of the PVC pipe were within 10 percent of predicted values, with the exception of the pinned-pinned test, which were as much as 25 percent less than predicted.
- All PVC strains followed the same trends as predicted, except for the liner/valley values for the fixed-pinned test.
- The interior gauges (valley 1, valley 2, and liner) in the PVC tests followed consistent patterns (i.e., the measured strain in the liner is always less than valley 2). Valley 2 always achieved less strain than valley 1. However,

TABLE B-3 Estimated maximum material strain levels in compression tests

Test No. (Material Type)	Location	E (MPa)	E psi	ε_c (%)	Combined Strains ε_{in} (%)	ε_{out} (%)	Comments
A12A-1 (PE)	midheight	525	76,134	0.33	1.51	-0.85	Does not account for lateral deflections
	ends	525	76,134	0.33	0.33	0.33	
A12A-2 (PE)	midheight	531	77,011	0.21	1.02	-0.95	
	ends	531	77,011	0.21	0.21	0.21	
A12A-3 (PE)	midheight	538	78,036	0.25	1.10	-0.99	
	ends	538	78,036	0.25	0.25	0.25	
A12A-4 (PE)	midheight	525	76,134	0.32	1.36	-1.22	
	ends	525	76,134	0.32	0.32	0.32	
A12A-5 (PE)	midheight	568	82,370	0.42	1.11	-0.85	
	ends	568	82,370	0.42	0.42	0.42	
A24A-1 (PE)	midheight	553	80,145	0.89	1.71	-0.38	
	ends	553	80,145	0.89	0.89	0.89	
A24A-2 (PE)	midheight	562	81,540	0.81	1.49	-0.23	
	ends	562	81,540	0.81	0.81	0.81	
A12A-6 (PE)	midheight	538	78,036	1.15	2.29	-0.98	
	fixed end	538	78,036	1.15	0.03	3.22	
A24A-3 (PE)	midheight	568	82,370	0.76	0.30	1.48	
	fixed end	568	82,370	0.76	1.14	0.17	
A24B-1 (PE)	midheight	553	80,145	1.31	2.27	-0.18	
	fixed end	553	80,145	1.31	-0.02	3.37	
A24C-1 (PE)	midheight	540	78,266	1.78	2.95	-0.10	
	fixed end	540	78,266	1.78	0.39	3.88	
A24D-1 A24E-1 (PE)	midheight	502	72,740	1.97	1.97	1.97	
	fixed end	502	72,740	1.97	1.97	1.97	
B48A-1 (PE)	midheight	525	76,134	1.35	2.36	0.01	Mid-height strains based on reduced cross section.
	fixed end	525	76,134	1.35	-0.19	3.32	
B48B-1 (PE)	midheight	509	73,751	2.69	5.29	-0.51	Mid-height strains based on reduced cross section.
	fixed end	509	73,751	2.69	2.03	2.03	
B48C-1 (PE)	midheight	519	75,224	1.81	2.57	-0.62	Mid-height strains based on reduced cross section.
	fixed end	519	75,224	1.81	1.15	2.85	
B18A-1 (PE)	midheight	549	79,547	0.93	2.24	-0.96	
	ends	549	79,547	0.93	0.63	0.93	
B18B-1 (PE)	midheight	551	79,897	1.11	2.73	-1.24	
	ends	551	79,897	1.11	1.11	1.11	
C24A-1 (PVC)	midheight	2,759	400,000	1.01	3.08	-1.61	
	ends	2,759	400,000	1.01	1.01	1.01	

TABLE B-3 *(Continued)*

Test No. (Material Type)	Location	E (MPa)	E (psi)	ε_c (%)	Combined Strains ε_{in} (%)	ε_{out} (%)	Comments
B36C-1 (PE)	midheight	541	78,500	1.58	3.23	-0.72	Fixed end reinforced. Mid-height strains based on reduced cross section.
	fixed end	541	78,500	1.58	NA	NA	
B36D-1 (PE)	midheight	523	75,815	2.26	3.68	0.25	Fixed end reinforced. Mid-height strains based on reduced cross section.
	fixed end	523	75,815	2.26	NA	NA	
D48A-1 (PE)	midheight	530	76,822	1.40	2.32	0.49	Fixed end reinforced.
	fixed end	530	76,822	1.40	NA	NA	
B36E-1 (PE)	midheight	521	75,512	2.89	5.25	-0.62	Fixed end reinforced. Mid-height strains based on reduced cross section
	fixed end	521	75,512	2.89	NA	NA	
D48D-1 (PE)	midheight	532	77,200	1.39	2.51	0.27	Fixed end reinforced. Strains based on reduced cross section
	fixed end	532	77,200	1.39	NA	NA	
E36A-1 (PE)	midheight	521	75,512	1.69	3.62	-0.94	Mid-height strains based on reduced cross section.
	fixed end	521	75,512	1.69	0.36	3.38	
E36C-1 (PE)	midheight	521	75,512	1.62	3.22	-0.57	Fixed end reinforced. Mid-height strains based on reduced cross section.
	fixed end	521	75,512	1.62	NA	NA	
C24B-1 (PVC)	midheight	2,484	360,186	1.00	2.64	-1.03	Mid-height strains based on reduced cross section
	fixed end	2,484	360,186	1.00	0.11	1.87	
C24B-2 (PVC)	midheight	2,498	362,152	1.36	1.40	1.30	Does not account for lateral deflections. Mid-height strains based on reduced cross section
	fixed end	2,498	362,152	1.36	1.15	1.33	
E36D-1 (PE)	midheight	609	88,322	2.06	2.37	1.57	All strains based on reduced cross section.
	fixed end	609	88,322	2.13	1.79	2.72	
C24C-1 (PVC)	midheight	2,705	392,274	1.68	1.73	1.61	Does not account for lateral deflections. All strains based on reduced cross section.
	fixed end	2,705	392,274	1.68	1.57	1.82	
C24D-1 (PVC)	midheight	2,633	381,739	1.45	1.49	1.39	Does not account for lateral deflections. All strains based on reduced cross section.
	fixed end	2,633	381,739	1.45	1.35	1.57	
C24E-1 (PVC)	midheight	2,621	380,060	1.71	1.76	1.64	Does not account for lateral deflections. All strains based on reduced cross section.
	fixed end	2,621	380,060	1.71	1.60	1.85	
E36E-1 (PE)	midheight	545	79,002	1.78	3.18	-0.15	Fixed end reinforced. All strains based on reduced cross section
	fixed end	545	79,002	1.78	NA	NA	
E36F-1 (PE)	midheight	466	67,585	2.29	3.22	0.94	All strains based on reduced cross section.
	fixed end	466	67,585	2.50	2.10	3.22	

TABLE B-3 *(Continued)*

Test No. (Material Type)	Location	E (MPa)	E (psi)	ε_c (%)	Combined Strains ε_{in} (%)	Combined Strains ε_{out} (%)	Comments
E36G-1 (PE)	midheight	679	98,466	3.22	4.06	1.88	All strains based on reduced cross section.
	fixed end	679	98,466	3.42	2.86	4.48	
C24F-1 (PVC)	midheight	2,250	326,302	2.20	2.27	2.11	Does not account for lateral deflections. All strains based on reduced cross section.
	fixed end	2,250	326,302	2.18	2.04	2.36	
C24G-1 (PVC)	midheight	2,759	400,000	2.12	2.19	2.04	Does not account for lateral deflections. All strains based on reduced cross section.
	fixed end	2,759	400,000	2.11	1.98	2.29	
A24F-1 (PE)	midheight	611	88,664	3.48	3.90	2.81	All strains based on reduced cross section.
	fixed end	611	88,664	3.50	3.26	3.93	
A24G-1 (PE)	midheight	611	88,664	4.52	5.06	3.62	All strains based on reduced cross section.
	fixed end	611	88,664	4.55	4.24	5.13	
A24H-1 (PE)	midheight	736	106,771	5.71	6.30	4.67	All strains based on reduced cross section.
	fixed end	736	106,771	5.74	5.35	6.49	
A24I-1 (PE)	midheight	502	72,740	3.59	3.97	2.96	All strains based on reduced cross section.
	fixed end	502	72,740	3.61	3.35	4.05	

Notes:
- All strains based on fully effective section unless noted otherwise.
- NA = strains cannot be accurately computed in locations of plywood reinforcement.
- Positive strain indicates compression.
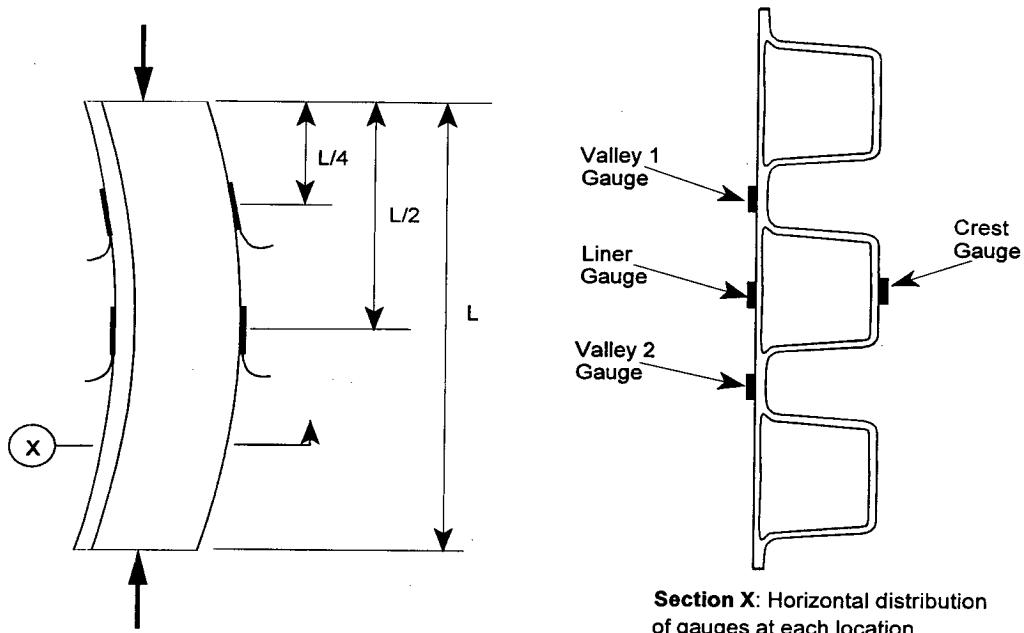
Section X: Horizontal distribution of gauges at each location.

Figure B-5.   Strain gauge locations on corrugation profile.

TABLE B-4   Polyethylene (PE) test results

Test (4)	Location on Specimen	Load (kN)	Deflection (mm)	Δ (1) (mm)	Moment (N-m)	Axial Stress (MPa)	Stress-in (MPa)	Stress-out (MPa)	Linear Prediction Strain-in valley, liner (%)	Strain-out crest (%)	Measured Strain-in valley (2) (%)	Strain-in liner (%)	Strain-out crest (%)
F - F	fixed end	9.12	-	0.00	-80.82	5.48	3.22	8.98	0.42	1.18			
	1/4 point	9.12	0.381	9.91	9.51	5.48	5.75	5.07	0.76	0.67	0.58	-	0.27
	mid height	9.12	0.508	13.21	39.62	5.48	6.59	3.77	0.87	0.50	0.40	-	0.19
	3/4 point	9.12	0.381	9.91	9.51	5.48	5.75	5.07	0.76	0.67	0.58	-	0.26
	fixed end	9.12	-	0.00	-80.82	5.48	3.22	8.98	0.42	1.18			
P - P	pinned end	10.50	-	0.00	0.00	6.31	6.31	6.31	0.83	0.83			
	1/4 point	10.50	0.381	9.91	103.99	6.31	9.21	1.81	1.21	0.24	0.48	-	0.32
	mid height	10.50	0.508	13.21	138.65	6.31	10.18	0.31	1.34	0.04	0.75	0.26	0.29
	3/4 point	10.50	0.381	9.91	103.99	6.31	9.21	1.81	1.21	0.24	0.48	-	0.27
	pinned end	10.50	-	0.00	0.00	6.31	6.31	6.31	0.83	0.83			
F - P	fixed end	9.52	-	0.00	-126.02	5.72	2.20	11.18	0.29	1.47			
	1/4 point	9.52	0.381	9.91	-0.22	5.72	5.72	5.73	0.75	0.76	0.58	-	0.28
	mid height	9.52	0.508	13.21	62.72	5.72	7.47	3.01	0.99	0.40	0.60	0.24	0.19
	3/4 point	9.52	0.381	9.91	62.79	5.72	7.47	3.00	0.99	0.40	0.57	-	0.30
	pinned end	9.52	-	0.00	0.00	5.72	5.72	5.72	0.75	0.75			

Specimen: 600-mm (24-in.)-Diameter Polyethylene (PE) Corrugated Pipe

Section Properties:

longitudinal width:	224 mm	I of section:	932358 mm^4
profile height:	66 mm	x bar:	26 mm
Area of section:	1664 mm^2	eccentricity	13 mm
Arc length of sample:	188 mm	chord length:	186 mm
Modulus of Elasticity (3):	759 MPa		

Notes:
1. Δ = distance from chord passing through N.A. at specimen ends to the N.A. at location of calculation
2. "Strain-in (Valley)" strain values are an average of the two (2) valley strain gauge outputs
3. Modulus of Elasticity is from AASHTO published values.
4. F = fixed-end condition, P = pinned-end condition
5. 1 in. = 25.4 mm, 1 kN = 224.8 lb, 1MPa = 145 psi

the difference in the PVC valley strain gauge readings was less than in the PE tests.

Discussion

As shown in Tables B-4 and B-5, the predicted strain differs from the measured strain to varying degrees. Uncertainty in the modulus of elasticity contributes to some of this variation. In addition, the actual restraint at the ends is unlikely to match the assumed condition precisely, particularly the pinned-pinned condition. Also, the specimen ends were not machined, and thus slight deviations from the plane and parallel condition can introduce additional errors. The data for the PVC matches the predictions more closely than the PE.

Strain gauging of PE is known to be difficult. The modulus of elasticity of PE is so low that the gauge can have a reinforcing effect and modify the strain field. In this case, strain gauges on the thin elements could also contribute to increased variability.

For the fixed-pinned tests, the measured strain trends more closely resemble the predicted fixed-fixed trends. A possible reason for this similarity is in the test setup. The rotation of the spherical head needed to be loosely restrained so the steel plate could be held in place without causing a safety hazard. This restraint created a degree of fixity in the "pinned" end. In addition, the point of rotation of this setup is approximately 5 in. below the end of the specimen. The spherical head is approximately 100 mm (4 in.) in diameter and has a 19-mm (¾-in.)-thick platen on top of the socket. On top of the platen is the 25-mm (1-in.)-thick steel loading plate. This condition also creates a degree of fixity in the setup, therefore, the "free end" is not allowed to rotate 100 percent freely.

Based on these results, the research team suggests that further testing be conducted with 15-deg specimens in the fixed-pinned condition. For testing shorter stub specimens (i.e., 35 deg and less), any of the three end conditions can be used to achieve good results. For PE, all end conditions induce compression in all elements of the cross section when the length of the specimen is less than 45 deg. Because of PVC's shallower corrugation height, tension is induced at the crest for the pinned-pinned setup and the fixed-pinned setup.

TABLE B-5   Polyvinyl chloride (PVC) test results

Test (4)	Location on Specimen	Load (kN)	Deflection (mm)	Δ(1) (mm)	Moment (N-m)	Axial Stress (MPa)	Stress-in (MPa)	Stress-out (MPa)	Linear Prediction		Measured		
									Strain-in valley, liner (%)	Strain-out crest (%)	Strain-in valley(2) (%)	Strain-in liner (%)	Strain-out crest (%)
	fixed end	18.59	-	0.00	-173.15	14.27	-1.20	33.90	-0.04	1.23			
	1/4 point	18.59	1.143	10.41	20.48	14.27	16.10	11.94	0.58	0.43	0.52	0.41	0.29
F - F	mid height	18.59	1.524	13.97	86.60	14.27	22.00	4.45	0.80	0.16	0.84	-	0.03
	3/4 point	18.59	1.143	10.41	20.48	14.27	16.10	11.94	0.58	0.43	0.60	0.48	0.23
	fixed end	18.59		0.00	-173.15	14.27	-1.20	33.90	-0.04	1.23			
	pinned end	13.92		0.00	0.00	10.68	10.68	10.68	0.39	0.39			
	1/4 point	13.92	2.464	10.41	144.99	10.68	23.63	-5.76	0.86	-0.21	0.62	-	-0.19
P - P	mid height	13.92	3.302	13.97	194.50	10.68	28.06	-11.38	1.02	-0.41	0.88	0.83	-0.48
	3/4 point	13.92	2.464	10.41	144.99	10.68	23.63	-5.76	0.86	-0.21	0.71	-	-0.30
	pinned end	13.92		0.00	0.00	10.68	10.68	10.68	0.39	0.39			
	fixed end	15.26		0.00	-212.37	11.71	-7.26	35.79	-0.26	1.30			
	1/4 point	15.26	1.346	10.41	-0.39	11.71	11.67	11.75	0.42	0.43	0.45	0.35	0.18
F - P	mid height	15.26	1.778	13.97	106.96	11.71	21.26	-0.42	0.77	-0.02	0.78	0.66	-0.13
	3/4 point	15.26	1.346	10.41	105.80	11.71	21.16	-0.29	0.77	-0.01	0.61	0.50	-0.06
	pinned end	15.26	-	0.00	0.00	11.71	11.71	11.71	0.42	0.42			

Specimen: 600-mm (24-in.)-Diameter Polyvinyl Chloride (PVC) Corrugated Pipe

Section Properties:

longitudinal width:	140 mm		I of section:	136441 mm^4
profile height:	28 mm		x bar:	12 mm
Area of section:	1303 mm^2		eccentricity:	14 mm
Arc length of sample:	186 mm		chord length:	183 mm
Modulus of Elasticity (3):	2759 MPa			

Notes:
1. Δ = distance from chord passing through N.A. at specimen ends to the N.A. at location of calculation
2. "Strain-in (Valley)" strain values are an average of the two (2) valley strain gauge outputs
3. Modulus of Elasticity is from AASHTO published values.
4. F = fixed-end condition, P = pinned-end condition
5. 1 in. = 25.4 mm, 1 kN = 224.8 lb, 1MPa = 145 psi

APPENDIX C

STRAIN LEVELS IN PLASTIC PIPE

INTRODUCTION

Design for resistance to local buckling in profile wall thermoplastic pipe is based on limiting strain levels. For an understanding of how any proposed design criteria for local buckling might affect current practice, it is useful to estimate strain levels in product tests and in ground.

During product development (and possibly during routine production), pipe should be tested to demonstrate the capacity to carry load in the field-installed condition. In current practice, such evaluation is primarily through the parallel plate test. The strain levels achieved in the parallel plate test in the pipe that were tested in compression (see Appendix B) as part of this project are investigated in the section below. Strain levels that might be anticipated under actual installed conditions are evaluated in the "In-Ground Conditions" section.

PARALLEL PLATE TEST

The principal quality control test for thermoplastic pipe is the parallel plate test. In this test, a pipe is compressed between two diametrically opposed plates. AASHTO M294 (HDPE) and M304 (PVC) require that all pipe

- Demonstrate a specified pipe stiffness at a deflection of 5 percent and
- Reach a deflection (reduction of vertical diameter) of 20 percent for HDPE pipe and 60 percent for PVC pipe without evidence of wall buckling, cracking, splitting, or delamination.

The equations that govern the parallel plate test are

$$F = \Delta y \frac{EI}{0.149R^3} \tag{C.1}$$

$$F = \Delta x \frac{EI}{0.137R^3} \tag{C.2}$$

$$M = FR[0.3183 - 0.50\sin(\theta)] \tag{C.3}$$

$$N = -0.5F\sin(\theta) \tag{C.4}$$

$$\varepsilon_b = \frac{Mc}{EI} \tag{C.5}$$

where

F = load applied in parallel plate test, kN/m, lb/in.
Δy = change in vertical diameter under load F, m, in.
E = modulus of elasticity of pipe material, kPa, psi
I = moment of inertia of pipe wall per unit length of pipe, m⁴/m, in.⁴/in.
R = centroidal radius of pipe, m, in.
Δx = change in horizontal diameter under load F, m, in.
M = bending moment per unit length of pipe, kN-m/m, in.-lb/in.
θ = angle from crown, degrees
N = compressive thrust per unit length of pipe, kN/m, lb/in.
ε_b = bending strain in pipe wall
$c = c_{in}, c_{out}$ = distance from centroid of pipe wall to inside or outside extreme fiber, m, in.

The above equations assume linear material behavior and linear geometric behavior, which are both violated at deflection levels of 20 percent. This means that load and stress predictions will overestimate actual test values; however, strain values are reasonably accurate, even if the nonlinearities are ignored. Given that the focus of the design method for local buckling is on strain levels, the linear equations are considered sufficiently accurate. An additional issue with the parallel plate test is the local deformation of the profile cross section where the pipe is in contact with the plates. This is also ignored in this analysis because the deformation varies with each profile geometry. The significance of this is discussed further below.

Equations C.1, C.3, and C.5 can be combined to predict bending strain as a function of pipe geometry and vertical deflection

$$\varepsilon_b = \frac{0.3183 - 0.5\sin(\theta)}{0.0744}\left(\frac{c}{R}\right)\left(\frac{\Delta y}{D}\right) \tag{C.6}$$

where

D = diameter to centroid of pipe wall, m, in.

Using Equation C.6, the strains achieved in the parallel plate test may be investigated. Table C-1 presents such calculations for several of the pipes included in the test program described in Appendix B. The table shows strains computed at the invert and springline and on the inner and outer surfaces of the pipe at a vertical deflection of 20 percent. Table C-1 indicates the following behavior at this deflection level:

- The parallel plate test produces relatively modest compression strains on the inside surface of most corrugated HDPE profiles—a maximum of 4 percent strain for the sections tested. This is because the centroidal axes of these pipes are relatively close to the inside surface (see c_{in} and c_{out} in Table C-1b).
- The compressive strain levels in the outside surface of the pipe are much higher than on the inside surface, up to 9 percent; however, these strains occur where the pipe is in contact with the load plates. This contact undoubtedly influences the behavior, thus the test may not truly evaluate the pipe capacity in compression at the calculated strain levels.
- Strains in the PVC pipe are smaller than the HDPE pipes because of the higher ratio of pipe diameter to profile depth. Given that M304 requires that PVC be deflected to a 60 percent deflection, the strains achieved during quality control testing would be higher than in the table;

however, the effect of the loading plate on the outside surface compression strains is still not known.
- The material strain rates that occur in the test are substantially lower for larger diameters. This is because the strain rate is specified in absolute terms (mm/minute) while the deflection is specified as a percentage of diameter. The ratio of diameter to profile depth also influences the strain rate, but to a lesser extent.
- The honeycomb profile is the only one that is symmetric about the centroidal axis, thus the strain levels are balanced between the inside and outside surface.

IN-GROUND CONDITIONS

In-ground strain levels are generally dominated by flexural strains, which result from pipe deflection. Deflection can be estimated in two ways: (1) theoretical predictions based on soil-structure interaction or (2) by assuming pipes are deflected to limiting deflection levels. Total strain is computed by adding flexural strains to hoop compression strains due to applied load. Both approaches to estimating flexural strain are used in the analysis reported below.

A small parametric study was conducted to investigate in-ground strain levels. The study considered pipe type, depth of fill, and backfill condition as variables. As suggested above, deflection levels are estimated both by theoretical pre-

TABLE C-1 Expected strain levels in parallel plate test

a. General pipe details and geometry

Diameter	Corr. Style	Manuf.	Element 1 (Crest)	Element 2 (Web)	Element 3 (Valley)	Element 4 (Liner)	Element 5	Total Profile Depth	Diam to Profile Depth
mm								mm	Ratio
457	Corr. PE	B	20.26	11.43	5.22	28.44		41.5	12
610	Corr. PE	A	34.79	16.59	2.19	24.24		66.4	10
914	Corr. PE	B	30.19	13.51	3.60	27.03		66.5	14
914	Corr. PE	E	16.89	10.94	5.85	21.96		83.2	12
1219	Corr. PE	B	22.77	12.98	6.48	29.67		74.4	17
610	Corr. PVC	C	8.09	5.32	1.72	9.41		27.7	22
1219	Hnycmb PE	D	20.00	20.00	4.29	8.62	8.62	66.1	19

HDPE - E =	620100	kPa
PVC - E =	2756000	kPa

b. Profile section properties

R	I	A	c-in	c-out
mm	mm^4/mm	mm^2/mm	mm	mm
246	1428	6.0	15.6	25.9
331	5021	7.8	29.1	37.3
482	6076	9.9	24.5	42.0
490	12311	14.2	32.7	50.5
644	8475	10.5	28.8	45.6
310	977	9.3	12.2	15.5
644	6961	10.9	33.0	33.0

c. Strains in Parallel Plate Test
20.0% Deflection

Diameter	Corr. Style	Load	Stiffness	Bending Moment Springline	Bending Moment Invert	springline inside	Bending Strains springline outside	invert inside	invert outside	Time to reach deflection	max strain rate*
mm		kN/m	kN/m/m	kN-m/m	kN-m/m	%	%	%	%	(min.)	%/min.
457	Corr. PE	36.5	370.9	1.63	2.86	-2.9%	4.8%	5.0%	-8.4%	7.2	0.70%
610	Corr. PE	70.5	533.2	4.24	7.43	-4.0%	5.1%	6.9%	-8.9%	9.6	0.72%
914	Corr. PE	41.4	215.0	3.63	6.35	-2.4%	4.0%	4.1%	-7.1%	14.4	0.29%
914	Corr. PE	79.8	407.3	7.10	12.45	-3.0%	4.7%	5.3%	-8.2%	14.4	0.37%
1219	Corr. PE	32.3	125.3	3.77	6.61	-2.1%	3.3%	3.6%	-5.7%	19.2	0.19%
610	Corr. PVC	73.9	596.1	4.17	7.30	-1.9%	2.4%	3.3%	-4.2%	9.6	0.34%
1219	Hnycmb PE	26.5	102.9	3.10	5.43	-2.4%	2.4%	4.2%	-4.2%	19.2	0.22%

*based on a load rate of
12.7   in./min.

Notes:
1. These calculations are made assuming linear elasticity. This likely significantly overpredicts load and bending moment; however, strains are reasonably accurate.
2. 1 psi = 6.89 kPa, 1 lb/in = 0.175 kN/m, 1 in. = 0.0254 m, 1 lb = 0.0044 kN
3. Deflection computed on the basis of inside pipe diameter

dictions based on the Spangler equation (Tables C-2 and C-3) and by assuming pipes are deflected to a specific deflection level of 7.5 percent (Tables C-4 and C-5). Flexural strains are estimated based on the shape factor concept used in fiberglass pipe design (AWWA, 1995). Using a shape factor of 6 provides allowance for non-elliptic deformations in the pipe. The shape factor for the parallel plate test is 4.28. Soil cover depths of 3 m, 6 m, and 9 m (10 ft, 20 ft, and 30 ft) and constrained soil modulus values of 7 MPa and 21 MPa (1,000 psi and 3,000 psi), representing silty soil at about 90 percent of maximum density per AASHTO T-99 and sand at about 95 percent of maximum, respectively, were evaluated. Deflection was computed using the Spangler Iowa formula with the soil prism load, a deflection lag factor of 1.5, and a bedding factor of 0.083. Hoop compression was computed using the Burns and Richard theory (full-slip) as simplified by McGrath. The study used the long-term modulus of elasticity. Two example spreadsheets (one each for PVC and PE)

used for these calculations are attached. Calculations were completed for 600-mm (24-in.)-diameter corrugated PE and corrugated PVC pipe.

Comparison of the four tables indicates the following:

- When installed to current specifications, theoretical deflections are much smaller than 7.5 percent; in good backfill conditions ($M_s = 3,000$ psi), predicted deflection levels are under 3 percent even at a depth of 9 m (30 ft).
- When the deflection level is fixed (Tables C-4 and C-5), the peak tensile strain decreases with increasing depth of fill; however, when deflections are calculated (Tables C-2 and C-3), the peak tensile and compressive strains increase with depth.
- For the two profiles evaluated, the outside compression strain is always greater than the inside compression strain.
- Hoop compression strains do not affect the total strain level in PVC as significantly as in HDPE.

TABLE C-2   Strain in 600-mm (24-in.)-diameter corrugated polyethylene (Spangler Deflection)

M_s MPa (psi)	VAF	Soil Depth m (ft)	Δ_y/D (%)	ϵ_h (%)	$\epsilon_{B\text{-}o}$ (outside) (%)	Combined strains		
						Outside		Inside
						$\epsilon_h + \epsilon_{B\text{-}o}$ (%)	$\epsilon_h - \epsilon_{B\text{-}o}$ (%)	$\epsilon_h - \epsilon_{B\text{-}i}$ (%)
7 (1,000)	0.55	3 (10)	2.2	-0.9	±1.6	0.6	-2.5	-1.8
		6 (20)	4.4	-1.8	±3.1	1.2	-4.9	-3.5
		9 (30)	6.6	-2.8	±4.6	1.9	-7.4	-5.3
21 (3,000)	0.30	3 (10)	0.8	-0.5	±0.5	0.0	-1.0	-0.8
		6 (20)	1.5	-1.0	±1.1	0.1	-2.1	-1.6
		9 (30)	2.2	-1.5	±1.6	0.1	-3.1	-2.4

TABLE C-3   Strain in 600-mm (24-in.)-diameter corrugated PVC (Spangler Deflection)

M_s MPa (psi)	VAF	Soil Depth m (ft)	Δ_y/D (%)	ϵ_h (%)	$\epsilon_{B\text{-}o}$ (outside) (%)	Combined strains		
						Outside		Inside
						$\epsilon_h + \epsilon_{B\text{-}o}$ (%)	$\epsilon_h - \epsilon_{B\text{-}o}$ (%)	$\epsilon_h - \epsilon_{B\text{-}i}$ (%)
7 (1,000)	0.89	3 (10)	2.2	-0.2	±0.7	0.5	-0.9	-0.7
		6 (20)	4.3	-0.4	±1.4	1.0	-1.7	-1.4
		9 (30)	6.5	-0.6	±2.0	1.5	-2.6	-2.1
21 (3,000)	0.70	3 (10)	0.8	-0.2	±0.2	0.1	-0.4	-0.3
		6 (20)	1.5	-0.3	±0.5	0.2	-0.8	-0.7
		9 (30)	2.2	-0.5	±0.7	0.2	-1.2	-1.0

Notes for Tables C-2 and C-3:
- Positive strain indicates tension.
- Bending and combined strains are computed at outside surface.
- For PE, inside bending strains will be 55 percent of outside bending strains.
- For PVC, inside bending strains will be 74 percent of outside bending strains.
- All loads are long-term service loads.
- Pipe stiffness is computed as $PS_B = E I / (0.149 R^3)$
- Bending strain is computed as: $\epsilon_B = D_f (C_x / R) (\Delta_y / D)$ with $D_f = 6$
- $K_x = 0.110$, and $D_l = 1.50$

TABLE C-4 Strain in 600-mm (24-in.)-diameter corrugated polyethylene (7.5 percent deflection)

M_s MPa (psi)	VAF	Soil Depth m (ft)	ϵ_h (%)	$\epsilon_{B\text{-}o}$ (outside) (%)	Combined Strains		
					$\epsilon_h + \epsilon_{B\text{-}o}$ (%)	$\epsilon_h - \epsilon_{B\text{-}o}$ (%)	$\epsilon_h - \epsilon_{B\text{-}i}$ (%)
7 (1,000)	0.55	3 (10)	-0.9	±5.3	4.3	-6.2	-3.8
		6 (20)	-1.8	±5.3	3.4	-7.1	-4.7
		9 (30)	-2.8	±5.3	2.5	-8.0	-5.6
21 (3,000)	0.30	3 (10)	-0.5	±5.3	4.8	-5.8	-3.4
		6 (20)	-1.0	±5.3	4.3	-6.3	-3.9
		9 (30)	-1.5	±5.3	3.8	-6.8	-4.4

TABLE C-5 Strain in 600-mm (24-in.)-diameter corrugated PVC (7.5 percent deflection)

M_s MPa (psi)	VAF	Soil Depth m (ft)	ϵ_h (%)	$\epsilon_{B\text{-}o}$ (outside) (%)	Combined Strains		
					$\epsilon_h + \epsilon_{B\text{-}o}$ (%)	$\epsilon_h - \epsilon_{B\text{-}o}$ (%)	$\epsilon_h - \epsilon_{B\text{-}i}$ (%)
7 (1,000)	0.55	3 (10)	-0.2	±2.4	2.2	-2.6	-2.0
		6 (20)	-0.4	±2.4	2.0	-2.8	-2.2
		9 (30)	-0.6	±2.4	1.8	-3.0	-2.4
21 (3,000)	0.30	3 (10)	-0.2	±2.4	2.2	-2.6	-1.9
		6 (20)	-0.3	±2.4	2.1	-2.7	-2.1
		9 (30)	-0.5	±2.4	1.9	-2.9	-2.3

- At 7.5 percent deflection, total compression strain in PE pipe is on the order of 5 to 8 percent, regardless of the installation type.

DISCUSSION

The analysis presented in this section indicates that, at currently allowed deflection levels of 7.5 percent, the in-ground compression strain levels are on the order of 7 to 9 percent for corrugated HDPE and on the order of 2.5 to 3 percent for corrugated PVC and always occur on the outside. This will vary as a function of the actual profile geometry. Using the shape factor method to estimate strains, the estimated bending strain levels should be conservative, but the method used to complete the calculations has been successfully used for other types of pipe for many years. These strain levels are comparable with the outside strain levels in the parallel plate test at a deflection level of 20 percent; however, the peak compression strains on the outside of the pipe occur at the location of the load plates. The influence of the plate on the pipe performance is not clear.

Inside compression strains at 7.5 percent deflection are on the order of 3.5 to 5.5 percent for corrugated HDPE and on the order of 2.0 to 2.5 percent for corrugated PVC. For HDPE, these values are generally less than achieved in the parallel plate test at 20 percent deflection.

The parallel plate test was developed to evaluate flexural properties of pipe and it does not appear to be suitable for evaluating the compression behavior of profile wall pipe.

Table C-1 also indicates that the strain rates are substantially different for the various profile geometries and diameters that were evaluated. It may be more appropriate to select parallel plate load rates that produce consistent strain rates.

APPENDIX D

EXAMPLE CALCULATIONS

This appendix contains sample calculations of the proposed design method. The first two examples are detailed, step-by-step calculations—one for an HDPE pipe and one for a PVC pipe. These calculations show all steps in evaluating a design for local buckling effects. Both designs are for pipe embedded in crushed stone at a depth of 6.7 m (20 ft) with ground water over the top of the pipe (1.5 m for the HDPE pipe and 3 m for the PVC pipe).

Included are spreadsheet calculations for five different pipes in two different soil conditions. Each pipe is subjected to several levels of hoop compression stress. The section is then evaluated using the design method and the allowable depth of fill and allowable deflections level are then back-calculated on the basis of the reduced cross-sectional area. The two soil conditions considered are a compacted crushed stone (M_s = 33 MPa [4,800 psi]) and a dense silty backfill (M_s = 13.8 MPa [2,000 psi]).

All of the calculations determine the allowable deflection by relating strain to deflection through the use of a shape factor. The shape factor is described in the body of the report. All of the calculations made herein were completed with D_f = 6. Lower values will be applicable in many design situations.

Design Example:	900 mm Corrugated PE,	Sn100 Backfill

DESIGN INPUT

Pipe Geometry, Pipe Section and Material Properties, Soil Properties

Inside diameter... $D_i = 914.4$ mm   50-year modulus.................... $E = 151.58$ MPa

Centroidal diameter....................................... $D_c = 979.9$ mm   50-year strength .... $F_y = 6.20$ MPa

Outside diameter.. $D_o = 1081.0$ mm   Earth load factor.................... $\gamma_E = 1.95$

Pipe wall area per inch length......................... $A = 14.1$ mm$^2 \cdot$mm^{-1} Bending combined factor......... $\gamma_B = 1.50$

Pipe wall mom. of inertia per in. length............ $I = 12290.3 \cdot \dfrac{mm^4}{mm}$ Shape factor........................... $D_f = 6.00$

Edge support coefficient.......... $k = 4.00$

Total depth of fil over top of pipe...................... $H = 6.71$ m

Resistance factor for the pipe... $\phi_p = 1.00$

Depth of water above springline....................... $Hs = 2.06$ m   Resistance factor for the soil.... $\phi_s = 0.90$

Unit weight of wet soil.................................... $\gamma_s = 18.85$ kN$\cdot$m^{-3}

Unit weight of bouyant soil............................. $\gamma_b = 11.78$ kN$\cdot$m^{-3}

Soil type (Sn, Si or Cl).............................. soiltype = "Sn"

Compaction (100, 95, 90 or 85). Note that 100 is not available for Si and Cl soils)............... comp = 100

Additional properties for global behavior of pipe wall

Centroidal radius of the pipe... $R_c := 0.5 \cdot D_c$ $R_c = 490.0$ mm

Distance to extreme inside fiber of the pipe wall............ $c_{in} := 0.5 \cdot (D_c - D_i)$ $c_{in} = 32.8$ mm

Distance to extreme outside fiber of the pipe wall.......... $c_{out} := 0.5 \cdot (D_o - D_c)$ $c_{out} = 50.5$ mm

Strain Limits

Factored hoop compression strain at yield strength (computed from long term modulus and strength)........... $\varepsilon_{hc} := \dfrac{F_y}{E}$ $\varepsilon_{hc} = 4.09\%$

Limiting total compression... $\varepsilon_{tc} := 1.5 \cdot \varepsilon_{hc}$ $\varepsilon_{tc} = 6.14\%$

Limiting total tension strain... $\varepsilon_{tt} := 1.5 \cdot 5.0 \cdot \%$ $\varepsilon_{tt} = 7.50\%$

Notes : Tension strain is based on a factor of safety times the allowable strain. The sign convention for strain assumes that tension is negative.

Design Example:	900 mm Corrugated PE,	Sn100 Backfill

Detailed pipe geometry (for local buckling calculation)

Crest (Element 1)

Web (Element 2) →

← Valley (Element 3)

Liner (Element 4)

Period

Width (b)

Height (h)

Idealized Corrugation
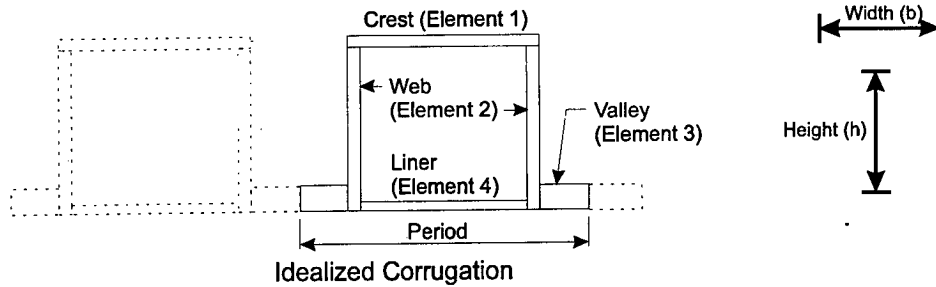
Pipe element dimensions

Index for defining the four section elements..... $i := 1, 2 .. 4$

Element Number:	Total Width:	Element Effective Buckling Width:	Element Thickness:	Width / Thickness:
$i =$	$\dfrac{b_i}{mm} =$	$\dfrac{w_i}{mm} =$	$\dfrac{t_i}{mm} =$	$w_i \cdot (t_i)^{-1} =$
1.00				16.89
2.00	91.24	79.81	4.72	10.94
3.00	71.15	62.53	5.71	5.85
4.00	25.20	50.39	8.61	21.94
	74.68	74.68	3.40	

Area of idealized geometry (compare to actual)..............

$$\frac{b_1 \cdot t_1 + 2 \cdot b_2 \cdot t_2 + 2 \cdot b_3 \cdot t_3 + b_4 \cdot t_4}{b_3 + t_2 + b_4 + t_2 + b_3} = 14.2 \cdot \frac{mm^2}{mm}$$

Period of the corrugations.. $Period := b_4 + 2 \cdot t_2 + 2 \cdot b_3$ Period = 136.50 mm

Overall area of each period... $A_g := Period \cdot A$ $A_g = 1931.17 \, mm^2$

Note: Full section properties include 2 each of elements 2 and 3.

| Design Example: | 900 mm Corrugated PE, | Sn100 Backfill |

SOIL PRESSURES AND CONSTRAINED MODULUS

Pressure due to soil above the water table........... $P_{sps} := \left[H - \left(Hs - \frac{1}{2} \cdot D_o\right)\right] \cdot \gamma_s$ $P_{sps} = 98 \cdot kN \cdot m^{-2}$

Pressure due to soil below the water table........... $P_{spb} := \gamma_b \cdot \left(Hs - \frac{1}{2} \cdot D_o + 0.11 \cdot D_o\right)$ $P_{spb} = 19 \cdot kN \cdot m^{-2}$

Total vertical soil pressure................................. $P_{sp} := \left(P_{sps} + P_{spb}\right)$ $P_{sp} = 117 \cdot kPa$

Hydrostatic water pressure at springline.............. $P_w := Hs \cdot 9.80 \cdot kN \cdot m^{-3}$ $P_w = 20 \cdot kPa$

Soil stiffness (interpolate from Table 18.1.4.3.1 on the basis of P_{sp}, note that hydrostatic pressure does not contribute to increasing effective soil stress)

$k_1 := type$ $k_1 = 1.00$

$k_2 := if(comp > 97, 1, if(comp > 92, 2, if(comp > 87, 3, 4)))$ $k_2 = 1.00$

Defining row number to be selected..........

$r := if(P_{sp} < 35 \cdot kPa, 1, if(P_{sp} < 69 \cdot kPa, 2, if(P_{sp} < 138 \cdot kPa, 3, if(P_{sp} < 275 \cdot kPa, 4, if(P_{sp} > 413 \cdot kPa, 6, 5$

                                                          $r = 3.00$

Defining column number to be selected.....

$n := if\left[k_1 < 1.5, k_2, if\left[k_1 < 2.5, (3 + k_2), (6 + k_2)\right]\right]$ $n = 1.00$

Vertical Soil Stress (kPa)   Matrix of M_s values (MPa) for various soils at selected soil stress levels

                           Sn100 Sn95 Sn90 Sn85 Si95 Si90 Si85 Cl95 Cl90 Cl85

$$Pmet := \begin{bmatrix} 7 \\ 35 \\ 69 \\ 138 \\ 275 \\ 413 \end{bmatrix} \quad Kmet := \begin{bmatrix} 16.2 & 13.8 & 8.8 & 3.2 & 9.8 & 4.6 & 2.5 & 3.7 & 1.8 & 0.9 \\ 23.8 & 17.9 & 10.3 & 3.6 & 11.5 & 5.1 & 2.7 & 4.3 & 2.2 & 1.2 \\ 29.0 & 20.7 & 11.2 & 3.9 & 12.2 & 5.2 & 2.8 & 4.8 & 2.4 & 1.4 \\ 37.9 & 23.8 & 12.4 & 4.5 & 13.0 & 5.4 & 3.0 & 5.1 & 2.7 & 1.6 \\ 51.7 & 29.3 & 14.5 & 5.7 & 14.4 & 6.2 & 3.5 & 5.6 & 3.2 & 2.0 \\ 64.1 & 34.5 & 17.2 & 6.9 & 15.9 & 7.1 & 4.1 & 6.2 & 3.6 & 2.4 \end{bmatrix}$$

$q := if(r > 5.5, 6, (r + 1))$ $Pmet_r = 69$ $Pmet_q = 138$

$Kmet_{r,n} = 29.0$ $Kmet_{q,n} = 37.9$

$warn1 := if(r > 5.5, 1, if(n > 4.5, if(n < 7.5, if(r > 4.5, 1, 0), 0), 0))$

$warn2 := if(warn1 > 0.5, \text{"VERTICAL PRESSURE EXCEEDS RANGE OF DATA - STOP ANALYSIS"}, \text{"Ms OKAY"})$

$$M_s := \left[\frac{\left(\dfrac{P_{sp}}{kPa} - Pmet_r\right)}{\left(Pmet_q - Pmet_r\right)} \cdot \left(Kmet_{q,n} - Kmet_{r,n}\right) + Kmet_{r,n}\right] \cdot MPa \qquad M_s = 35.2 \cdot MPa$$

Is the computed value valid? $warn2 = \text{"Ms OKAY"}$

Design Example:	900 mm Corrugated PE,	Sn100 Backfill

HOOP COMPRESSION CAPACITY (ignoring local buckling)

Hoop stiffness factor......................... $S_H := \dfrac{\phi_s \cdot M_s \cdot R_c}{E \cdot A}$ $S_H = 7.235$

Vertical arching factor...................... $VAF := 0.76 - 0.71 \cdot \left(\dfrac{S_H - 1.17}{S_H + 2.92} \right)$ $VAF = 0.34$

Ultimate thrust............................... $T_s := \gamma_E \cdot 0.5 \cdot D_o \cdot (VAF \cdot P_{sp} + P_w)$ $T_s = 62.77 \bullet \dfrac{kN}{m}$

Ultimate hoop compression stress.... $\sigma_{ch} := \dfrac{T_s}{A}$ $\sigma_{ch} = 4.43 \bullet MPa$

Ultimate hoop compression strain..... $\varepsilon_c := \dfrac{\sigma_{ch}}{E}$ $\varepsilon_c = 2.92 \bullet \%$

Check hoop compression capacity

$Status := if\left(\phi_p \cdot F_y > \sigma_{ch}, \text{"OK"}, \text{"NG"} \right)$ $Status = \text{"OK"}$

$Adequacy_h := \dfrac{\phi_p \cdot F_y}{\sigma_{ch}}$ $Adequacy_h = 1.40$

CAPACITY OF SECTION (considering local buckling)

$$\varepsilon_c = 2.92\% \qquad \lambda_i := \frac{w_i}{t_i} \cdot \left(\frac{\varepsilon_c}{k}\right)^{0.5} \qquad \rho_i := \text{if}\left[\lambda_i > 0.673, \frac{1}{\lambda_i} \cdot \left(1 - \frac{0.22}{\lambda_i}\right), 1\right]$$

i =

1.00
2.00
3.00
4.00

Slenderness factors:

$\lambda_i =$

1.44
0.94
0.50
1.88

Fractional Effectiveness of each element:

$\rho_i =$

0.59
0.82
1.00
0.47

Effective wall area.........................
$$A_{eff} := \frac{1}{\text{Period}} \cdot \left[A_g - \sum_i \left(1 - \rho_i\right) \cdot w_i \cdot t_i - \left(1 - \rho_2\right) \cdot w_2 \cdot t_2\right]$$
$$A_{eff} = 11.06 \cdot \frac{mm^2}{mm}$$

$$\sigma_{bck} := \frac{T_s}{A_{eff}}$$
$$\sigma_{bck} = 5.67 \cdot MPa$$

Recheck the hoop compression with the reduced area

$$\text{Status} := \text{if}\left(\phi_p \cdot F_y > \sigma_{bck}, \text{"OK"}, \text{"NG"}\right)$$
Status = "OK"

$$\text{Adequacy}_{bck} := \frac{\phi_p \cdot F_y}{\sigma_{bck}}$$
$$\text{Adequacy}_{bck} = 1.09$$

SUMMARY OF HOOP COMPRESSION CALCULATIONS

	Ultimate Hoop Compression Stress	Ratio of ultimate applied hoop compression stress to ultimate hoop compression capacity
Based on gross area	$\sigma_{ch} = 643 \cdot psi$	$\text{Adequacy}_h = 1.40$
Based on local buckling	$\sigma_{bck} = 823 \cdot psi$	$\text{Adequacy}_{bck} = 1.09$

Effective Area (% of gross area)

$$A_{\%eff} := \frac{A_{eff}}{A}$$
$$A_{\%eff} = 78 \cdot \%$$

| Design Example: | 900 mm Corrugated PE, | Sn100 Backfill |

CHECK ALLOWABLE DEFLECTION BASED ON AVAILABLE STRAIN CAPACITY

Hoop strain:.. $\varepsilon_c := \dfrac{\sigma_{bck}}{E}$ $\qquad$ $\varepsilon_c = 3.74\%$

Allowable tension strain capacity for bending.................... $\varepsilon_{bt} := \left(\phi \cdot \varepsilon_{tt} + \varepsilon_c \cdot \dfrac{1}{\gamma_E}\right) \cdot \dfrac{1}{\gamma_B}$ $\qquad$ $\varepsilon_{bt} = 6.28\%$

Allowable compression strain capacity for bending............. $\varepsilon_{bc} := \left(\phi \cdot \varepsilon_{tc} - \varepsilon_c \cdot \dfrac{\gamma_B}{\gamma_E}\right) \cdot \dfrac{1}{\gamma_B}$ $\qquad$ $\varepsilon_{bc} = 2.17\%$

Use **AWWA Manual M45** *Manual of Water Supply Practices*
Fiberglass Pipe Design Eq. 5-6 to relate strain to deflection: $\qquad$ $\varepsilon_b = D_f * c/R * \Delta/D$

Case One - Positive bending with crest in compression

Limiting allowable deflection based on tension on inside............... $\Delta_1 := \varepsilon_{bt} \cdot \left(\dfrac{1}{D_f}\right) \cdot \left(\dfrac{R_c}{c_{in}}\right)$ $\qquad$ $\Delta_1 = 15.6\%$

Limiting allowable deflection based on compression on outside..... $\Delta_2 := \varepsilon_{bc} \cdot \left(\dfrac{1}{D_f}\right) \cdot \left(\dfrac{R_c}{c_{out}}\right)$ $\qquad$ $\Delta_2 = 3.51\%$

Case Two - Negative bending with valley in compression

Limiting allowable deflection based on compression on inside........ $\Delta_3 := \varepsilon_{bc} \cdot \left(\dfrac{1}{D_f}\right) \cdot \left(\dfrac{R_c}{c_{in}}\right)$ $\qquad$ $\Delta_3 = 5.42\%$

Limiting allowable deflection based on tension on outside............ $\Delta_4 := \varepsilon_{bt} \cdot \left(\dfrac{1}{D_f}\right) \cdot \left(\dfrac{R_c}{c_{out}}\right)$ $\qquad$ $\Delta_4 = 10.1\%$

Determine the service level deflection by extracting the
minimum factored deflection from the above two cases................. $\Delta_{SLD} := \min\left[\begin{bmatrix} \Delta_1 \\ \Delta_2 \\ \Delta_3 \\ \Delta_4 \end{bmatrix}\right]$ $\qquad$ $\Delta_{SLD} = 3.5\%$

DESIGN SUMMARY:

Depth of fill.. $H = 6.71$ m

Density of fill... $\gamma_s = 18.85 \cdot kN \cdot m^{-3}$

Hoop Thrust Evaluation................................ Adequacy $_{bck} = 1.09$

Allowable bending deflection........................ $\Delta_{SLD} = 3.5\%$

$\Delta_{hoop} := \varepsilon_c \cdot \gamma_E^{-1}$ $\qquad$ $\Delta_{hoop} = 1.9\%$

Total allowable change in vertical diameter.... $\Delta_{SLD} + \Delta_{hoop} = 5.43\%$

| Design Example: | 600 mm Corrugated PVC, | Sn100 Backfill |

DESIGN INPUT

Pipe Geometry, Pipe Section and Material Properties, Soil Properties

Inside diameter... $D_i = 609.6$ mm

50-year modulus..................... $E = 1088.62$ MPa

Centroidal diameter....................................... $D_c = 634.0$ mm

50-year strength .... $F_y = 17.91$ MPa

Outside diameter.. $D_o = 665.0$ mm

Earth load factor..................... $\gamma_E = 1.95$

Pipe wall area per inch length......................... $A = 9.3$ mm$^2 \cdot$mm^{-1}

Bending combined factor......... $\gamma_B = 1.50$

Pipe wall mom. of inertia per in. length............ $I = 983.2 \cdot \dfrac{mm^4}{mm}$

Shape factor........................... $D_f = 6.00$

Total depth of fil over top of pipe...................... $H = 6.71$ m

Edge support coefficient......... $k = 4.00$

Resistance factor for the pipe... $\phi_p = 1.00$

Depth of water above springline....................... $Hs = 1.86$ m

Resistance factor for the soil.... $\phi_s = 0.90$

Unit weight of wet soil................................... $\gamma_s = 18.85$ kN$\cdot$m^{-3}

Unit weight of bouyant soil............................. $\gamma_b = 11.78$ kN$\cdot$m^{-3}

Soil type (Sn, Si or Cl).............................. soiltype = "Sn"

Compaction (100, 95, 90 or 85). Note that 100 is not available for Si and Cl soils)................ comp = 100

Additional properties for global behavior of pipe wall

Centroidal radius of the pipe... $R_c := 0.5 \cdot D_c$ $R_c = 317.0$ mm

Distance to extreme inside fiber of the pipe wall............. $c_{in} := 0.5 \cdot (D_c - D_i)$ $c_{in} = 12.2$ mm

Distance to extreme outside fiber of the pipe wall.......... $c_{out} := 0.5 \cdot (D_o - D_c)$ $c_{out} = 15.5$ mm

Strain Limits

Factored hoop compression strain at yield strength (computed from long term modulus and strength).......... $\varepsilon_{hc} := \dfrac{F_y}{E}$ $\varepsilon_{hc} = 1.65$ %

Limiting total compression... $\varepsilon_{tc} := 1.5 \cdot \varepsilon_{hc}$ $\varepsilon_{tc} = 2.47$ %

Limiting total tension strain... $\varepsilon_{tt} := 1.5 \cdot 3.5 \cdot \%$ $\varepsilon_{tt} = 5.25$ %

Notes : Tension strain is based on a factor of safety times the allowable strain. The sign convention for strain assumes that tension is negative.

Design Example: **600 mm Corrugated PVC,**   **Sn100 Backfill**

Detailed pipe geometry (for local buckling calculation)

Crest (Element 1)

Web (Element 2)

Valley (Element 3)

Liner (Element 4)

Period

Width (b)

Height (h)

Idealized Corrugation
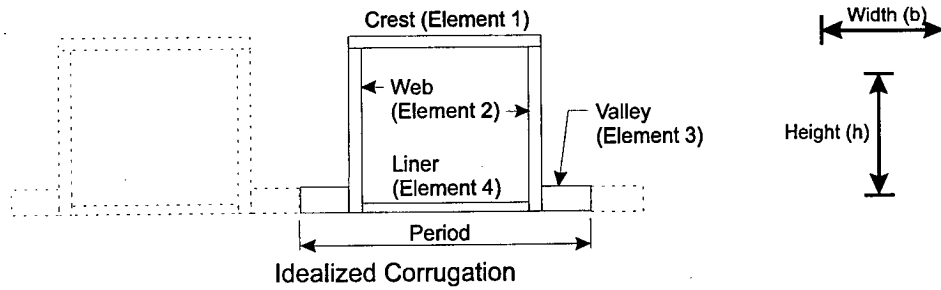
Pipe element dimensions

Index for defining the four section elements..... $i := 1, 2 .. 4$

Element Number:	Total Width:	Element Effective Buckling Width:	Element Thickness:	Width / Thickness:
$i =$	$b_i :=$	$w_i :=$	$t_i :=$	$w_i \cdot (t_i)^{-1} =$
1.00	$1.351 \cdot in$	$1.053 \cdot in$	$0.130 \cdot in$	8.10
2.00	$0.959 \cdot in$	$0.764 \cdot in$	$0.149 \cdot in$	5.13
3.00	$0.168 \cdot in$	$0.336 \cdot in$	$0.195 \cdot in$	1.72
4.00	$1.267 \cdot in$	$1.267 \cdot in$	$0.135 \cdot in$	9.39

Area of idealized geometry (compare to actual)..............
$$\frac{b_1 \cdot t_1 + 2 \cdot b_2 \cdot t_2 + 2 \cdot b_3 \cdot t_3 + b_4 \cdot t_4}{b_3 + t_2 + b_4 + t_2 + b_3} = 9.3 \circ \frac{mm^2}{mm}$$

Period of the corrugations.. $Period := b_4 + 2 \cdot t_2 + 2 \cdot b_3$ $Period = 48.29 \circ mm$

Overall area of each period... $A_g := Period \cdot A$ $A_g = 450.11 \circ mm^2$

Note: Full section properties include 2 each of elements 2 and 3.

Design Example:	600 mm Corrugated PVC,	Sn100 Backfill

SOIL PRESSURES AND CONSTRAINED MODULUS

Pressure due to soil above the water table........... $P_{sps} := \left[H - \left(Hs - \frac{1}{2} \cdot D_o \right) \right] \cdot \gamma_s$ $\qquad$ $P_{sps} = 98 \cdot kN \cdot m^{-2}$

Pressure due to soil below the water table........... $P_{spb} := \gamma_b \cdot \left(Hs - \frac{1}{2} \cdot D_o + 0.11 \cdot D_o \right)$ $\qquad$ $P_{spb} = 19 \cdot kN \cdot m^{-2}$

Total vertical soil pressure................................. $P_{sp} := \left(P_{sps} + P_{spb} \right)$ $\qquad$ $P_{sp} = 116.4 \cdot kPa$

Hydrostatic water pressure at springline.............. $P_w := Hs \cdot 9.80 \cdot kN \cdot m^{-3}$ $\qquad$ $P_w = 18 \cdot kPa$

Soil stiffness (interpolate from Table 18.1.4.3.1 on the basis of P_{sp}, note that hydrostatic pressure does not contribute to increasing effective soil stress)

$k_1 := type$ $\qquad$ $k_1 = 1.00$

$k_2 := if(comp > 97, 1, if(comp > 92, 2, if(comp > 87, 3, 4)))$ $\qquad$ $k_2 = 1.00$

Defining row number to be selected..........

$r := if(P_{sp} < 35 \cdot kPa, 1, if(P_{sp} < 69 \cdot kPa, 2, if(P_{sp} < 138 \cdot kPa, 3, if(P_{sp} < 275 \cdot kPa, 4, if(P_{sp} > 413 \cdot kPa, 6, 5)))))$

$\qquad\qquad\qquad r = 3.00$

Defining column number to be selected.....

$n := if\left[k_1 < 1.5, k_2, if\left[k_1 < 2.5, (3 + k_2), (6 + k_2) \right] \right]$ $\qquad$ $n = 1.00$

Vertical Soil Stress (kPa)

Matrix of M_s values (MPa) for various soils at selected soil stress levels

Sn100 Sn95 Sn90 Sn85 Si95 Si90 Si85 Cl95 Cl90 Cl85

$$Pmet := \begin{bmatrix} 7 \\ 35 \\ 69 \\ 138 \\ 275 \\ 413 \end{bmatrix} \qquad Kmet := \begin{bmatrix} 16.2 & 13.8 & 8.8 & 3.2 & 9.8 & 4.6 & 2.5 & 3.7 & 1.8 & 0.9 \\ 23.8 & 17.9 & 10.3 & 3.6 & 11.5 & 5.1 & 2.7 & 4.3 & 2.2 & 1.2 \\ 29.0 & 20.7 & 11.2 & 3.9 & 12.2 & 5.2 & 2.8 & 4.8 & 2.4 & 1.4 \\ 37.9 & 23.8 & 12.4 & 4.5 & 13.0 & 5.4 & 3.0 & 5.1 & 2.7 & 1.6 \\ 51.7 & 29.3 & 14.5 & 5.7 & 14.4 & 6.2 & 3.5 & 5.6 & 3.2 & 2.0 \\ 64.1 & 34.5 & 17.2 & 6.9 & 15.9 & 7.1 & 4.1 & 6.2 & 3.6 & 2.4 \end{bmatrix}$$

$q := if(r > 5.5, 6, (r + 1))$ $\qquad$ $Pmet_r = 69$ $\qquad$ $Pmet_q = 138$

$Kmet_{r,n} = 29.0$ $\qquad$ $Kmet_{q,n} = 37.9$

$warn1 := if(r > 5.5, 1, if(n > 4.5, if(n < 7.5, if(r > 4.5, 1, 0), 0), 0))$

$warn2 := if(warn1 > 0.5, "VERTICAL PRESSURE EXCEEDS RANGE OF DATA - STOP ANALYSIS", "Ms OKAY")$

$$M_s := \left[\frac{\left(\frac{P_{sp}}{kPa} - Pmet_r \right)}{(Pmet_q - Pmet_r)} \cdot (Kmet_{q,n} - Kmet_{r,n}) + Kmet_{r,n} \right] \cdot MPa \qquad M_s = 35.1 \cdot MPa$$

Is the computed value valid? $\qquad$ $warn2 = "Ms OKAY"$

Design Example:	600 mm Corrugated PVC,	Sn100 Backfill

HOOP COMPRESSION CAPACITY (ignoring local buckling)

Hoop stiffness factor....................... $S_H := \dfrac{\phi_s \cdot M_s \cdot R_c}{E \cdot A}$ $S_H = 0.987$

Vertical arching factor..................... $VAF := 0.76 - 0.71 \cdot \left(\dfrac{S_H - 1.17}{S_H + 2.92} \right)$ $VAF = 0.79$

Ultimate thrust............................... $T_s := \gamma_E \cdot 0.5 \cdot D_o \cdot \left(VAF \cdot P_{sp} + P_w \right)$ $T_s = 71.71 \cdot \dfrac{kN}{m}$

Ultimate hoop compression stress.... $\sigma_{ch} := \dfrac{T_s}{A}$ $\sigma_{ch} = 7.69 \cdot MPa$

Ultimate hoop compression strain..... $\varepsilon_c := \dfrac{\sigma_{ch}}{E}$ $\varepsilon_c = 0.71 \cdot \%$

Check hoop compression capacity

$Status := if\left(\phi_p \cdot F_y > \sigma_{ch}, "OK", "NG" \right)$ $Status = "OK"$

$Adequacy_h := \dfrac{\phi_p \cdot F_y}{\sigma_{ch}}$ $Adequacy_h = 2.33$

Design Example:	600 mm Corrugated PVC,	Sn100 Backfill

CAPACITY OF SECTION (considering local buckling)

$$\varepsilon_c = 0.71\,\% \qquad \lambda_i := \frac{w_i}{t_i} \cdot \left(\frac{\varepsilon_c}{k}\right)^{0.5} \qquad \rho_i := if\left[\lambda_i > 0.673, \frac{1}{\lambda_i} \cdot \left(1 - \frac{0.22}{\lambda_i}\right), 1\right]$$

i =

| 1.00 |
| 2.00 |
| 3.00 |
| 4.00 |

Slenderness factors:

λ_i =

| 0.34 |
| 0.22 |
| 0.07 |
| 0.39 |

Fractional
Effectiveness of
each element:

ρ_i =

| 1.00 |
| 1.00 |
| 1.00 |
| 1.00 |

Effective wall area.........................
$$A_{eff} := \frac{1}{Period}\left[A_g - \sum_i (1 - \rho_i) \cdot w_i \cdot t_i - (1 - \rho_2) \cdot w_2 \cdot t_2\right] \qquad A_{eff} = 9.32 \cdot \frac{mm^2}{mm}$$

$$\sigma_{bck} := \frac{T_s}{A_{eff}} \qquad\qquad \sigma_{bck} = 7.69 \cdot MPa$$

Recheck the hoop
compression with
the reduced area

$$Status := if\left(\phi_p \cdot F_y > \sigma_{bck}, "OK", "NG"\right) \qquad Status = "OK"$$

$$Adequacy_{bck} := \frac{\phi_p \cdot F_y}{\sigma_{bck}} \qquad\qquad Adequacy_{bck} = 2.33$$

SUMMARY OF HOOP COMPRESSION CALCULATIONS

	Ultimate Hoop Compression Stress	Ratio of ultimate applied hoop compression stress to ultimate hoop compression capacity
Based on gross area	$\sigma_{ch} = 1116 \cdot psi$	$Adequacy_h = 2.33$
Based on local buckling	$\sigma_{bck} = 1116 \cdot psi$	$Adequacy_{bck} = 2.33$

Effective Area (% of gross area)

$$A_{\%eff} := \frac{A_{eff}}{A} \qquad\qquad A_{\%eff} = 100 \cdot \%$$

Design Example:	600 mm Corrugated PVC,	Sn100 Backfill

CHECK ALLOWABLE DEFLECTION BASED ON AVAILABLE STRAIN CAPACITY

Hoop strain:.. $\varepsilon_c := \dfrac{\sigma_{bck}}{E}$ $\varepsilon_c = 0.71\%$

Allowable tension strain capacity for bending.................... $\varepsilon_{bt} := \left(\phi \cdot \varepsilon_{tt} + \varepsilon_c \cdot \dfrac{1}{\gamma_E}\right) \cdot \dfrac{1}{\gamma_B}$ $\varepsilon_{bt} = 3.74\%$

Allowable compression strain capacity for bending............ $\varepsilon_{bc} := \left(\phi \cdot \varepsilon_{tc} - \varepsilon_c \cdot \dfrac{\gamma_B}{\gamma_E}\right) \cdot \dfrac{1}{\gamma_B}$ $\varepsilon_{bc} = 1.28\%$

Use AWWA Manual M45 *Manual of Water Supply Practices Fiberglass Pipe Design* Eq. 5-6 to relate strain to deflection: $\varepsilon_b = D_f * c/R * \Delta/D$

Case One - Positive bending with crest in compression

Limiting allowable deflection based on tension on inside............... $\Delta_1 := \varepsilon_{bt} \cdot \left(\dfrac{1}{D_f}\right) \cdot \left(\dfrac{R_c}{c_{in}}\right)$ $\Delta_1 = 16.2\%$

Limiting allowable deflection based on compression on outside..... $\Delta_2 := \varepsilon_{bc} \cdot \left(\dfrac{1}{D_f}\right) \cdot \left(\dfrac{R_c}{c_{out}}\right)$ $\Delta_2 = 4.38\%$

Case Two - Negative bending with valley in compression

Limiting allowable deflection based on compression on inside....... $\Delta_3 := \varepsilon_{bc} \cdot \left(\dfrac{1}{D_f}\right) \cdot \left(\dfrac{R_c}{c_{in}}\right)$ $\Delta_3 = 5.56\%$

Limiting allowable deflection based on tension on outside.............. $\Delta_4 := \varepsilon_{bt} \cdot \left(\dfrac{1}{D_f}\right) \cdot \left(\dfrac{R_c}{c_{out}}\right)$ $\Delta_4 = 12.8\%$

Determine the service level deflection by extracting the minimum factored deflection from the above two cases................. $\Delta_{SLD} := \min\left[\begin{bmatrix}\begin{bmatrix}\Delta_1 \\ \Delta_2 \\ \Delta_3 \\ \Delta_4\end{bmatrix}\end{bmatrix}\right]$ $\Delta_{SLD} = 4.4\%$

DESIGN SUMMARY:

Depth of fill... $H = 6.71 \text{ m}$

Density of fill... $\gamma_s = 18.85 \cdot kN \cdot m^{-3}$

Hoop Thrust Evaluation............................... Adequacy$_{bck}$ = 2.33

Allowable bending deflection........................ $\Delta_{SLD} = 4.4\%$

$\Delta_{hoop} := \varepsilon_c \cdot \gamma_E^{-1}$ $\Delta_{hoop} = 0.4\%$

Total allowable change in vertical diameter.... $\Delta_{SLD} + \Delta_{hoop} = 4.74\%$

Example Calculations

Section: A24   Corrugated HDPE   24 in. Inside Diameter

	Element 1 (Crest)	Element 2 (Web)	Element 3 (Valley)	Element 4 (Liner)			
I (in.)	2.62	1.94	0.24	2.31	E =	22000 psi	
t (in.)	0.08	0.10	0.22	0.10	k =	4	
w (in.)	2.42	1.71	0.47	2.31	Ag =	0.92 in^2	0.308 in.^2/in.
w/t	32.14	16.59	2.19	24.24	Ig =	0.58 in^4	0.195 in.^4/in.
					h =	2.02 in	

Installation Conditions

							SI	
			c-in (y-bar) =	0.87 in.	c-in/(c-in+cout)=	0.43	7.815811	area
Ms =	2000 psi		c-out (y-bar) =	1.15 in.	EA/R =	525.9	13.7931	Ms
Soil density =	120 pcf		R-centr. =	12.87 in.			3.6	depth
Design Factors			Df =	6.00			3.83%	defl
Earth load factor =	2	Limiting total compressive strain =		-6.14%			6.206897	
omb str. load factor =	1.5	Limiting tensile strain =		7.50%			17.93103	
Phi-soil =	0.9							
Phi-pipe =	1.00							

Positive moment is compression on the liner side.
Evaluate elements 1, 3, and 4 on combined strain, evaluate Element 2 based on hoop compression strain
Positive stress/strain = Tension

A. Check on Basis of Maximum Possible Deflection

Positive moment region (Bending causes tension on inside surface)

Factored Comp Stress (psi)	Factored Comp strain (%)	Available for Bending Strain-in (%)	Bending Strain-out (%)	Factored Vert. Defl. (%)	Total Strain-in (%)	Total Strain-out (%)	rho Elem. 1	Elem. 2	Elem. 3	Elem. 4	Effective Area (in^2/in.)	Effective I (in.^4/in.)	Area Reduction (%)	I Reduction (%)	Factored Load Carrying Capacity (lbs/in.)	Hoop Stiffness Factor (psi)	VAF	Allowable Depth of Fill (ft)	Allowable Deflection (%)
0	0.00%	7.50%	-6.14%	11.5%	4.67%	-6.14%	0.237	1.000	1.000	1.000	0.26	0.121	16%	38%	0	3.42	0.51	0.0	7.65%
-200	-0.91%	8.18%	-5.45%	10.2%	3.24%	-6.36%	0.233	0.913	1.000	1.000	0.25	0.109	20%	44%	98	3.42	0.51	4.1	6.80%
-400	-1.82%	8.86%	-4.77%	8.9%	1.81%	-6.59%	0.229	0.718	1.000	1.000	0.22	0.089	29%	54%	175	3.42	0.51	7.4	5.95%
-600	-2.73%	9.55%	-4.09%	7.7%	0.38%	-6.82%	0.226	0.613	1.000	1.000	0.20	0.080	33%	59%	246	3.42	0.51	10.3	5.10%
-655	-2.98%	9.73%	-3.90%	7.3%	-0.01%	-6.88%	0.225	0.591	1.000	1.000	0.20	0.079	34%	60%	264	3.42	0.51	11.1	4.87%
-800	-3.64%	10.23%	-3.41%	6.4%	-1.04%	-7.05%	0.222	0.544	1.000	0.664	0.17	0.068	45%	65%	273	3.42	0.51	11.5	4.25%
-900	-4.09%	10.57%	-3.07%	5.7%	-1.76%	-7.16%	0.221	0.518	1.000	0.537	0.16	0.063	49%	67%	283	3.42	0.51	11.9	3.83%

Negative moment region (Bending causes tension on outside surface)

Comp Stress (psi)	Comp strain (%)	Available for Bending Strain-in (%)	Bending Strain-out (%)	Factored Vert. Defl. (%)	Total Strain-in (%)	Total Strain-out (%)	rho Elem. 1	Elem. 2	Elem. 3	Elem. 4	Effective Area (in^2/in.)	Effective I (in.^4/in.)	Area Reduction (%)	I Reduction (%)	Factored Load Carrying Capacity (lbs/in.)	Hoop Stiffness Factor (psi)	VAF	Allowable Depth of Fill (ft)	Allowable Deflection (%)
0	0.00%	-6.14%	7.500%	14.0%	-5.70%	7.50%	1.000	1.000	1.000	0.319	0.26	0.154	16%	21%	0	3.42	0.51	0.0	7.02%
-200	-0.91%	-5.45%	8.18%	13.4%	-6.36%	6.26%	1.000	0.913	1.000	0.304	0.24	0.143	20%	27%	98	3.42	0.51	4.1	6.71%
-400	-1.82%	-4.77%	8.86%	11.7%	-6.59%	4.46%	1.000	0.718	1.000	0.299	0.22	0.126	29%	35%	175	3.42	0.51	7.4	5.87%
-600	-2.73%	-4.09%	9.55%	10.1%	-6.82%	2.65%	1.000	0.613	1.000	0.294	0.20	0.119	34%	39%	245	3.42	0.51	10.3	5.03%
-655	-2.98%	-3.90%	9.73%	9.6%	-6.88%	2.16%	1.000	0.591	1.000	0.293	0.20	0.118	35%	39%	263	3.42	0.51	11.1	4.80%
-800	-3.64%	-3.41%	10.23%	8.4%	-7.05%	0.85%	1.000	0.544	1.000	0.290	0.19	0.116	37%	40%	311	3.42	0.51	13.1	4.19%
-900	-4.09%	-3.07%	10.57%	7.5%	-7.16%	-0.06%	1.000	0.518	1.000	0.287	0.19	0.115	38%	41%	343	3.42	0.51	14.5	3.77%

Section: B48   Corrugated HDPE   48 in. Inside Diameter

	Element 1 (Crest)	Element 2 (Web)	Element 3 (Valley)	Element 4 (Liner)				
I (in.)	3.50	2.56	0.91	3.56	E =	22000 psi		
t (in.)	0.14	0.19	0.28	0.12	k =	4		
w (in.)	3.12	2.28	1.82	3.56	Ag =	2.40 in^2	0.417 in.^2/in.	
w/t	22.29	12.00	6.50	29.67	Ig =	2.65 in^4	0.459 in.^4/in.	
					h =	2.70 in		

Installation Conditions

		c-in (y-bar) =	1.10 in.	c-in/(c-in+cout)= 0.41
Ms =	2000 psi	c-out (y-bar) =	1.60 in.	EA/R = 365.2
Soil density =	120 pcf	R-centr. =	25.10 in.	
Design Factors		Df =	6.00	
Earth load factor =	2	Limiting total compressive strain =	-6.14%	
omb str. load factor =	1.5	Limiting tensile strain =	7.50%	
Phi-soil =	0.9			
Phi-pipe	1.00			

SI
10.58157 area
13.7931 Ms
3.8 depth
5.34% defl

Positive moment is compression on the liner side.
Evaluate elements 1, 3, and 4 on combined strain, evaluate Element 2 based on hoop compression strain
Positive stress/strain = Tension

A. Check on Basis of Maximum Possible Deflection

Positive moment region (Bending causes tension on inside surface)

Factored Comp Stress (psi)	Factored Comp strain (%)	Available for Bending Strain-in (%)	Factored Bending Strain-out (%)	Factored Vert. Defl. (%)	Total Strain-in (%)	Total Strain-out (%)	rho Elem. 1	Elem. 2	Elem. 3	Elem. 4	Effective Area (in^2/in.)	Effective I (in.^4/in.)	Area Reduction (%)	I Reduction (%)	Factored Load Carrying Capacity (lbs/in.)	Hoop Stiffness Factor (psi)	VAF	Allowable Depth of Fill (ft)	Allowable Deflection (%)
0	0.00%	7.50%	-6.14%	16.0%	4.20%	-6.14%	0.333	1.000	1.000	1.000	0.36	0.305	14%	34%	0	4.93	0.42	0.0	10.67%
-200	-0.91%	8.18%	-5.45%	14.2%	2.82%	-6.36%	0.328	1.000	1.000	1.000	0.36	0.303	14%	34%	144	4.93	0.42	3.8	9.48%
-400	-1.82%	8.86%	-4.77%	12.4%	1.44%	-6.59%	0.323	0.900	1.000	1.000	0.34	0.274	18%	40%	274	4.93	0.42	7.3	8.30%
-600	-2.73%	9.55%	-4.09%	10.7%	0.07%	-6.82%	0.318	0.785	1.000	1.000	0.32	0.246	23%	47%	387	4.93	0.42	10.3	7.11%
-655	-2.98%	9.73%	-3.90%	10.2%	-0.31%	-6.88%	0.316	0.761	1.000	0.890	0.31	0.236	26%	49%	406	4.93	0.42	10.9	6.79%
-800	-3.64%	10.23%	-3.41%	8.9%	-1.31%	-7.05%	0.313	0.706	1.000	0.513	0.27	0.208	35%	55%	436	4.93	0.42	11.7	5.93%
-900	-4.09%	10.57%	-3.07%	8.0%	-1.99%	-7.16%	0.311	0.675	1.000	0.427	0.26	0.198	37%	57%	469	4.93	0.42	12.5	5.34%

Negative moment region (Bending causes tension on outside surface)

Comp Stress (psi)	Comp strain (%)	Available for Bending Strain-in (%)	Bending Strain-out (%)	Factored Vert. Defl. (%)	Total Strain-in (%)	Total Strain-out (%)	rho Elem. 1	Elem. 2	Elem. 3	Elem. 4	Effective Area (in^2/in.)	Effective I (in.^4/in.)	Area Reduction (%)	I Reduction (%)	Factored Load Carrying Capacity (lbs/in.)	Hoop Stiffness Factor (psi)	VAF	Allowable Depth of Fill (ft)	Allowable Deflection (%)
0	0.00%	-6.14%	7.500%	19.6%	-5.13%	7.50%	1.000	1.000	0.953	0.278	0.36	0.388	14%	16%	0	4.93	0.42	0.0	9.78%
-200	-0.91%	-5.45%	8.18%	20.8%	-6.36%	7.07%	1.000	1.000	0.892	0.252	0.35	0.378	16%	18%	141	4.93	0.42	3.8	10.40%
-400	-1.82%	-4.77%	8.86%	18.2%	-6.59%	5.16%	1.000	0.900	0.882	0.247	0.33	0.352	20%	23%	267	4.93	0.42	7.1	9.10%
-600	-2.73%	-4.09%	9.55%	15.6%	-6.82%	3.26%	1.000	0.785	0.873	0.244	0.31	0.328	25%	29%	376	4.93	0.42	10.0	7.80%
-655	-2.98%	-3.90%	9.73%	14.9%	-6.88%	2.73%	1.000	0.761	0.870	0.242	0.31	0.323	26%	30%	404	4.93	0.42	10.8	7.45%
-800	-3.64%	-3.41%	10.23%	13.0%	-7.05%	1.35%	1.000	0.706	0.864	0.240	0.30	0.314	28%	32%	478	4.93	0.42	12.8	6.50%
-900	-4.09%	-3.07%	10.57%	11.7%	-7.16%	0.40%	1.000	0.675	0.859	0.238	0.29	0.309	30%	33%	527	4.93	0.42	14.1	5.85%

Example Calculations

Section: C24   Corrugated PVC   24 in. Inside Diameter
         Element 1 Element 2 Element 3 Element 4
         (Crest)   (Web)   (Valley)   (Liner)   E =   158000 psi
I (in.)   1.35   0.96   0.17   1.27   k =   4
t (in.)   0.13   0.15   0.20   0.14   Ag =   0.70 in^2   0.367 in.^2/in.
w (in.)   1.05   0.79   0.34   1.27   Ig =   0.11 in^4   0.060 in.^4/in.
w/t   8.09   5.32   1.72   9.41   h =   1.09 in

Installation Conditions
                                          c-in (y-bar) =   0.48 in.   c-in/(c-in+cout)=   0.44   SI
                    Ms =   2000 psi   c-out (y-bar) =   0.61 in.   EA/R =   4650   9.328244 area
           Soil density =   120 pcf   R-centr. =   12.48 in.   13.7931 Ms
Design Factors   Df =   6.00   14.3 depth
      Earth load factor =   2   Limiting total compressive strain = -2.47%   2.81% defl
    omb str. load factor = 1.5   Limiting tensile strain =   5.25%
           Phi-soil =   0.9
           Phi-pipe =   1.00

Positive moment is compression on the liner side.
Evaluate elements 1, 3, and 4 on combined strain, evaluate Element 2 based on hoop compression strain
Positive stress/strain = Tension

A. Check on Basis of Maximum Possible Deflection

Positive moment region (Bending causes tension on inside surface)

Factored Comp Stress (psi)	Factored Comp strain (%)	Available for Bending Strain-in (%)	Bending Strain-out (%)	Factored Vert. Defl. (%)	Total Strain-in (%)	Total Strain-out (%)	Elem. 1	Elem. 2	Elem. 3	Elem. 4	Effective Area (in^2/in.)	Effective I (in.^4/in.)	Area Reduction (%)	I Reduction (%)	Factored Load Carrying Capacity (lbs/in.)	Hoop Stiffness Factor (psi)	VAF	Allowable Depth of Fill (ft)	Allowable Deflection (%)
0	0.00%	5.25%	-2.47%	8.4%	1.94%	-2.47%	1.000	1.000	1.000	1.000	0.37	0.060	0.0%	0.0%	0	0.39	0.93	0.0	5.62%
-600	-0.38%	5.53%	-2.18%	7.5%	1.34%	-2.56%	1.000	1.000	1.000	1.000	0.37	0.060	0.0%	0.0%	441	0.39	0.93	10.9	4.97%
-1000	-0.63%	5.72%	-1.99%	6.8%	0.94%	-2.63%	1.000	1.000	1.000	1.000	0.37	0.060	0.0%	0.0%	735	0.39	0.93	18.1	4.54%
-1222	-0.77%	5.83%	-1.89%	6.4%	0.71%	-2.66%	1.000	1.000	1.000	1.000	0.37	0.060	0.0%	0.0%	898	0.39	0.93	22.2	4.30%
-1800	-1.14%	6.10%	-1.61%	5.5%	0.13%	-2.75%	1.000	1.000	1.000	1.000	0.37	0.060	0.0%	0.0%	1322	0.39	0.93	32.7	3.67%
-2200	-1.39%	6.29%	-1.42%	4.9%	-0.27%	-2.82%	0.996	1.000	1.000	1.000	0.37	0.059	0.1%	0.2%	1614	0.39	0.93	39.9	3.24%
-2600	-1.65%	6.48%	-1.23%	4.2%	-0.67%	-2.88%	0.990	1.000	1.000	1.000	0.37	0.059	0.3%	0.5%	1905	0.39	0.93	47.0	2.81%

Negative moment region (Bending causes tension on outside surface)

Comp Stress (psi)	Comp strain (%)	Available for Bending Strain-in (%)	Bending Strain-out (%)	Factored Vert. Defl. (%)	Total Strain-in (%)	Total Strain-out (%)	Elem. 1	Elem. 2	Elem. 3	Elem. 4	Effective Area (in^2/in.)	Effective I (in.^4/in.)	Area Reduction (%)	I Reduction (%)	Factored Load Carrying Capacity (lbs/in.)	Hoop Stiffness Factor (psi)	VAF	Allowable Depth of Fill (ft)	Allowable Deflection (%)
0	0.00%	-2.47%	5.250%	10.7%	-2.47%	3.13%	1.000	1.000	1.000	0.950	0.36	0.059	1%	1%	0	0.39	0.93	0.0	5.35%
-600	-0.38%	-2.18%	5.53%	9.5%	-2.56%	2.39%	1.000	1.000	1.000	0.940	0.36	0.059	1%	2%	434	0.39	0.93	10.7	4.73%
-1000	-0.63%	-1.99%	5.72%	8.6%	-2.63%	1.90%	1.000	1.000	1.000	0.933	0.36	0.059	2%	2%	722	0.39	0.93	17.8	4.32%
-1222	-0.77%	-1.89%	5.83%	8.2%	-2.66%	1.62%	1.000	1.000	1.000	0.930	0.36	0.059	2%	2%	882	0.39	0.93	21.8	4.09%
-1800	-1.14%	-1.61%	6.10%	7.0%	-2.75%	0.91%	1.000	1.000	1.000	0.920	0.36	0.058	2%	2%	1296	0.39	0.93	32.0	3.50%
-2200	-1.39%	-1.42%	6.29%	6.2%	-2.82%	0.42%	1.000	1.000	1.000	0.914	0.36	0.058	2%	2%	1582	0.39	0.93	39.1	3.09%
-2600	-1.65%	-1.23%	6.48%	5.4%	-2.88%	-0.08%	1.000	1.000	1.000	0.908	0.36	0.058	2%	2%	1866	0.39	0.93	46.1	2.68%

Example Calculations

Section: D48   Honeycombed HDPE   48 in. Inside Diameter

	Element 1 (Liner 1-top)	Element 2 Liner 2-bot	Element 3 (Web 1c)	Element 4 Web 2trto	Element 5 Web 3trbo			
I (in.)	2.53	2.53	1.00	1.00	1.00	E =	22000 psi	
t (in.)	0.09	0.09	0.10	0.10	0.10	k =	4	0.430 in.^2/in.
w (in.)	1.88	1.88	0.88	1.00	1.00	Ag =	1.09 in^2	0.444 in.^4/in.
w/t	20.00	20.00	4.29	8.62	8.62	Ig =	1.12 in^4	
						h =	2.66 in.	

Installation Conditions

c-in (y-bar) = 1.332 in.   c-in/(c-in+cout)= 0.50   **SI**

Ms = 2000 psi   c-out (y-bar) = 1.332 in.   EA/R = 373.4   10.91939 area

Soil density = 120 pcf   R-centr. = 25.33 in.   13.7931 Ms

Design Factors   Df = 6.0   6.3 depth

Earth load factor = 2   Limiting total compressive strain = -6.14%   4.86% defl

Comb str. load factor = 1.5   Limiting tensile strain = 7.50%

Phi-soil = 0.9

Phi-pipe = 1.00

Positive moment is compression on the liner side.

Evaluate elements 1 and 2 on combined strain, evaluate other elements based on hoop compression strain

Positive stress/strain = Tension

A. Check on Basis of Maximum Possible Deflection

Positive moment region (Bending causes tension on inside surface)

Factored Comp Stress (psi)	Factored Comp strain (%)	Available for Bending Strain-in (%)	Bending Strain-out (%)	Factored Vert. Defl. (%)	Total Strain-in (%)	Total Strain-out (%)	Elem. 1	Elem. 2	Elem. 3	Elem. 4	Elem. 5	Effective Area (in^2/in.)	Effective I (in.^4/in.)	Area Reduction (%)	I Reduction (%)	Factored Load Carrying Capacity (lbs/in.)	Hoop Stiffness Factor (psi)	VAF	Allowable Depth of Fill (ft)	Allowable Deflection (%)
0	0.00%	7.50%	-6.14%	19.5%	6.14%	-6.14%	0.368	1.000	1.000	1.000	1.000	0.37	0.33	14%	25%	0	8.04	0.32	0.0	9.73%
-200	-0.91%	8.18%	-5.45%	17.3%	4.55%	-6.36%	0.362	1.000	1.000	1.000	1.000	0.37	0.33	14%	25%	148	8.04	0.32	5.3	8.65%
-400	-1.82%	8.86%	-4.77%	15.1%	2.95%	-6.59%	0.356	1.000	1.000	1.000	1.000	0.37	0.39	14%	12%	295	8.04	0.32	10.6	7.57%
-600	-2.73%	9.55%	-4.09%	13.0%	1.36%	-6.82%	0.351	1.000	1.000	0.971	0.971	0.36	0.38	15%	14%	437	8.04	0.32	15.6	6.49%
-655	-2.98%	9.73%	-3.90%	12.4%	0.93%	-6.88%	0.349	1.000	1.000	0.947	0.947	0.36	0.38	16%	15%	472	8.04	0.32	16.8	6.19%
-800	-3.64%	10.23%	-3.41%	10.8%	-0.23%	-7.05%	0.346	1.000	1.000	0.891	0.891	0.35	0.36	18%	18%	561	8.04	0.32	20.0	5.40%
-900	-4.09%	10.57%	-3.07%	9.7%	-1.02%	-7.16%	0.343	0.774	1.000	0.858	0.858	0.32	0.33	25%	25%	583	8.04	0.32	20.8	4.86%

Negative moment region (Bending causes tension on outside surface)

Comp Stress (psi)	Comp strain (%)	Available for Bending Strain-in (%)	Bending Strain-out (%)	Factored Vert. Defl. (%)	Total Strain-in (%)	Total Strain-out (%)	Elem. 1	Elem. 2	Elem. 3	Elem. 4	Elem. 5	Effective Area (in^2/in.)	Effective I (in.^4/in.)	Area Reduction (%)	I Reduction (%)	Factored Load Carrying Capacity (lbs/in.)	Hoop Stiffness Factor (psi)	VAF	Allowable Depth of Fill (ft)	Allowable Deflection (%)
0	0.00%	-6.14%	7.500%	19.5%	-6.14%	6.14%	1.000	0.368	1.000	1.000	1.000	0.37	0.22	14%	51%	0	8.04	0.32	0.0	9.73%
-200	-0.91%	-5.45%	8.18%	17.3%	-6.36%	4.55%	1.000	0.362	1.000	1.000	1.000	0.37	0.22	14%	51%	148	8.04	0.32	5.3	8.65%
-400	-1.82%	-4.77%	8.86%	15.1%	-6.59%	2.95%	1.000	0.356	1.000	1.000	1.000	0.37	0.42	14%	5%	295	8.04	0.32	10.6	7.57%
-600	-2.73%	-4.09%	9.55%	13.0%	-6.82%	1.36%	1.000	0.351	1.000	0.971	0.971	0.36	0.41	15%	7%	437	8.04	0.32	15.6	6.49%
-655	-2.98%	-3.90%	9.73%	12.4%	-6.88%	0.93%	1.000	0.349	1.000	0.947	0.947	0.36	0.41	16%	8%	472	8.04	0.32	16.8	6.19%
-800	-3.64%	-3.41%	10.23%	10.8%	-7.05%	-0.23%	1.000	0.346	1.000	0.891	0.891	0.35	0.39	18%	11%	561	8.04	0.32	20.0	5.40%
-900	-4.09%	-3.07%	10.57%	9.7%	-7.16%	-1.02%	0.774	0.343	1.000	0.858	0.858	0.32	0.36	25%	20%	583	8.04	0.32	20.8	4.86%

Example Calculations

Section: E36   Corrugated HDPE   36 in. Inside Diameter

	Element 1	Element 2	Element 3	Element 4				
	(Crest)	(Web)	(Valley)	(Liner)				
I (in.)	3.59	2.80	0.99	2.94	E =	22000 psi		
t (in.)	0.19	0.23	0.34	0.13	k =	4		
w (in.)	3.14	2.46	1.98	2.94	Ag =	2.99 in^2	0.557 in.^2/in.	
w/t	16.89	10.94	5.85	21.96	Ig =	4.00 in^4	0.745 in.^4/in.	
					h =	2.99 in		

Installation Conditions

SI

			c-in (y-bar) =	1.28 in.	c-in/(c-in+cout)=	0.43	14.15725 area
Ms =	2000 psi		c-out (y-bar) =	1.71 in.	EA/R =	635.9	13.7931 Ms
Soil density =	120 pcf		R-centr. =	19.28 in.			5.5 depth
Design Factors			Df =	6.00			3.86% defl
Earth load factor =	2	Limiting total compressive strain =	-6.14%				
omb str. load factor =	1.5	Limiting tensile strain =	7.50%				
Phi-soil =	0.9						
Phi-pipe	1.00						

Positive moment is compression on the liner side.
Evaluate elements 1, 3, and 4 on combined strain, evaluate Element 2 based on hoop compression strain
Positive stress/strain = Tension

A. Check on Basis of Maximum Possible Deflection

Positive moment region (Bending causes tension on inside surface)

Factored Comp Stress (psi)	Factored Comp strain (%)	Available for Bending Strain-in (%)	Available for Bending Strain-out (%)	Factored Vert. Defl. (%)	Total Strain-in (%)	Total Strain-out (%)	rho Elem. 1	rho Elem. 2	rho Elem. 3	rho Elem. 4	Effective Area (in^2/in.)	Effective I (in.^4/in.)	Area Reduction (%)	I Reduction (%)	Factored Load Carrying Capacity (lbs/in.)	Hoop Stiffness Factor (psi)	VAF	Allowable Depth of Fill (ft)	Allowable Deflection (%)
0	0.00%	7.50%	-6.14%	11.6%	4.61%	-6.14%	0.428	1.000	1.000	1.000	0.49	0.532	13%	29%	0	2.83	0.55	0.0	7.71%
-200	-0.91%	8.18%	-5.45%	10.3%	3.19%	-6.36%	0.421	1.000	1.000	1.000	0.49	0.529	13%	29%	194	2.83	0.55	5.0	6.85%
-400	-1.82%	8.86%	-4.77%	9.0%	1.77%	-6.59%	0.414	0.951	1.000	1.000	0.47	0.504	15%	32%	378	2.83	0.55	9.7	6.00%
-600	-2.73%	9.55%	-4.09%	7.7%	0.35%	-6.82%	0.408	0.837	1.000	1.000	0.45	0.455	20%	39%	535	2.83	0.55	13.8	5.14%
-655	-2.98%	9.73%	-3.90%	7.4%	-0.04%	-6.88%	0.407	0.812	1.000	1.000	0.44	0.446	21%	40%	576	2.83	0.55	14.8	4.90%
-800	-3.64%	10.23%	-3.41%	6.4%	-1.07%	-7.05%	0.402	0.756	1.000	0.709	0.40	0.407	27%	45%	647	2.83	0.55	16.7	4.28%
-900	-4.09%	10.57%	-3.07%	5.8%	-1.78%	-7.16%	0.399	0.724	1.000	0.580	0.39	0.387	31%	48%	697	2.83	0.55	17.9	3.86%

Negative moment region (Bending causes tension on outside surface)

Comp Stress (psi)	Comp strain (%)	Available for Bending Strain-in (%)	Available for Bending Strain-out (%)	Factored Vert. Defl. (%)	Total Strain-in (%)	Total Strain-out (%)	rho Elem. 1	rho Elem. 2	rho Elem. 3	rho Elem. 4	Effective Area (in^2/in.)	Effective I (in.^4/in.)	Area Reduction (%)	I Reduction (%)	Factored Load Carrying Capacity (lbs/in.)	Hoop Stiffness Factor (psi)	VAF	Allowable Depth of Fill (ft)	Allowable Deflection (%)
0	0.00%	-6.14%	7.500%	14.1%	-5.64%	7.50%	1.000	1.000	0.984	0.351	0.51	0.665	9%	11%	0	2.83	0.55	0.0	7.07%
-200	-0.91%	-5.45%	8.18%	13.7%	-6.36%	6.35%	1.000	1.000	0.951	0.332	0.50	0.656	10%	12%	201	2.83	0.55	5.2	6.84%
-400	-1.82%	-4.77%	8.86%	12.0%	-6.59%	4.53%	1.000	0.951	0.942	0.327	0.49	0.632	12%	15%	391	2.83	0.55	10.1	5.98%
-600	-2.73%	-4.09%	9.55%	10.3%	-6.82%	2.71%	1.000	0.837	0.932	0.322	0.46	0.587	17%	21%	553	2.83	0.55	14.2	5.13%
-655	-2.98%	-3.90%	9.73%	9.8%	-6.88%	2.21%	1.000	0.812	0.930	0.321	0.45	0.579	18%	22%	596	2.83	0.55	15.3	4.89%
-800	-3.64%	-3.41%	10.23%	8.5%	-7.05%	0.90%	1.000	0.756	0.923	0.317	0.44	0.561	21%	25%	705	2.83	0.55	18.2	4.27%
-900	-4.09%	-3.07%	10.57%	7.7%	-7.16%	-0.01%	1.000	0.724	0.919	0.315	0.43	0.552	22%	26%	778	2.83	0.55	20.0	3.85%

APPENDIX E

RECOMMENDED BALLOT ITEMS TO INCORPORATE FINDINGS INTO AASHTO SPECIFICATIONS

This section of the report contains recommended specification language to incorporate the findings of this project into AASHTO Specifications.

NCHRP Project 20-7, Task 89
LRFD Specifications for Plastic Pipe and Culverts

Proposed Revisions to AASHTO LRFD Specifications for Thermoplastic Pipe

12.5.3 Strength Limit State

No proposed changes to specification requirements.

C12.5.3

Add:

Thermoplastic pipe have many profile wall geometries and some of these are made up of thin sections that may be limited based on local buckling. The strength limit state for wall area includes evaluating the section capacity for local buckling.

12.5.5 Resistance Factors

Add to table 12.5.5-1, under "Thermoplastic Pipe"

PE and PVC pipe:
    flexure   1.0

12.6.1 Loading

Add to second sentence:

Earth surcharge, live load surcharge, downdrag forces and <u>external hydrostatic pressure</u> shall be evaluated where construction or site conditions warrant.

C12.6.1

External hydrostatic pressure, if present, can add significantly to the total thrust in a buried pipe.

12.12.3.1 GENERAL

Buried plastic pipe shall be investigated at the strength limit state for thrust, buckling and <u>combined compression strain</u>.

12.12.3.1

The limit state for combined strain is new. Total compressive strain in an element can result in local buckling and total tensile strain can result in cracking.

12.12.3.5 WALL RESISTANCE

Add:

If the evaluation for local buckling capacity in Section 12.12.3.8 results in a reduced total area, then the reduced area shall be used in evaluating the factored resistance.

12.12.3.8 RESISTANCE OF WALL TO LOCAL BUCKLING OF PIPE WALL

Elements of profile wall pipe shall be designed to resist local buckling in accordance with the following sections.

12.12.3.8.1 Idealized Wall Profile

Profile wall pipe shall be idealized as straight elements. Each element shall be assigned width based on the clear distance between the adjoining elements and a thickness based on the thickness at the center of the element. See Fig. 12.12.3.8.1-1 for the idealization of a typical corrugated profile.
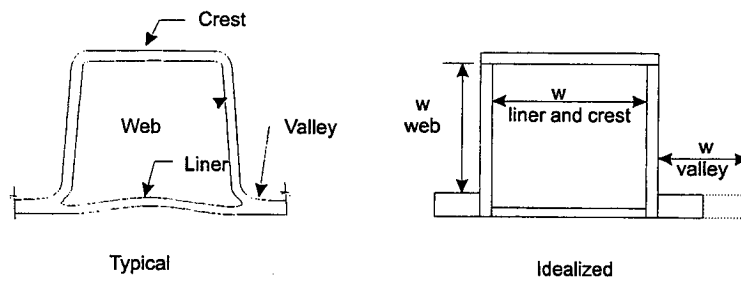
C12.12.3.5

The local buckling evaluation reduces the capacity of pipe wall sections with low ratios of width to thickness.

Figure 12.12.3.8.1-1. Typical and idealized cross-section of profile wall pipe.

12.12.3.8.2 Slenderness and Effective Width

To evaluate local buckling, the effective width of each element is evaluated as:

$$b = \rho w \qquad (12.12.3.8.2\text{-}1)$$

where:

$$\rho = \frac{(1 - 0.22/\lambda)}{\lambda} \qquad (12.12.3.8.2\text{-}2)$$

$$\lambda = \frac{w}{t}\sqrt{\frac{\varepsilon}{k}} > 0.673 \qquad (12.12.3.8.2\text{-}3)$$

b = element effective width, mm, in.
ρ = effective width factor
w = total clear width of element between supporting elements
λ = slenderness factor
t = thickness of element, in., mm
ε = strain in element
k = edge support coefficient

The total effective area is the gross section area reduced by the ineffective area which is evaluated using Eqs. 12.12.3.8-1 to 3.

C12.12.3.8.2

The resistance to local buckling is based on the effective width concept used by the cold formed steel industry (AISI, 1997). This theory assumes that even though buckling is initiated in the center of a plate element, the element still has substantial strength at the edges where the element is supported. This concept is demonstrated in Fig. C12.12.3.8.2-1.
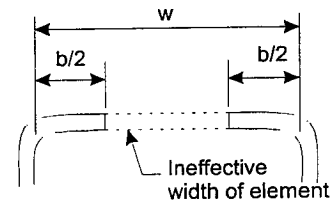

Figure 12.12.3.8.2-1. Effective width concept.

The strain in the element used to evaluate the effective width is based on the total thrust and the total wall area. Strain should be computed using the 50-year modulus of elasticity.

With the limitation that total strain is restricted to 50% more than the compression strain, the section is limited by pure compression. When bending is added, the reduction in compression on one side of the section compensates for the increased compression on the other side.

12.12.3.9 COMBINED STRAIN

Total compressive strain in a pipe wall due to thrust and bending shall not exceed the limiting combined compressive strain, ε_c:

$$\varepsilon_c \geq \varepsilon_b + [T_L/A_{eff}/E_{50}](\gamma_B/\gamma) \qquad (12.12.3.9\text{-}1)$$

where:

ε_c = factored limiting combined compressive strain
= $1.5\,F_u/E_{50}$

γ_B = 1.5, factor of safety on combined strain

A_{eff} = Effective area of pipe wall, the lesser of the gross area or the reduced area computed based on local buckling mm²/mm, in.²/in.

E_{50} = 50-year modulus of elasticity, MPa, ksi

Bending strain at the service limit is ε_c/k.

C12.12.3.9

The criteria for combined compressive strain is based on limiting local buckling. A higher strain limit is allowed for combined strain because the web elements, which are subjected primarily to bending, are less likely to buckle and increase the stability of elements near the crest and valley.

12.12.3.9.1 Bending Strain

In the absence of a more detailed analysis, the bending strain may be computed based on the empirical relationship between strain and deflection:

$$\varepsilon_b = \gamma_B D_f \left(\frac{c}{R}\right)\left(\frac{\Delta}{D}\right) \qquad (12.12.3.9.1\text{-}1)$$

where:

ε_b = factored bending strain

Df = shape factor from Table 12.12.3.9.1-1

f = distance from neutral axis to extreme fiber, mm (in.)

R = radius to centroid of pipe, mm (in.)

Δ = allowable deflection of pipe, reduction of vertical diameter due to bending, mm (in.)

D = diameter to centroid of pipe wall, mm (in.)

Elements whose centroid is less than c/3 from the centroid of the profile wall need not be evaluated for combined strain.

More detailed analyses must consider the likelihood of inconsistent soil support to the pipe in the haunch zone and of local deformations during placement and compaction of backfill.

C12.12.3.9.1

The empirical shape factor is used in the design of fiberglass pipe and is presented in AWWA Manual of Practice M45 *Fiberglass Pipe Design*. It demonstrates that bending strains are highest in low stiffness pipe backfilled in soils that require substantial compactive effort (silts and clays) and are lowest in high stiffness pipe backfilled in soils that require little compactive effort (sands and gravels).

One method of using the shape factor and combined bending strain is to evaluate the limiting deflection that can be allowed in the field with the calculated compressive thrust. In this approach, the total compressive strain is assumed to be at the limiting value. The bending strain is computed as the difference between the limiting compressive strain and the hoop strain, and an allowable deflection is computed from Eq. 12.12.3.9.1-1. For example:

$$\varepsilon_b = \varepsilon_c - T_L/A_{eff}/E_{50} * \gamma_B/\gamma \qquad (C12.12.3.9.1\text{-}1)$$

$$\Delta = \frac{\varepsilon_b}{\gamma_B D_f}\left(\frac{R}{c}\right)D \qquad (C12.12.3.9.1\text{-}2)$$

and the total allowable vertical deflection is:

$$\Delta_{all} = \Delta + T_L/A_{eff}/E_{50}/\gamma \qquad (C12.12.3.9.1\text{-}3)$$

Table 12.12.3.9.1-1 does not cover all possible backfills and density levels. Designers should interpolate or extrapolate the table as necessary for specific projects.

TABLE 12.12.3.9-1 Shape Factors Based On Pipe Stiffness, Backfill and Compaction Level

| Pipe Stiffness (F/Δy, kPa) | Pipe Zone Embedment Material and Compaction Level | | | |
| | Gravel (1) | | Sand (2) | |
	Dumped to Slight (3)	Moderate to High (4)	Dumped to Slight (3)	Moderate to High(4)
62	5.5	7.0	6.0	8.0
124	4.5	5.5	5.0	6.5
248	3.8	4.5	4.0	5.5
496	3.3	3.8	3.5	4.5

1. GW, GP, GW-GC, GW-GM, GP-GC and GP-GM per ASTM D 2487 (includes crushed rock).
2. SW, SP, SM, SC, GM and GC or mixtures per ASTM D 2487.
3. < 85% of maximum dry density per AASHTO T-99, < 40% relative density (ASTM D 4253 and D 4254).
4. ≥ 85% of maximum dry density per AASHTO T-99, ≥ 40% relative density (ASTM D 4253 and D 4254).

The **Transportation Research Board** is a unit of the National Research Council, which serves the National Academy of Sciences and the National Academy of Engineering. The Board's mission is to promote innovation and progress in transportation by stimulating and conducting research, facilitating the dissemination of information, and encouraging the implementation of research results. The Board's varied activities annually draw on approximately 4,000 engineers, scientists, and other transportation researchers and practitioners from the public and private sectors and academia, all of whom contribute their expertise in the public interest. The program is supported by state transportation departments, federal agencies including the component administrations of the U.S. Department of Transportation, and other organizations and individuals interested in the development of transportation.

The National Academy of Sciences is a private, nonprofit, self-perpetuating society of distinguished scholars engaged in scientific and engineering research, dedicated to the furtherance of science and technology and to their use for the general welfare. Upon the authority of the charter granted to it by the Congress in 1863, the Academy has a mandate that requires it to advise the federal government on scientific and technical matters. Dr. Bruce M. Alberts is president of the National Academy of Sciences.

The National Academy of Engineering was established in 1964, under the charter of the National Academy of Sciences, as a parallel organization of outstanding engineers. It is autonomous in its administration and in the selection of its members, sharing with the National Academy of Sciences the responsibility for advising the federal government. The National Academy of Engineering also sponsors engineering programs aimed at meeting national needs, encourages education and research, and recognizes the superior achievements of engineers. Dr. William A. Wulf is president of the National Academy of Engineering.

The Institute of Medicine was established in 1970 by the National Academy of Sciences to secure the services of eminent members of appropriate professions in the examination of policy matters pertaining to the health of the public. The Institute acts under the responsibility given to the National Academy of Sciences by its congressional charter to be an adviser to the federal government and, upon its own initiative, to identify issues of medical care, research, and education. Dr. Kenneth I. Shine is president of the Institute of Medicine.

The National Research Council was organized by the National Academy of Sciences in 1916 to associate the broad community of science and technology with the Academy's purpose of furthering knowledge and advising the federal government. Functioning in accordance with general policies determined by the Academy, the Council has become the principal operating agency of both the National Academy of Sciences and the National Academy of Engineering in providing services to the government, the public, and the scientific and engineering communities. The Council is administered jointly by both the Academies and the Institute of Medicine. Dr. Bruce M. Alberts and Dr. William A. Wulf are chairman and vice chairman, respectively, of the National Research Council.

Abbreviations used without definitions in TRB publications:

AASHO	American Association of State Highway Officials
AASHTO	American Association of State Highway and Transportation Officials
ASCE	American Society of Civil Engineers
ASME	American Society of Mechanical Engineers
ASTM	American Society for Testing and Materials
FAA	Federal Aviation Administration
FHWA	Federal Highway Administration
FRA	Federal Railroad Administration
FTA	Federal Transit Administration
IEEE	Institute of Electrical and Electronics Engineers
ITE	Institute of Transportation Engineers
NCHRP	National Cooperative Highway Research Program
NCTRP	National Cooperative Transit Research and Development Program
NHTSA	National Highway Traffic Safety Administration
SAE	Society of Automotive Engineers
TCRP	Transit Cooperative Research Program
TRB	Transportation Research Board
U.S.DOT	United States Department of Transportation

THE NATIONAL ACADEMIES
Advisers to the Nation on Science, Engineering, and Medicine

National Academy of Sciences
National Academy of Engineering
Institute of Medicine
National Research Council